

University of Kentucky

UKnowledge

Theses and Dissertations--Pharmacology and
Nutritional Sciences

Pharmacology and Nutritional Sciences


2023

AGE-ASSOCIATED INCREASE OF GAMMA DELTA T CELLS IN VISCERAL ADIPOSE TISSUE AND MECHANISMS OF THEIR ACCUMULATION

Sujata Mukherjee

University of Kentucky, sujata.mukherjee@uky.edu

Author ORCID Identifier:

 <https://orcid.org/0000-0003-4024-4977>

Digital Object Identifier: <https://doi.org/10.13023/etd.2023.280>

[Right click to open a feedback form in a new tab to let us know how this document benefits you.](#)

Recommended Citation

Mukherjee, Sujata, "AGE-ASSOCIATED INCREASE OF GAMMA DELTA T CELLS IN VISCERAL ADIPOSE TISSUE AND MECHANISMS OF THEIR ACCUMULATION" (2023). *Theses and Dissertations--Pharmacology and Nutritional Sciences*. 50.

https://uknowledge.uky.edu/pharmacol_etds/50

This Doctoral Dissertation is brought to you for free and open access by the Pharmacology and Nutritional Sciences at UKnowledge. It has been accepted for inclusion in Theses and Dissertations--Pharmacology and Nutritional Sciences by an authorized administrator of UKnowledge. For more information, please contact UKnowledge@lsv.uky.edu.

STUDENT AGREEMENT:

I represent that my thesis or dissertation and abstract are my original work. Proper attribution has been given to all outside sources. I understand that I am solely responsible for obtaining any needed copyright permissions. I have obtained needed written permission statement(s) from the owner(s) of each third-party copyrighted matter to be included in my work, allowing electronic distribution (if such use is not permitted by the fair use doctrine) which will be submitted to UKnowledge as Additional File.

I hereby grant to The University of Kentucky and its agents the irrevocable, non-exclusive, and royalty-free license to archive and make accessible my work in whole or in part in all forms of media, now or hereafter known. I agree that the document mentioned above may be made available immediately for worldwide access unless an embargo applies.

I retain all other ownership rights to the copyright of my work. I also retain the right to use in future works (such as articles or books) all or part of my work. I understand that I am free to register the copyright to my work.

REVIEW, APPROVAL AND ACCEPTANCE

The document mentioned above has been reviewed and accepted by the student's advisor, on behalf of the advisory committee, and by the Director of Graduate Studies (DGS), on behalf of the program; we verify that this is the final, approved version of the student's thesis including all changes required by the advisory committee. The undersigned agree to abide by the statements above.

Sujata Mukherjee, Student

Dr. Marlene Starr, Major Professor

Dr. Rolf J Craven, Director of Graduate Studies

AGE-ASSOCIATED INCREASE OF $\gamma\delta$ T CELLS IN VISCERAL ADIPOSE TISSUE
AND MECHANISMS OF THEIR ACCUMULATION

DISSERTATION

A dissertation submitted in partial fulfillment of the
requirements for the degree of Doctor of Philosophy in Pharmacology in the
College of Medicine
at the University of Kentucky

By

Sujata Mukherjee

Lexington, Kentucky

Director: Dr. Marlene E. Starr, Associate Professor of Surgery

Lexington, Kentucky

2023

Copyright © Sujata Mukherjee 2023
<https://orcid.org/0000-0003-4024-4977>

ABSTRACT OF DISSERTATION

AGE-ASSOCIATED INCREASE OF $\gamma\delta$ T CELLS IN VISCERAL ADIPOSE TISSUE AND MECHANISMS OF THEIR ACCUMULATION

Chronic systemic inflammation, known as inflammaging is considered a hallmark of aging and associated diseases. While adipose tissue has long been considered only as a caloric reservoir regulating systemic energy homeostasis, research in the past couple of decades substantiate its endocrine function to secrete an array of inflammatory mediators and hormones, which have physiological effects on multiple organ systems, and contribute to inflammaging. Redistribution of adipose tissue from subcutaneous to visceral depots, changes in the immune profile and the chronic inflammatory state are among the major sources of adipose tissue dysfunction with aging.

This dissertation is focused on identifying and characterizing a unique population of T cells, called $\gamma\delta$ T cells, in visceral adipose tissue (VAT) with aging. My studies identified an age-associated increase in $\gamma\delta$ T cell numbers in VAT and a progressive trend of accumulation of these cells over the lifespan in C57BL/6J mice. Importantly, this accumulation is also consistent in humans. I explored the role of VAT resident $\gamma\delta$ T cells in inflammation using a genetic deletion model that lacks $\gamma\delta$ T cells (TCR δ KO) and showed that lack of $\gamma\delta$ T cells results in reduced inflammation both locally and systemically. The potential for $\gamma\delta$ T cells to promote inflammation with aging set the stage to understand the maintenance of this population in VAT and the mechanisms for the age-associated accumulation. I evaluated several physiological mechanisms that may contribute to $\gamma\delta$ T cells accumulation. Using isochronic parabiotic pairs of wild-type (WT) and TCR δ KO mice at young and old age, I found minimal recruitment of peripheral $\gamma\delta$ T cells into VAT without a significant change by aging, suggesting a minor contribution of migration to $\gamma\delta$ T cell accumulation with aging. Since the number of T cells are tightly regulated within a

tissue to maintain homeostasis, I further evaluated two potential driving forces, proliferation, and programmed cell death as mechanisms to increase the number of $\gamma\delta$ T cells in VAT with aging. Studies using Ki67 as a proliferation marker and *in vivo* EdU incorporation demonstrated that the absolute number of proliferating $\gamma\delta$ T cells per gram of VAT significantly increased in the aged VAT compared to young and middle age, indicating that an increase in the local proliferating $\gamma\delta$ T cell population contributes to the age-associated accumulation. Analysis of apoptosis via caspase activity, revealed a decrease in apoptosis in $\gamma\delta$ T cells with a concomitant increase in the live population among the middle-aged group of mice that continued into the aged. Comparative studies in peripheral lymph nodes showed the expected increase in apoptosis among the aged, suggesting that $\gamma\delta$ T cells are protected from age-associated apoptosis specifically in VAT. Changes in VAT microenvironment with age that led to a reduction in apoptosis will be an interesting avenue for future research. Collectively, these data suggest that an increased number of tissue-resident proliferating $\gamma\delta$ T cells and increased survival of $\gamma\delta$ T cell populations, rather than peripheral migration, account for the age-associated $\gamma\delta$ T cell accumulation observed in VAT. These findings are important to better understand how adipose tissue dysfunction and related changes in its immune profile contribute to inflammaging among the elderly.

KEYWORDS: Aging, adipose tissue, gamma delta T cells, inflammation, migration, proliferation

Sujata Mukherjee
(Name of Student)

06/12/2023
Date

AGE-ASSOCIATED INCREASE OF $\gamma\delta$ T CELLS IN VISCERAL ADIPOSE TISSUE
AND MECHANISMS OF THEIR ACCUMULATION

By
Sujata Mukherjee

Dr. Marlene Starr

Director of Dissertation

Dr. Rolf J. Craven

Director of Graduate Studies

06/12/2023

Date

DEDICATION

To my beloved husband

ACKNOWLEDGMENTS

It is a privilege to express my gratefulness towards those who were my strengths during this incredible journey of graduate school. First, I express my profound respect and admiration for my Ph.D. advisor Dr. Marlene Starr for her valuable guidance and mentorship. I was fortunate to receive endless encouragements and support throughout the ups and downs of my PhD training which helped me to grow into a better researcher. I would like to thank my committee members Dr. Michael Kilgore, Dr. Donald Cohen, and Dr. Hiroshi Saito, for their continuous support and guidance.

I would like to thank Dr. Maria Bruno for training me in numerous valuable techniques and helping me with my research projects in the lab. I am grateful to Jennifer Strange and Cuiping Zhang for assisting with their flow cytometry expertise. I am thankful to William Titlow for his assistance with my experiments. I want to convey my deepest appreciation to Dr. Donald Cohen and Dr. Octavio Gonzalez at the University of Kentucky, and Dr. Jonathan Boyson at the University of Vermont for their help in my dissertation projects.

I would also like to thank the Department of Pharmacology and Nutritional Sciences for providing me with all the necessary guidance and assistance for the successful completion of my PhD. A special thanks to Dr. Rolf Craven and Dr. Nada Porter for being exceptionally supportive to the students. I would also like to thank the Nutritional Sciences and Pharmacology Students association for their continuous support. I thank the University of Kentucky graduate school and College of Medicine for providing me with the opportunity to complete my successful PhD training.

Most importantly, I would like to express my deepest gratitude and appreciation to my loving and caring husband, Dr. Arnab K Majee. I would like to thank him for providing me with motivation and tremendous support on a daily basis. My graduate school journey would not have been the same without him. A special thanks to my friends, Dr. Rakshamani Tripathi, Dr. Himi Tripathi, Dr. Maria Bruno, Dr. Anastasia Lyon and Dr. Meagan Kingren for their support and help through every phase of my graduate school. Lastly, I would like to thank my entire family who helped me achieve my goals.

TABLE OF CONTENTS

ACKNOWLEDGMENTS iii

LIST OF TABLES viii

LIST OF FIGURES ix

CHAPTER 1. INTRODUCTION 1

 1.1 Aging 1

 1.1.1 Global burden of aging 1

 1.1.2 Epidemiology and related diseases 2

 1.2 Adipose tissue in aging 4

 1.2.1 Adipose tissue dysfunction with aging 4

 1.2.2 Adipose tissue as a source of inflammaging 5

 1.3 $\gamma\delta$ T cells 6

 1.3.1 Age-associated alterations of $\gamma\delta$ T cells in circulation 6

 1.3.2 Age-associated alterations of $\gamma\delta$ T cells in other tissues 7

 1.3.3 Abundance and distribution in adipose tissue 8

 1.3.4 Subpopulations studied in mouse adipose tissue 8

 1.3.5 Adipose tissue-residency in mouse model 9

 1.3.6 Effect of obesity on adipose-resident $\gamma\delta$ T cells 10

 1.3.7 Regulatory roles of $\gamma\delta$ T cells in adipose tissue biology 10

 1.3.7.1 $\gamma\delta$ T cells are major producers of IL-17 in adipose tissue 10

 1.3.7.2 $\gamma\delta$ T cells as a metabolic regulator in adipose tissue 11

 1.3.7.3 Thermogenic role of $\gamma\delta$ T cells in adipose tissue 11

 1.3.8 IL-17 producing $\gamma\delta$ T cells in other tissues with chronic inflammation 12

 1.3.9 Goal of this dissertation 13

CHAPTER 2. MATERIALS AND METHODSS 15

 2.1 Animals and husbandry 15

2.2	Parabiosis	15
2.3	Murine sample collection.....	17
2.4	Human sample acquisition.....	18
2.5	Tissue processing for single-cell suspensions	18
2.5.1.	Adipose tissue	18
2.5.2	Blood.....	18
2.5.3	Liver, Spleen and Lymph node.....	19
2.5.4	Skin	19
2.6	Flow cytometry	19
2.7	Quantitative real-time RT-PCR	22
2.8	Plasma IL-6 ELISA	23
2.9	<i>In vivo</i> cell proliferation study with EdU.....	23
2.10	Analysis of apoptosis.....	24
2.11	TCR-V γ /V δ PCR	24
2.12	Statistical analyses	25
CHAPTER 3. ACCUMULATION OF $\gamma\delta$ T CELLS IN VISCERAL ADIPOSE TISSUE (VAT) WITH AGING PROMOTES CHRONIC INFLAMMATION.....		26
3.1	Objective.....	26
3.2	Results.....	26
3.2.1	$\gamma\delta$ T cells are increased by aging specifically in VAT	26
3.2.2	Trend of $\gamma\delta$ T cells accumulation in VAT over the lifespan in mice	31
3.2.3	$\gamma\delta$ T cells in VAT predominantly express IL-17A	35
3.2.4	Reduced inflammation in aged mice lacking $\gamma\delta$ T cells (TCR δ KO)	38
3.3	Conclusions.....	44
CHAPTER 4. THE CONTRIBUTIONS OF MIGRATION, PROLIFERATION AND APOPTOSIS IN AGE-ASSOCIATED $\gamma\delta$ T CELLS ACCUMULATION IN VAT		45

4.1 Objective.....	45
4.2 Results.....	45
4.2.1 Minimal peripheral migration of $\gamma\delta$ T cells was found in young and aged mice.....	45
4.2.2 Proliferating VAT-resident $\gamma\delta$ T cells increase in the aged	48
4.2.3 Apoptosis of VAT-resident $\gamma\delta$ T cells declines at middle age.....	53
4.3 Conclusions.....	59
CHAPTER 5. THE SUBPOPULATIONS OF $\gamma\delta$ T CELLS IN VAT	60
5.1 Objective.....	60
5.2 Results.....	60
5.2.1 TCR-V γ /V δ profiling by PCR	60
5.2.2 TCR-V γ /V δ profiling by flow cytometry	65
5.3 Conclusions.....	71
CHAPTER 6. DISCUSSION, LIMITATIONS AND FUTURE DIRECTIONS.....	72
6.1 $\gamma\delta$ T cells progressively accumulate in VAT over the lifespan in mice	72
6.2 Adipose tissue-resident $\gamma\delta$ T cells promote inflammation.....	73
6.3 Adipose tissue-resident $\gamma\delta$ T cells mediate cellular homeostasis	75
6.4 Peripheral migration plays a minor role in age-associated $\gamma\delta$ T cell accumulation in VAT.....	76
6.5 Increased number of proliferating $\gamma\delta$ T cells contribute to age-associated accumulation in VAT.....	77
6.6 Decreased apoptosis beginning at middle-age contributes to increased survival and age-associated accumulation of $\gamma\delta$ T cells in VAT.....	78
6.7 Limitations and future directions	81
REFERENCES	85

VITA..... 91

LIST OF TABLES

Table 2.1 Antibodies used for the flow cytometry studies	21
Table 2.2 Cell identification schemes	22
Table 2.3 Primers used for gene expression analysis with PCR.....	25
Table 5.1 Antibodies used for the flow cytometry studies with γ chains	65
Table 6.1 Nonstandard abbreviations and acronyms	83

LIST OF FIGURES

Fig. 1.1 Projected population growth in USA	2
Fig. 1.2 Lifespan in C57BL/6J mice in comparison to human life.....	3
Fig. 1.3 Age-associated adipose tissue dysfunction	4
Fig. 2.1 In-house developed clear plexiglass barrier for parabiosis pair acclimatization.	17
Fig. 2.2 Experimental design for EdU pulsing in young and aged mice to analyze in vivo proliferation.....	23
Fig. 3.1 $\gamma\delta$ T cells are increased by aging in visceral adipose tissue (VAT)	28
Fig. 3.2 $\gamma\delta$ T cells are increased by aging specifically in VAT	28
Fig. 3.3 $\gamma\delta$ T cells increase in human VAT by aging.....	29
Fig. 3.4 Age-associated changes in the T_{conv} cells in VAT.....	29
Fig. 3.5 Representative flow cytometry plots to identify $\gamma\delta$ T and T_{conv} cells.....	30
Fig. 3.6 Accumulation of $\gamma\delta$ T and T_{conv} cells in VAT over the lifespan in mice.....	33
Fig. 3.7 Age and corresponding adiposity in mice	33
Fig. 3.8 $\gamma\delta$ T and T_{conv} cell profiling in lymph nodes (LN) over the lifespan.....	34
Fig. 3.9 Representative flow cytometry plots to identify $\gamma\delta$ T and T_{conv} cells based on IL-17A or IFN γ production.....	35
Fig. 3.10 $\gamma\delta$ T cells in VAT predominantly express IL-17A	36
Fig. 3.11 IL-17A and IFN γ producing T_{conv} cells in VAT	36
Fig. 3.12 IL-17A and IFN γ in splenic T cells	37
Fig. 3.13 Reduced inflammation in aged mice lacking $\gamma\delta$ T cells (TCR δ KO).....	39
Fig. 3.14 Non-immune cells are the primary IL-6 producers which decreased in aged mice lacking $\gamma\delta$ T cells (TCR δ KO)	41
Fig. 3.15 IL-6 expression in tissues of WT vs. TCR δ KO mice.....	41
Fig. 3.16 Representative flow cytometry plots to identify IL-6 positive cells in the CD45 positive immune cells versus CD45 negative non-immune cells	41

Fig. 3.17 Representative flow cytometry plots to identify IL-6 positive cells in stromal vascular cellular (SVFC) compartments	42
Fig. 3.18 Representative flow cytometry plots to identify immune cells among SVFC ..	43
Fig. 4.1 Peripheral migration has a minimal role in age-associated $\gamma\delta$ T cell accumulation in VAT	47
Fig. 4.2 Representative flow cytometry plots for proliferating T cells.....	49
Fig. 4.3 Proliferating $\gamma\delta$ T cell profiling in VAT with aging.....	50
Fig. 4.4 Proliferating T_{conv} cell profiling in VAT with aging	51
Fig. 4.5 Proliferating $\gamma\delta$ T and T_{conv} cell profiling in LN with aging	52
Fig. 4.6 $\gamma\delta$ T cells in VAT are protected from apoptosis at the middle age	55
Fig. 4.7 Analysis of apoptosis in T_{conv} cells in VAT with aging.	56
Fig. 4.8 Analysis of apoptosis in $\gamma\delta$ T cells in LN with aging.....	57
Fig. 4.9 Analysis of apoptosis in T_{conv} cells in LN with aging	58
Fig. 5.1 Age-associated comparison of relative gene expressions of γ - δ chains by PCR	61
Fig. 5.2 Gene expression analysis on individual samples by PCR	64
Fig. 5.3 Antibody co-expression for different γ chains.....	70
Fig. 6.1 A putative model demonstrating the interplay of global mechanisms to $\gamma\delta$ T cells accumulation in VAT with aging.....	80

Chapter 1 INTRODUCTION

1.1 Aging

1.1.1 Global Burden of aging

Environmental and internal challenges lead to accumulation of a wide variety of molecular and cellular damage over time which persistently deteriorate physiological functions, a process known as biological aging[1]. Since the late 21st century, advancement of healthcare and technological innovations have given rise to higher life expectancy with a comfortable lifestyle[2]. Approximately 12.7% of the world population are aged i.e., 60 years or older, which is estimated to more than double to 2.1 billion by 2050[3, 4]. “Greying” of United States is particularly interesting as the aged population over 65 years are expected to outnumber the children under the age 5 in the next decade changing the population pyramid into a slow growing demography[5, 6]. US Census bureau predicted that the aged population over 65 years will become 23.4% of the total population compared to 19.8% of children under 18 years (Fig 1.1)[7], which is unprecedented. The National Institute of Aging has invested significant resources in elevating the quality of life among the elderly to maintain their physical, mental, and social well-being[8]. “Healthy aging” has been trending among the elderly in the high economy countries which consists of consuming healthy food and engaging in regular exercise, and social activities for mental well-being[2, 9, 10]. However, the majority of the older population suffers from frailty, and neurodegenerative and chronic diseases, thus increasing the financial, social and public health burden that makes aging a global issue[11].

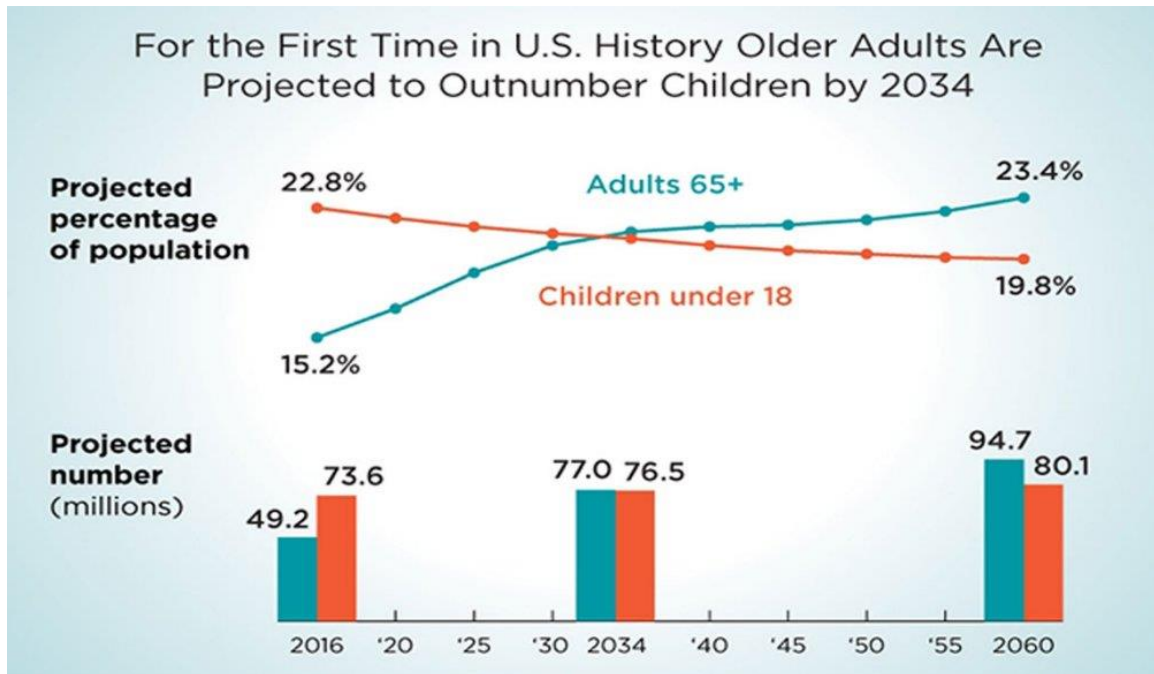


Fig. 1.1 Projected population growth in USA. Taken from National Population Projection 2017 by US Census Bureau.

1.1.2 Epidemiology and related diseases

Aging research has flourished over the last 50 years [12-16]. The aged population is currently divided into 3 generations which span over three decades. The “young old” are in their 60s and early 70s who are healthy and often working actively. The “old”, who are in their 70s and 80s, show the onset of frailty and suffer from chronic illness. The “old-old” are representative of the sick, disabled, dependent and nearing death[17]. Age-related diseases result from systemic failure of bodily functions which increase morbidity and mortality. Examples of age-associated pathologies include neurodegenerative Alzheimer’s and senile dementia; metabolic syndromes such as type 2 diabetes and insulin resistance; cardiovascular complications such as coronary artery diseases, hypertension, stroke; chronic inflammation mediated diseases such as osteoarthritis, frailty, and cancer. Tremendous advancements in biomedical research over the past century led to basic understanding of biological mechanisms of aging. However, the recent focus of research has been shifted to adapting translational interventions for deleterious cellular and molecular mechanisms to prevent unwanted pathophysiology[18]. Geriatric epidemiology

even recognizes the “life course approach”[19] which helps to identify risk factors at any stages of life that eventually develop into age-associated diseases[20]. Over the years many age-related diseases have been recapitulated in C57BL/6 mice which is arguably the ideal model to study aging as human age equivalency is most well-characterized in these mice (Fig 1.2)[21]

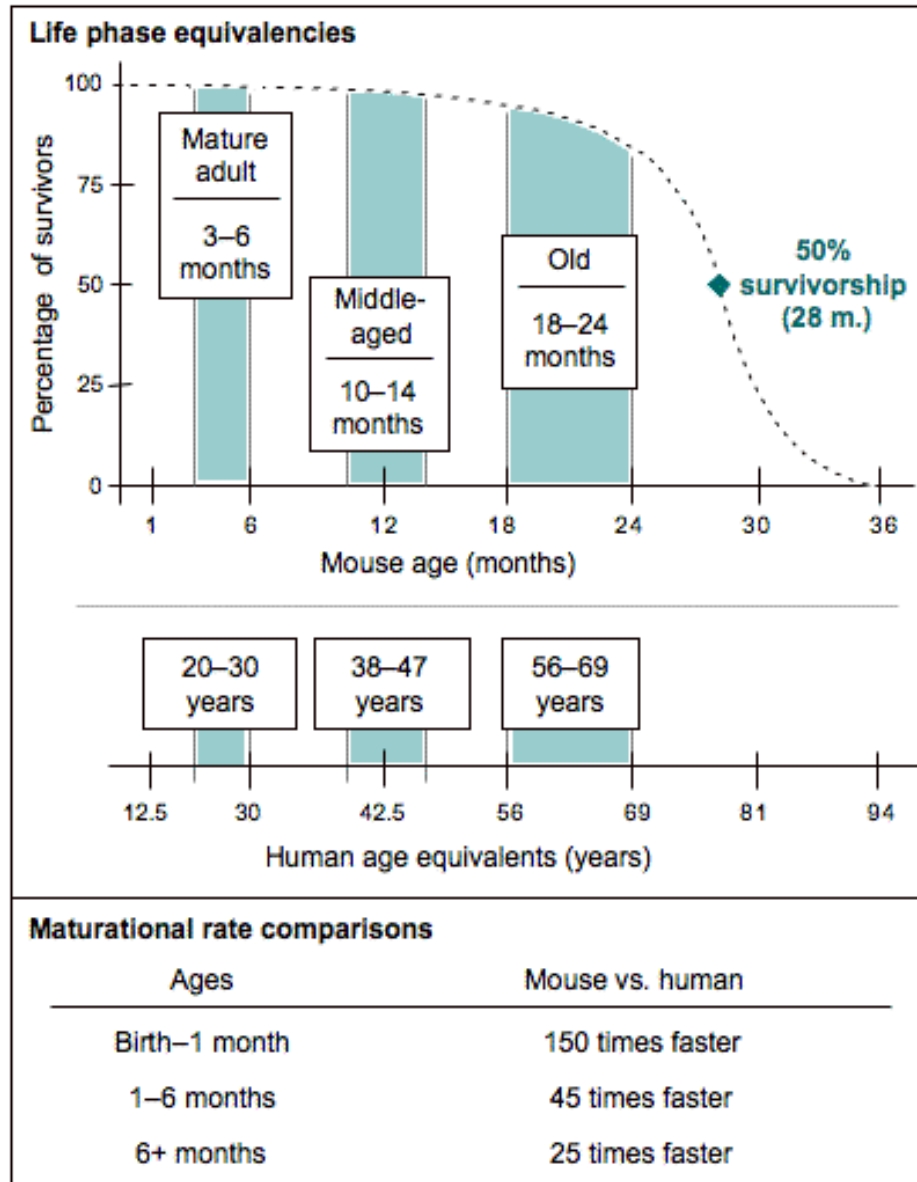


Fig. 1.2 Lifespan in C57BL/6J mice in comparison to human life. Taken from Flurkey, Curren, and Harrison, *The Mouse in Biomedical Research*, 2007.

1.2 Adipose tissue in aging

1.2.1 Adipose tissue dysfunction with aging

Adipose tissue gained a lot of interest in the past two decades as it plays a major role in biological aging besides acting as an active endocrine organ and energy reservoir. While subcutaneous fat primarily helps to insulate the body from cold, provides protection to tissues and organs as well as plays a major role in obesity-related insulin resistance[22], visceral fat tissue contributes to metabolic and chronic inflammatory disorders which are carried out by the release of cytokines, chemokines and adipokines[23]. Adipose depot redistribution with aging from subcutaneous depot to visceral depot represents the onset of chronic sterile inflammation[24]. Age-associated adipose tissue dysfunction results from a combination of adipose redistribution, chronic inflammation within adipose tissue, decline in progenitor cell function, preadipocytes and immune cell senescence which give rise to senescence associated secretory phenotype (SASP), ectopic lipid accumulation, changes in adipose derived hormones, reduced mi-RNA processing, and decrease in brown and beige fat function

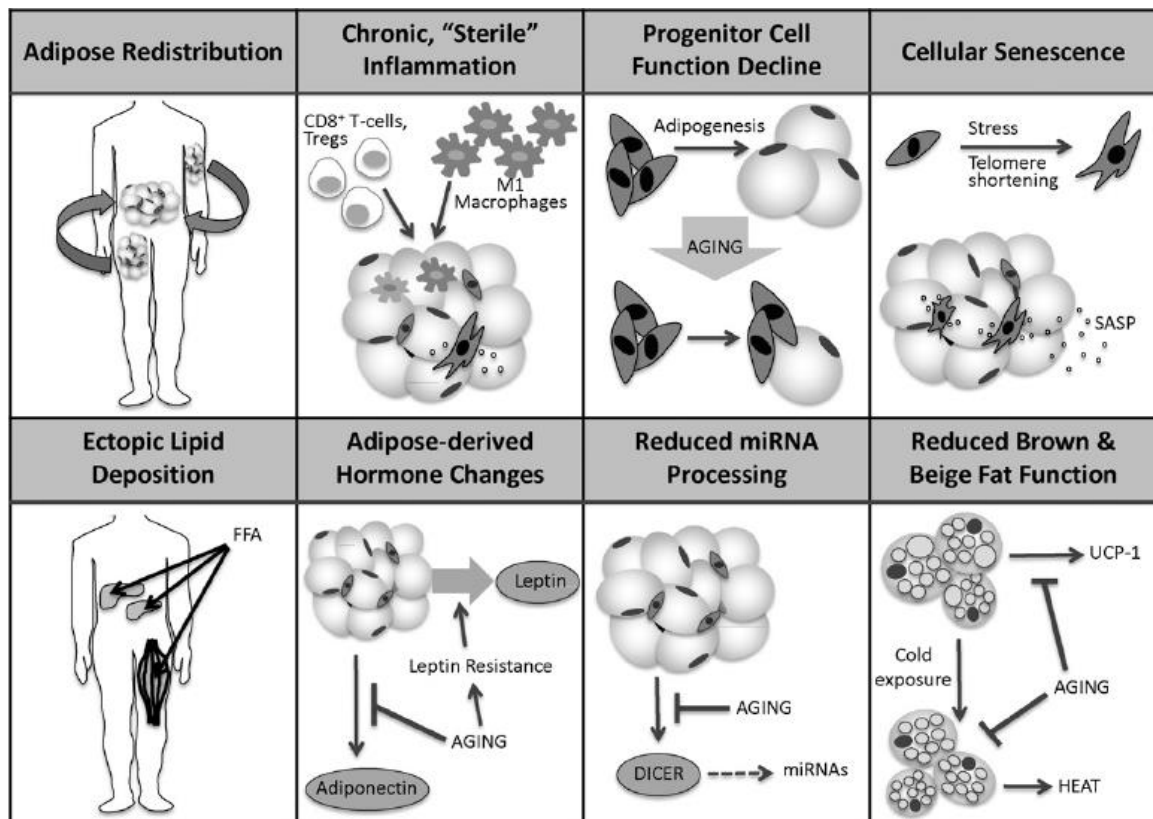


Fig. 1.3 Age-associated adipose tissue dysfunction. Taken from Palmer et al. 2016.

fat function (Fig 1.3)[25]. These changes collectively impart a profound impact on insulin sensitivity and metabolic and cardiovascular health[25-30].

1.2.2 Adipose tissue as a source of inflammaging

Chronic, systemic, sterile, low-grade inflammation, termed inflammaging[31], has revolutionized the conceptual understanding of age-associated pathophysiology and its underlying mechanisms[32]. Morphological and functional changes due to adipose tissue dysfunction are considered a major contributor of inflammaging. Increased oxidative stress in adipose tissue with age leads to DNA damage which triggers senescence via p53/ p21 signaling pathways[33]. Senescent preadipocytes accumulate in adipose tissue as clearance of these cells are compromised with aging. The elevated levels of proinflammatory cytokines and chemokines released from the senescent cells known as SASP serves as an inflammaging inducer[26, 34]. In fact, adipose tissue has been used as a target of therapeutic interventions to reduce the burden of inflammaging associated diseases by using calorie restriction and senolytic treatments. Other than senescence, hypoxia, fibrosis, inflammasome activation[33], exogenous and endogenous fatty acids, various molecular mechanisms such as JAK/STAT, Wnt/ β -catenin, PI3K/AKT, NF- κ B and MAPK signaling pathways have been linked to adipose tissue mediated inflammaging[26]. Adipose resident macrophages[33, 35], neutrophils, eosinophils, B cells and conventional T cells have been well characterized as contributors of inflammaging[33, 36]. However, no studies have reported adipose specific $\gamma\delta$ T cells in the context of aging.

1.3 $\gamma\delta$ T cells

$\gamma\delta$ T cells are the prototype of ‘unconventional’ T cells and represent a unique subset that possess characteristics of both innate and adaptive immune system[37]. The T cell receptor (TCR) of $\gamma\delta$ T cells consist of one of the gammas and one of the delta chains which undergo V(D)J recombination of 7 gamma and 6 delta chains giving rise to different subpopulations of $\gamma\delta$ T cells[38]. $\gamma\delta$ T cells have been widely studied in the context of pathogen infections[39-42] and autoimmune diseases such as rheumatoid arthritis, ankylosing spondylitis, and systemic lupus erythematosus[43, 44]. However, preferential enrichment of $\gamma\delta$ T cells in peripheral tissues rather than lymphoid organs provide important clues to its physiological role in tissue homeostasis[45, 46]. $\gamma\delta$ T cells also demonstrate developmental preprogramming of effector functions in thymus with respect to specific cytokine (i.e., IL-17A or IFN γ) production[46]. Recent studies highlighted roles of $\gamma\delta$ T cells in epithelial and mucosal tissue repair[47, 48], immune surveillance and wound healing[46], cancer immunotherapy[49], thermogenesis[45] and inflammation[50, 51].

1.3.1 Age-associated alterations of $\gamma\delta$ T cells in circulation

Several clinical studies showed age-associated decline in $\gamma\delta$ T populations, both in number and frequency in circulation in humans indicating a selective depletion of these cells which can be potentially linked to increased susceptibility to infectious diseases and overall vulnerability with aging[52-58]. The gender as well affect both number of total $\gamma\delta$ T cells and specifically V δ 2⁺ T cells, which are significantly higher in male compared to female[57]. The functionality of aging V δ 2⁺ $\gamma\delta$ T cells in circulation is sustained via co-stimulatory molecules, as these cells showed high cytokine production in response to PMA/ionomycin stimulation compared to age-matched $\alpha\beta$ T cells, exemplifying a functional dichotomy in circulating lymphocytes with aging[59]. Due to the presence of an inflamed environment in the elderly, $\gamma\delta$ T cells remain in a basal-activated state, as shown by the activation marker CD69. These cells also appear to be primarily TNF α producing[54, 55]. Age-associated reduction in $\gamma\delta$ T cell numbers is associated with two schools of thoughts. First, a significant decrease in V δ 2⁺ subpopulation in the aged, which

further showed proliferative defect by reduced expansion *in vitro*[56, 57, 59, 60]. Second, higher sensitivity to apoptosis in $\gamma\delta$ T cells induced by both CD95, an apoptotic related marker and TNF α [60]. Overall, the decrease in $\gamma\delta$ T cell numbers is likely due to a combination of both mechanisms. Several studies consistently showed that CD27⁺V δ 2⁺ $\gamma\delta$ T cells are decreased with age[58] due to higher activation-induced cell death and low proliferative capacity in V δ 2⁺ T cells via mitogen-induced downregulation of Bcl-2 protein expression compared to V δ 1⁺ T cells[57]. On the other hand, V δ 1⁺ subpopulations proportionately increase in the aged circulation without any significant difference in the *in vitro* expansion compared to young, suggesting an immunosenescent-specific subpopulation of $\gamma\delta$ T cells in the elderly[56]. Next-generation sequencing study additionally corroborated the age-associated shift of V γ and V δ gene usage in the memory $\gamma\delta$ T cell subset in humans, from V γ 9/V δ 2 dominance in young to V γ 2/V δ 1 dominance in elderly[61]. Although decreased frequency and number of V δ 2⁺ $\gamma\delta$ T cells in circulation of elderly has been repeatedly reported, Mazzocchi et. al. showed that elderly males (age range 67-69 years) not only showed an increase in $\gamma\delta$ -TCR expressing cells in the circulation but also showed a clear circadian rhythmicity with an increase during noon compared to young middle-aged males[62]. Aging also alters the functionality of human peripheral $\gamma\delta$ T cells as increased TNF α production was reported in a study[56]. How age impacts on $\gamma\delta$ T cell functionality and interferes with cellular crosstalk among immune cell populations leading inflammaging requires further exploration.

1.3.2 Aging-associated alterations of $\gamma\delta$ T cells in other tissues

A few studies showed an age-associated increase of IL-17A producing $\gamma\delta$ T cells in tissues other than VAT. While V γ 6⁺ $\gamma\delta$ T cells increased by aging (compared between young (3mo) and aged (>21mo) in the peripheral lymph nodes (pLNs) of mice, V γ 1 and V γ 4 populations showed an age-associated decrease. Although the composition of $\gamma\delta$ T cell subsets in the pLN pool changes with age, no age-associated changes were observed in function or on the transcriptomic profile. Furthermore, selective activation of pLN-resident V γ 6⁺ $\gamma\delta$ T cells made them pro-tumorigenic in old mice and migrate into tumor to enhance tumor growth, in an experimental lung cancer model[63, 64]. Another study showed that

lung resident IL-17A-producing $\gamma\delta$ T cells increase in the aged mice (20-24mo) with altered gene expressions that changes their immune functions to play anti-tumor roles in lung melanoma, substantiating the use of $\gamma\delta$ T cells in anti-tumor immunotherapy in the elderly population[65]. $\gamma\delta$ T cells have shown dichotomic role in cancer progression in the literature, and whether aging induces the protective or tumorigenic potential of these unique cells requires further study.

1.3.3 Abundance and distribution of $\gamma\delta$ T cells in adipose tissue

$\gamma\delta$ T cells are reportedly enriched in adipose tissues compared to other peripheral organs in young mice. The visceral white adipose tissues (VAT) consisting of perigonadal (epididymal and parametrial), omental, and perirenal depots have the highest abundance of $\gamma\delta$ T cells, ranging from about 5-25% of total CD3⁺ lymphocytes, while subcutaneous white adipose tissue has the least (less than 7%)[45, 50]. Subcutaneous brown adipose tissue (BAT), on the other hand, has a similar abundance of $\gamma\delta$ T cells to VAT[45]. In contrast to adipose tissues, peripheral organs have relatively scarce $\gamma\delta$ T populations (i.e., lung showed a range from ~2-4%, liver has up to 10% and spleen has the least (less than 2%), which is similar to the circulation [45, 51]. Whole-mount tissue imaging revealed that $\gamma\delta$ T cells are dispersed throughout visceral adipose tissue and not present within specific neural or lymphoid niches[66]. Importantly, Kohlgruber et al. also confirmed the presence of $\gamma\delta$ T cells in the VAT of humans[45].

1.3.4 Subpopulations studied in mouse adipose tissue

$\gamma\delta$ T cells are generally divided into two functionally distinct subtypes based on production of either IL-17A or IFN γ [67–69]. The programming of these cells is decided in the thymus during embryonic development and surface markers are one of the key factors used to distinguish these populations. IFN γ -producing $\gamma\delta$ T cells are CD27⁺, while IL-17 producing $\gamma\delta$ T cells are CD27^{neg}. CD27, a costimulatory molecule of the tumor necrotic factor receptor superfamily, not only marks these populations, but acts as a regulator of their differentiation during thymic development and imprinting[70]. Within the adipose

tissue, both CD27⁺ and CD27^{neg} $\gamma\delta$ T cells have been identified[45, 50, 66]. Kohlgruber et al. performed the most comprehensive phenotyping of adipose tissue $\gamma\delta$ T cells to date and characterized two major functionally and phenotypically distinct populations in young C57BL/6 mice (1-7mo). The CD27^{neg} population was confirmed to be IL-17 producing and further distinguished from the CD27⁺ population by high expression of CD3 and intracellular expression of the transcription factor PLZF which regulates a series of biological processes including development, differentiation, and function of innate immune cells[71]. Thus, based on the present knowledge, $\gamma\delta$ T cells in adipose tissue can be characterized and functionally demarcated as CD3^{hi}CD27^{neg}PLZF^{pos} IL-17-producing innate-like $\gamma\delta$ T cells and CD3^{lo}CD27⁺PLZF^{neg} IFN γ -producing $\gamma\delta$ T cells[45]. In addition, $\gamma\delta$ T cells in the adipose tissue are almost exclusively negative for CD4 and CD8[72] which often serve to classify conventional $\alpha\beta$ T cells.

With respect to γ/δ -TCR profiling, Mehta et al. detected the expression of V γ 1, V γ 2, V γ 4, V γ 6 and V δ 1, V δ 3, V δ 4 (Heilig & Tonegawa nomenclature[73]) genes in VAT of young mice by PCR[50]. Flow cytometric analyses confirmed that VAT of young mice is primarily composed of V γ 6⁺ cells, which correspond to the more abundant CD3 ϵ ^{hi}CD27^{neg}PLZF^{pos} IL-17A-producing population, while the CD3 ϵ ^{lo}CD27⁺ PLZF^{neg} IFN- γ -producing population appears to contain both V γ 1⁺ and V γ 4⁺ cells[45].

1.3.5 Adipose tissue-residency in mouse model

Recent *in vivo* studies demonstrated that $\gamma\delta$ T cells are a self-sustaining adipose tissue-resident population using parabiotic pairs of congenic CD45.1 and CD45.2 mice, in which more than 90% of the VAT $\gamma\delta$ T cells did not passively migrate between animals[45, 66]. Interestingly, VAT $\gamma\delta$ T cells are uniquely tissue-resident while $\gamma\delta$ T cells in other tissues including spleen, liver, lungs and bone marrow are reconstituted from the circulation[45, 66]. CD8⁺ T_{conv} cells are likewise reconstituted from the circulating population in all tissues including VAT[45]. Phenotypic characterization of VAT $\gamma\delta$ T cells has been reported using surface expression of CD69, a type II C lectin receptor important for T_{RM} differentiation and considered as the signature phenotype of tissue-resident

memory cells (T_{RM})[74]. Flow cytometry studies demonstrate that the majority of VAT $\gamma\delta$ T cells are $CD69^+$ showing the characteristic T_{RM} phenotype[51]. NanoString analysis confirmed that VAT $\gamma\delta$ T cells, have distinct transcriptomes compared to circulating $\gamma\delta$ T cells indicating the presence of a functionally distinct resident $\gamma\delta$ T cell population in VAT[51].

1.3.6 Effect of obesity on adipose-resident $\gamma\delta$ T cells

Since adipose tissue possesses remarkable plasticity, adapting to physiological changes, studies using high-fat diet-fed animals are often used to investigate obesity-induced alterations. Several studies reported an effect of obesity on adipose-resident $\gamma\delta$ T cells in murine model[50, 51, 72, 75]. Twelve weeks of high fat diet (HFD) feeding to 1mo old mice caused an increase in $\gamma\delta$ T cell percentage in inguinal fat depots which was proportional to adiposity[75]. Eighteen weeks of HFD feeding to 1.5mo old mice caused an increase in IL-17A producing $\gamma\delta$ T cells per gram of inguinal fat [72]. Two independent studies with short term (5weeks) milk fat diet [50] and long term (young mice were fed for 20 weeks starting weaning and aged mice for 12 months starting at 11 months of age) high fat diet [51] similarly reported an increase of $\gamma\delta$ T cell in epididymal fat depot, which was proportional to the increase of fat mass. Collectively, these studies suggest that diet-induced obesity increase $\gamma\delta$ T cell population in adipose tissue. The molecular mechanisms of the adipose specific increase in $\gamma\delta$ T cells in obesity require further research.

1.3.7 Regulatory roles of $\gamma\delta$ T cells in adipose tissue biology

1.3.7.1 $\gamma\delta$ T cells are major producers of IL-17 in adipose tissue

IL-17A is a pro-inflammatory cytokine that has been associated with inducing inflammatory responses in several metabolic diseases, such as obesity and T2 diabetes as well as infectious and autoimmune diseases[39-42, 76, 77]). IL-17A, the founding member of a family of six cytokines (IL-17A through IL-17F), signals through ubiquitously present multimeric receptor complexes composed of IL-17RA and IL-17RC[78]. IL-17A-producing Th17 cells, a subtype of activated $CD4^+$ T cells, have gained significant interest

recently as they show selective expansion and elevated IL-17A levels in the context of obesity-related inflammatory conditions[78, 79]. Recent studies indicated that IL-17A exerts several regulatory roles in adipose tissue. In adipose tissue, $\gamma\delta$ T cells are reportedly the primary producers of IL17A[45, 72, 80]. which raises the premise that $\gamma\delta$ T cells may be involved in regulatory functions via IL-17A.

1.3.7.2 $\gamma\delta$ T cells as a metabolic regulator in adipose tissue

A few studies reported the role of $\gamma\delta$ T cells during obesity in regulating the metabolic phenotype. One study with TCR δ KO mice showed $\gamma\delta$ T cells are likely to contribute to hyperinsulinemia and impaired insulin sensitivity[51]. Moreover, $\gamma\delta$ T cells promote inflammation and thereby further contribute to insulin resistance in metabolically active organs such as liver and skeletal muscles[50]. Another study using aged TCR δ KO mice showed that lack of $\gamma\delta$ T cells is associated with improved metabolic fitness in terms of higher respiratory exchange ratio and increased energy expenditure[51].

Additionally, IL-17A, which is likely produced by $\gamma\delta$ T cells has been shown to modulate metabolic processes in adipose tissue. IL-17A inhibits glucose uptake by cultured preadipocytes. Lack of IL-17 in knock-out model showed enhanced glucose tolerance and insulin sensitivity, and greater fasting glucose levels without obesity, indicating that IL-17 contributes to systemic glucose homeostasis. Next, several studies have found that IL-17A and IL-17F inhibit adipogenesis[72, 78, 81] and in human mesenchymal stem cells (MSC), IL-17 impairs adipocyte differentiation[78]. IL-17A promotes obesity via phosphorylation of PPAR γ in adipocytes[82]. IL-17 receptor knock-out mice showed rapid weight gain and metabolic phenotypes such as reduced energy expenditure and reduced oxygen consumption, impaired glucose tolerance, and increased lipid accumulation in brown adipose tissue[80].

1.3.7.3 Thermogenic role of $\gamma\delta$ T cells in adipose tissue

Susceptibility to diet-induced obesity and glucose tolerance are interconnected with defective adipose thermogenesis[80]. Indeed, a few studies noted the role of $\gamma\delta$ T cells in

thermogenesis which is likely mediated via IL-17A. Kohlgruber et al. shared their discovery that innate-like IL-17A-producing $V\gamma 6^+$ $\gamma\delta$ T cells participate in body temperature homeostasis via crosstalk with adipose stromal cells, which produce IL-33 and exert downstream effects on Treg cell accumulation[45, 83]. Thermogenic adipose tissue is stimulated by sympathetic nervous system to produce heat via adaptive thermogenesis. $V\gamma 6^+$ $\gamma\delta$ T cells, in particular, promote adaptive thermogenesis while maintaining whole-body energy homeostasis. Recent findings demonstrate $\gamma\delta$ T/ IL-17F/IL-17RC/TGF β 1 axis is critical for sympathetic innervation in multiple tissues, such as adipose tissue, salivary glands and lungs, via $\gamma\delta$ T derived IL-17F mediated IL-17RC signaling pathway. Ablation of adipose specific IL-17RC reduces TGF β 1 expression in parenchymal cells in brown adipose tissue, impairing various physiological functions, while restoring TGF β 1 expression rescues local sympathetic innervation. Adipocyte specific IL-17RCKO mice showed impaired cold tolerance and higher lipid content, confirming the importance of IL-17RC signaling in UCP1-positive thermogenic adipocytes. Adipocyte IL-17RC helps with oxygen expenditure which helps in not gaining weight. Lack of IL-17RC led to impaired glucose tolerance, aggravated liver steatosis, and enlarged inguinal and VAT on high fat diet. Impaired thermogenesis and decreased cold tolerance in IL-17RCKO mice is due to lower oxygen consumption, which results from inefficient beta3adrenergic receptor activation. IL-17RC helps in functional sympathetic innervation as IL-17RCKO shows reduced growth and maturation of sympathetic axons in BAT, possibly due to deficiency in neurotrophic factors. This study uncovered an immune-regulatory mechanism of sympathetic innervation in multiple tissues including BAT[80]. It will be interesting to see whether the $\gamma\delta$ T/ IL-17F/IL-17RC/TGF β 1 axis plays the same role in humans.

1.3.8 IL-17 producing $\gamma\delta$ T cells in other tissues with chronic inflammation

$\gamma\delta$ T cells are the primary source of IL-17A in other tissues and other chronic inflammatory diseases. In the progression of age-related macular degeneration (AMD), $\gamma\delta$ T cells are the primary infiltrated lymphocytes, which act as a major source of IL-17 as one of the pro-inflammatory signals during degeneration of the retinal pigment epithelium (RPE)[84]. In skin inflammation, IL-23-responsive dermal $\gamma\delta$ T cells are the major IL-17

producers in the skin and a potential target for the treatment of psoriasis[47]. Furthermore, adipose tissue and skin inflammations are linked via $\gamma\delta$ T cells as adiponectin, an adipose tissue derived hormone, directly acts on IL-17A producing dermal $V\gamma 4^+$ $\gamma\delta$ T cells to suppress IL-17A synthesis via receptor AdipoR1[85].

1.3.9 Goal of this dissertation

While most of the previous studies have focused on adipose tissue specific $\gamma\delta$ T cells in the context of high-fat diet induced obesity, no studies described changes in adipose specific $\gamma\delta$ T cells in the context of aging. This dissertation characterizes the age-associated $\gamma\delta$ T cell accumulation in VAT and studies mechanisms of their accumulation. In aim 1, I determined whether $\gamma\delta$ T cells accumulate in VAT with aging to define their role in inflammaging. My studies focus on quantifying $\gamma\delta$ T cells in mice and humans across the lifespan in various tissues, including VAT, peripheral lymph node (LN), and skin along with other tissues studied before. Previous studies provide the rationale to study the role of $\gamma\delta$ T cells in visceral adipose tissue inflammation in the context of aging as aging is now considered a disease for which chronic inflammation is a common denominator. My study also characterizes VAT $\gamma\delta$ T cells based on IL-17A and IFN γ production in young and aged mice. The PCR study further demonstrates the presence of different subpopulations in young and aged VAT and compares whether there are any age-associated changes in gene expressions.

In aim 2, I explored the physiological mechanisms of $\gamma\delta$ T cell accumulation in VAT. While $\gamma\delta$ T cells have been shown to be tissue-resident, it is possible that circulating $\gamma\delta$ T cells may infiltrate into VAT and then gain tissue-residency. Moreover, VAT of aged mice is known to produce increased levels of inflammatory cytokines and chemokines which may facilitate $\gamma\delta$ T cells recruitment from the periphery. My parabiosis study explores this possibility. Additionally, the molecular mechanisms of maintenance of the VAT resident $\gamma\delta$ T cell population are still obscure. Since the number of T cells are tightly regulated within a tissue to maintain homeostasis, I evaluated two potential driving forces. My studies explore the proliferation and apoptosis status of VAT $\gamma\delta$ T cell while comparing it with T_{conv} cells and lymphocytes in other peripheral organs. Collectively, my research

will aid in better understanding the deleterious effects of adipose tissue immune system on aging.

Chapter 2 MATERIALS AND METHODS

2.1 Animals and husbandry

Male and female C57BL/6 mice were obtained from The Jackson Laboratory (Stock 664) or the National Institute on Aging. T cell receptor delta chain knockout mice (TCR δ KO, B6.129P2-Tcrdtm1Mom/J, Stock 2120) were obtained from The Jackson Lab and bred in-house. Different age groups of mice were utilized, and age is specified for each experiment in figure legends. Mice were housed in pressurized intraventilated cages and maintained in an environment under controlled temperature (21–23 °C), humidity (30–70%), and lighting (14 h/10 h, light/dark) with free access to drinking water and chow (Teklad Global No. 2918). All procedures were approved by the Institutional Animal Care and Use Committee at the University of Kentucky and performed in accord with the National Institutes of Health guidelines for ethical animal treatment.

2.2 Parabiosis

Isochronic parabiosis pairs were constructed using age- and sex- matched WT and TCR δ KO male and female mice (male to male or female to female). Aged male mice were acclimated for pairing for 2 weeks using an in-house developed clear plexiglass barrier. After removal of the barrier, pairs were cohoused for an additional 2 weeks before surgery to assure compatibility (Fig 2.1). Aged female mice were cohoused for at least 2 weeks prior to surgery. Surgeries were performed following the protocol described by Paniz Kamran et al.[86]. Briefly, C57BL/6 and TCR δ KO mice were placed one-at-a-time into an induction chamber and anesthetized with isoflurane, 4-5%, provided by a precision vaporizer. The mouse was transferred to a prep area where it received ophthalmic ointment, Meloxicam-5 mg/kg SQ, Buprenorphine SR-LAB (Zoopharm)-1mg/kg SQ, and enrofloxacin-10mg/kg SQ. The appropriate side of the mouse was then clipped of fur and the mouse was then transferred to a heated surgical platform and placed on one of two separate side-by-side nose cones and anesthesia was maintained at 1.5-2% isoflurane. The process was repeated for the second mouse. With the mice positioned in lateral recumbency, back-to-back, the exposed side of each mouse was aseptically prepped using

betadine followed by isopropyl alcohol for a total of three cycles. A sterile surgical drape was then placed over the mice, with an opening to expose only the operation area. Using sharp scissors, an incision was made through the skin of each mouse extending from 5mm above the elbow to 5mm below the knee joint. The skin adjoining the incision was gently separated from underlying tissue to create a 5mm flap surrounding the incision. The exposed olecranon of each mouse was joined tightly using 3-0 Prolene suture secured with a double surgical knot. The knee joints were joined in a similar manner. The skin along the ventral side of the incision was then approximated and joined with 5-0 Vicryl suture in a continuous pattern beginning and ending with a secure knot. The mice were placed in the prone position where the dorsal side of the incision was approximated and joined in the same manner. The entire ventral and dorsal suture lines were inspected for integrity and continuity, with special attention given to the areas where they were joined at the front and hind limbs. The mice were transferred to a warmed clean cage and were each administered 1ml of warm sterile physiological saline SQ. The mice were monitored until they recovered from anesthesia and were ambulatory. The mice were then returned to the vivarium, where they were given moistened food on the floor of the cage and a water bottle with an extended sipper tube for access to water. The mice were monitored twice daily for the first 3 days post-op, and then once daily for the next week for weight loss, normal activity, inquisitiveness, condition of hair coat, eating, drinking, hydration, appearance of eyes, and ambulation. The surgical incision sites were observed for complications (e.g., red edges, swelling, exudates, or displaced sutures). The mice were given additional doses of meloxicam at 24- and 48-hours post-op. Remaining exposed sutures were removed at 14 days post-op. Parabiotic pairs were euthanized 4 weeks later to harvest blood and tissues for flow cytometry analysis.

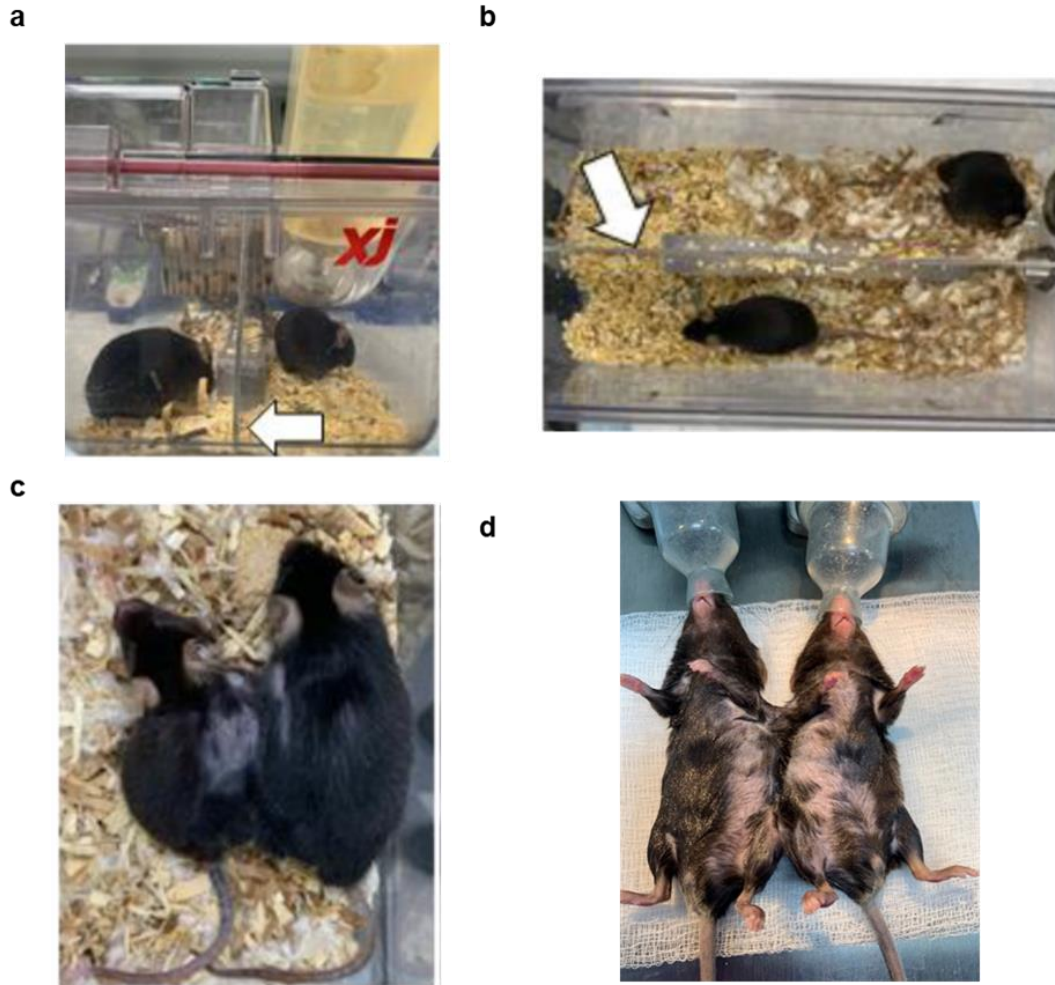


Fig. 2.1 In-house developed clear plexiglass barrier for parabiosis pair acclimatization. a) front view b) top view c) parabiotic pair d) parabiosis pair before euthanasia.

2.3 Murine sample collection

Mice were deeply anesthetized by isoflurane inhalation, laparotomy performed, and blood collected from the inferior vena cava (IVC) by syringe needle with 10% volume of 0.1 M sodium citrate. Blood was immediately centrifuged ($2500 \times g$, 4°C , 15min) to obtain plasma which was stored at -80°C . Subsequently, the IVC was cut, and the entire vasculature was perfused with 30 mL physiological saline through the cardiac ventricles to eliminate circulating cells. For protein or gene expression analyses, tissues were carefully dissected, flash frozen in liquid nitrogen, and stored at -80°C . For flow cytometry studies, whole blood was collected into tubes and fresh tissues (visceral gonadal fat pads (VAT),

subcutaneous inguinal fat pads (SAT), spleen, liver (a portion of left lateral lobe), lymph nodes (inguinal and brachial) and dorsal portion of skin) were dissected after perfusion and kept on ice until processing.

2.4 Human sample acquisition

Fresh visceral adipose tissue specimens (mesenteric fat, perirenal fat, and omentum) were obtained from patients undergoing surgery at the University of Kentucky Medical Center. Sample collection was facilitated in a deidentified manner through the University of Kentucky Center for Clinical and Translational Science and approved by the University of Kentucky Institutional Review Board (Study #44734). Specimens were retrieved from the operating room and kept on ice until processing.

2.5 Tissue processing for single-cell suspensions

2.5.1 Adipose tissue

VAT and SAT were dissected from mice, weighed, and minced with scissors. Minced tissues were transferred to ice cold digestion buffer (0.5% BSA in HBSS with $\text{Ca}^{2+}\text{Mg}^{2+}$) with collagenase (1 mg/mL) and incubated on a tube rocker at 37°C for 50 min with vigorous shaking by hand every 10 min. Prior to the final 10 min, 10mM EDTA was added. Digested cells were passed through a 200- μm strainer and centrifuged ($500 \times g$, 10 min, 4°C) to separate mature adipocytes from stromal vascular fraction (SVF) cells. The top adipocyte layer was aspirated and discarded. The cell pellet containing SVF cells was treated with 3mL red blood cell (RBC) lysis buffer for 5 min, passed through a 70- μm strainer and centrifugation repeated. SVF cells were resuspended in an appropriate volume of digestion buffer for subsequent processing/analysis. Human VAT was processed in a similar fashion.

2.5.2 Blood

RBC lysis buffer (20mL) was added to whole blood (approx. 1-mL per mouse) in a 50 mL conical tube. Cell suspensions were incubated on ice for 5 min with occasional

shaking, passed through a 70 μ m strainer, washed, and centrifuged. RBC lysis was repeated, followed by another round of centrifugation. White blood cells (WBC) were resuspended in an appropriate volume of digestion buffer for subsequent processing/analysis.

2.5.3 Liver, Spleen and Lymph node

Tissues were dissected from mice, weighed (liver and spleen) mashed with a 5 mL syringe plunger through a 100 μ m cell strainer, washed with 20 mL digestion buffer and centrifuged at 500 \times g for 10 min. RBC lysis was performed for liver and spleen cells, followed by passing through a 70- μ m strainer. After a second round of centrifugation, cells were resuspended in digestion buffer for subsequent processing/analysis.

2.5.4 Skin

A 3 \times 3 cm area of skin was shaved on the dorsal aspect of the mouse, Nair was applied for 3 min, and the skin was washed thoroughly with running water. Subsequently, a 2 \times 2 cm piece of skin was excised and scraped of excess adipose/connective tissue. Skin was minced in a 35-mm Petri dish containing 2 mL of digestion cocktail (300 μ g/mL Liberase, 50 U/mL DNase I in 5% FBS-RPMI) and incubated at 37 $^{\circ}$ C for 90 min with agitation every 30 min. Digested skin was then mashed through a 100 μ m cell strainer and washed. Samples were centrifuged at 350 \times g for 5 min, the supernatant aspirated, and the pellet treated with RBC lysis buffer. Cells were passed through a 70 μ m cell strainer, another round of centrifugation performed, and the resulting pellet resuspended in an appropriate volume of digestion buffer.

2.6 Flow cytometry

Single cell suspensions in 250 μ L of Dulbecco's Phosphate Buffered Saline (DPBS, gibco 14190-144) were stained with Fixable Viability Dye eFluor 450 (eBioscience 65-0843-14) according to the manufacturer's protocol, and Fc receptor blocking was performed using TruStain FcX (Biolegend 156603) for 10 min on ice in 250 μ L of buffer containing DPBS with 1mM EDTA, 25mM HEPES, 1% FBS. Cells were further incubated for 30 min at 4 $^{\circ}$ C in the dark with respective antibodies for cell surface staining; antibodies

used are described in Table 2.1 and cell surface identifiers are described in Table 2.2. For cell surface analyses only, stained cells were fixed with 4% paraformaldehyde (Biolegend 420801) for 20 min. For human samples, the same procedure was performed with Human TruStain FcX™ (BioLegend 422302), and antibodies as noted in Table 1. For intracellular staining with IL-17A, IFN γ and IL-6, SVF cells were first incubated *in vitro* with GolgiPlug protein transport inhibitor (BD 555029) in 5% FBS-RPMI for 4 h at 5% CO₂, 37 °C. For intracellular staining with Ki67, SVF cells were permeabilized following surface staining according to standard protocol (Invitrogen 00-5523-00). Following cell surface staining and fixation, cells were permeabilized according to standard protocol (BD 51-2091KZ) and intracellular staining was performed using antibodies for IFN γ , IL-17A, IL-6, Ki67 and respective isotype controls (see Table 2.1). For detection of IFN γ and IL-17A, cells were also treated with Cell Stimulation Cocktail (Invitrogen 00-4970-93) during protein transport inhibition. For intracellular staining of IL-6, cell stimulation was not performed. Murine and human cells were analyzed on a FACSymphony A3 Cell Analyzer (BD, San Jose, CA). Analysis of flow cytometry data was performed using the FlowJo data analysis software (FlowJo, LLC, Ashland, OR).

Table 2.1 Antibodies used for the Flow cytometry studies.

Antigen	Conjugate	Manufacturer	Identifier
Mouse			
CD45	APC/Cyanine7 Brilliant Violet 510	BioLegend BioLegend	103116 103138
CD3	FITC PE/Cyanine7	BioLegend BioLegend	100204 100219
TCR γ/δ	APC-Vio 770 PerCP-Vio 700 PerCP/Cy5.5	Miltenyi Biotec Miltenyi Biotec BioLegend	130-126-042 130-117-665 118118
CD11b	APC	BioLegend	101212
Ly6G	PerCP/Cyanine5.5	BioLegend	127616
CD4	PE/Cyanine7	BioLegend	100422
CD8 α	Brilliant Violet 711	BD Biosciences	563046
CD11c	APC/Cyanine7	BioLegend	117324
CD206	Brilliant Violet 711	BioLegend	141727
CD34	Brilliant Violet 421	BioLegend	152207
CD31	PE/Cyanine7	BioLegend	102417
IL-6	PE	BioLegend	504503
IgG1, κ (Isotype for IL-6)	PE	BioLegend	400408
CD44	PE	BioLegend	103008
CD62L	Brilliant Violet 421	BioLegend	104436
CD69	PE-CF594	BD Biosciences	562455
IL-17A	Brilliant Violet 605	BioLegend	506927
IgG1, κ (Isotype for IL-17A)	Brilliant Violet 605	BioLegend	400433
IFN- γ	Alexa Fluor® 700	BioLegend	505823
IgG1, κ (Isotype for IFN- γ)	Alexa Fluor® 700	BioLegend	400420
Ki-67	FITC	BioLegend	652410
IgG _{2a} , κ (Isotype for Ki-67)	FITC	BD Pharmingen	20624A
Human			
CD45	APC	Invitrogen	17-0459-42
CD3	PE/Cyanine7	Invitrogen	25-0036-42
TCR γ/δ	FITC	Invitrogen	11-9959-42

Table 2.2 Cell Identification Schemes.

Cell type	Identification Scheme
Immune	CD45 ⁺
Non-Immune	CD45 ^{neg}
Lymphocytes (total)	Lymphocyte gate
$\gamma\delta$ T cells	Lymphocyte gate, CD45 ⁺ , CD3 ⁺ , TCR $\gamma\delta$ ⁺
T _{conv} cells	Lymphocyte gate, CD45 ⁺ , CD3 ⁺ , TCR $\gamma\delta$ ^{neg}
CD4 ⁺ T _{conv} cell	Lymphocyte gate, CD45 ⁺ , CD3 ⁺ , TCR $\gamma\delta$ ^{neg} , CD4 ⁺
CD8 ⁺ T _{conv} cell	Lymphocyte gate, CD45 ⁺ , CD3 ⁺ , TCR $\gamma\delta$ ^{neg} , CD8 α ⁺
DN (Double-Negative) T _{conv} cell	Lymphocyte gate, CD45 ⁺ , CD3 ⁺ , TCR $\gamma\delta$ ^{neg} , CD4 ^{neg} , CD8 α ^{neg}
Naïve T cell	Lymphocyte gate, CD45 ⁺ , CD3 ⁺ , CD44 ^{low} , CD62L ^{hi} , CD69 ^{neg}
Central memory T cell	Lymphocyte gate, CD45 ⁺ , CD3 ⁺ , CD44 ^{hi} , CD62L ^{hi} , CD69 ^{neg}
Effector memory T cell	Lymphocyte gate, CD45 ⁺ , CD3 ⁺ , CD44 ^{hi} , CD62L ^{low} , CD69 ^{neg}
Tissue-resident T cell	Lymphocyte gate, CD45 ⁺ , CD3 ⁺ , CD44 ^{hi} , CD62L ^{low} , CD69 ⁺
Macrophages (total)	CD45 ⁺ , CD11b ⁺ , Ly6G ^{neg}
M1 macrophages	CD45 ⁺ , CD11b ⁺ , Ly6G ^{neg} , CD11c ⁺ , CD206 ^{neg} or CD206 ^{low}
M2 macrophages	CD45 ⁺ , CD11b ⁺ , Ly6G ^{neg} , CD11c ^{neg} , CD206 ⁺
DN (Double-Negative) macrophages	CD45 ⁺ , CD11b ⁺ , Ly6G ^{neg} , CD11c ^{neg} , CD206 ^{neg}
Neutrophils	CD45 ⁺ , CD11b ⁺ , Ly6G ⁺
Endothelial cells	CD45 ^{neg} , CD31 ⁺
Preadipocytes and adipose-derived stem cells (ADSC)	CD45 ^{neg} , CD31 ^{neg}

2.7 Quantitative real-time RT-PCR

Frozen tissues were homogenized with TRIzol reagent following the standard protocol. For adipose tissues, prior to the addition of chloroform, the homogenate was centrifuged at 10,000 rpm for 10 min and the upper lipid layer aspirated. Total cellular RNA was purified using PureLink RNA MiniKit (Invitrogen 12183018A), the concentration was determined by reading the absorbance at 260, and the 260:280 absorbance ratio was used to assess RNA purity (NanoDrop). Equivalent amounts of RNA were reverse transcribed into cDNA using SuperScript III First-Strand Synthesis SuperMix (Invitrogen 11752–050), according to the manufacturer's protocol. TaqMan assays were purchased from ThermoFisher Scientific, and qRT-PCR was performed on a QuantStudio 3 Real-Time PCR machine (Applied Biosystems). Target gene expression was normalized to hypoxanthine-guanine phosphoribosyl transferase (HPRT) expression

as an endogenous control, and fold change was calculated as $2^{-(\Delta\Delta CT)}$, using the mean ΔCT of the control group as a calibrator. TaqMan assays used were Mm00446190_m1 and Mm03024075_m1 for IL-6 and HPRT, respectively.

2.8 Plasma IL-6 ELISA

IL-6 level in plasma was determined by using Mouse IL-6 ELISA kit according to manufacturer's protocol (Invitrogen BMS603-2).

2.9 *In vivo* cell proliferation study with EdU

Stock solution of 5-ethynyl-2'-deoxyuridine (EdU) at 40mg/mL was prepared by dissolving 10 mg in 250 μ l of DMSO and kept at -20°C. Each mouse was injected with 1 mg dosage using 25 μ l of stock solution and 375 μ l PBS to make 400 μ l of total injection volume. Mice were given intraperitoneal injections every day 24 hours apart for 3 consecutive days and were sacrificed on day 4th (Fig 2.2). VAT was processed until single cell suspension to stain for viability and antibodies against cell surface markers (Supplementary Table 2.1) followed by EdU staining according to manufacturer's guidelines using the Click-iT Plus EdU Alexa Fluor 594 flow cytometry assay kit (Invitrogen C10646).

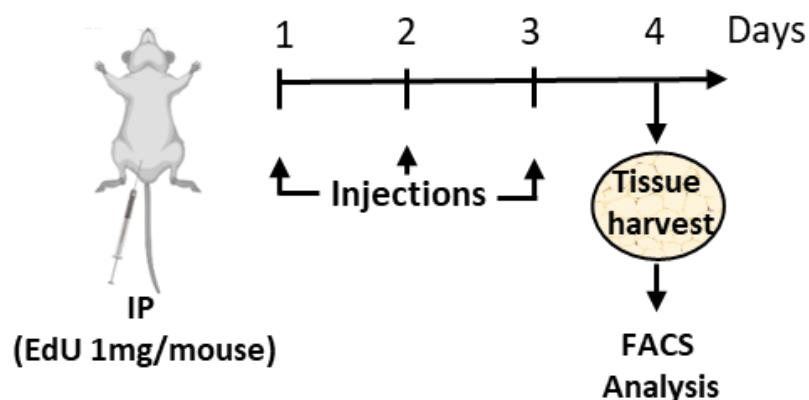


Fig. 2.2. Experimental design for EdU pulsing in young and aged mice to analyze *in vivo* proliferation. IP: Intraperitoneal injection.

2.10 Analysis of apoptosis

VAT and lymph nodes were collected from mice and processed until single cell suspension. Untreated cells were directly resuspended into the buffer containing DPBS with 1mM EDTA, 25mM HEPES, 1% FBS and proceed to Fc receptor blocking followed by surface staining in 250 μ L of the same buffer. Then the cells were stained with CellEvent™ Caspase-3/7 Green Flow Cytometry Assay Kit according to manufacturer's protocol (Invitrogen C10740). In order to block BCL2, cells ($\sim 1 \times 10^6$) were incubated with 2 μ M of ABT737 (Selleck chemicals) together with 1.6 μ M of S63845 (Sigma-Aldrich) or 0.2% DMSO for 3hrs at 37 °C with 5% CO₂. Then the cells were washed with buffer containing DPBS with 1mM EDTA, 25mM HEPES, 1% FBS and proceed to Fc receptor blocking. Then the cells were further processed as same as the untreated as mentioned above.

2.11 TCR-V γ /V δ PCR

RNA was extracted from frozen tissues (VAT, blood, spleen) by methods described in Section 2.7 Quantitative real-time RT-PCR. RNA was reverse transcribed using SuperScript™ III First-Strand Synthesis SuperMix for qRT-PCR (Invitrogen 11752050) and the resulting cDNA was amplified by use of Taq PCR Kit (New England Biololabs E5000S). The primers used to detect γ/δ chains were described previously[87] and are listed in Table 2.3, according to the nomenclature of Heilig and Tonegawa[73]. The following reaction conditions were used: denaturation at 94°C, annealing between 46-55°C (see Table. 2.3 for specific temperature), and extension at 72°C; for 38 cycles. PCR products were run on individual samples as well as pooled (n=4) on a 2% agarose gel and visualized using ethidium bromide on the ChemiDoc MP Imaging System (Bio-Rad).

Table 2.3 Primers used for gene expression analysis with PCR.

Gene	Forward primer (5'-3')	Reverse Primer (5'-3')	Annealing (°C)
V γ 1	V γ 1 CGGCAAAAAGCAAAAAGT	C γ 4 GGAGACAAAGGTAGGTCCCAGC	55
V γ 2	V γ 2 TTGGTACCGGCAAAAACAAATCA	C γ 2 CAATACACCCTTATGACATCG	46
V γ 4	V γ 4 CTGCAACCCCTACCCATAT	C γ 1 CCACCACTCGTTTCTTTAGG	55
V γ 5	V γ 5 AGGATCCCGCTTGAAATGGATGAGA		55
V γ 6	V γ 6 GATCCAAGAGGAAAGGAAAGACGGC		55
V γ 7	V γ 7 GATCCAACTTCGTCAGTTCCACAAC		55
V δ 1	V δ 1 AATAGCAATTCTACTGATGGTGG	C δ 1 CGAATCCACAATCTTCTTG	46
V δ 2	V δ 2 AGTCCTCAGTCTCTGACAATC		46
V δ 3	V δ 3 CCAGATTCAATGGAAAGTAC		55
V δ 4	V δ 4 GTACAAACAGCAAGGAGGGCAGG		55
V δ 5	V δ 5 CCAGACAGTGGCAAGCGGCACTG		55
V δ 6	V δ 6 TCAAGTCCATCAGCCTTGTC		55
β -Actin	CTTCTTTGCAGCTCCTTCGTTG	TTCTCCATGTCGTCCCAGTTGG	55

2.12 Statistical analysis

Comparisons of continuous variables were analyzed first using overall two-way ANOVA, Hotelling's T² tests, or Student's t-test. Multiple comparisons of continuous variables were then performed using Fisher's Least Significant Difference. Correlation between continuous variables was analyzed using Pearson's Correlation Coefficient. All analyses were done using R (R Core Team, Vienna, Austria). All analyses were performed by collaborating statistician Dr. Arnold Stromberg at the University of Kentucky.

Chapter 3 ACCUMULATION OF $\gamma\delta$ T CELLS IN VISCERAL ADIPOSE TISSUE WITH AGING PROMOTES CHRONIC INFLAMMATION

3.1 Objective

Adipose tissue dysfunction is a major contributor to chronic inflammation in aging. The majority of the current knowledge about age-associated changes in the adipose resident immune profile is focused on macrophages and conventional T cells. Very little is known about the role of $\gamma\delta$ T cells in adipose tissue, especially as it pertains to aging. Previous studies from Dr. Starr's lab reported age-associated changes in gene expression in visceral adipose tissue (VAT). Particularly, T-cell receptor gamma, constant region (Tcrg-C), a gene expressed exclusively by $\gamma\delta$ T cells, showed a significant 6-fold increase in the aged (24 months old) compared to young (4 months old) male mice[88]. The objective of this chapter is to elucidate whether this upregulated gene expression results in an actual increase of the number of $\gamma\delta$ T cells within VAT by aging. I have used flow cytometry analysis to quantify $\gamma\delta$ T cells in VAT over the lifespan in mice and in humans. Then I performed cytokine profiling of $\gamma\delta$ T cells between young and aged VAT to understand functional changes of these cells with aging. Furthermore, a genetic deficient model, TCR delta knock out (TCR δ KO) mice were used to understand the functional role of $\gamma\delta$ T cells in aged VAT inflammation. Utilizing IL-6, which is a well-known inflammaging marker, I have determined whether the state of age-associated inflammation is affected by the absence of $\gamma\delta$ T cells. Moreover, I have evaluated whether $\gamma\delta$ T cells play a role in cellular homeostasis within VAT by contributing to the maintenance of cellular architecture.

3.2 Results

3.2.1 $\gamma\delta$ T cells are increased by aging specifically in VAT

We evaluated whether the age-associated increase in gene expression corresponds to an increase in $\gamma\delta$ T cell number with age by surveying $\gamma\delta$ T cells in the stromal vascular fraction (SVF) of gonadal visceral adipose tissue (VAT) by flow cytometry (Fig. 3.1a, Representative plots). Male mice showed a significant increase in the percentage of $\gamma\delta$ T cells by aging. Female mice showed a similar trend, though not reaching significance (Fig.

3.1b). Both males and females displayed a significant increase in the total number of $\gamma\delta$ T cells in VAT (Fig. 3.1c), which remained significant after adjusting for fat mass (Fig. 3.1d), suggesting that the increase is independent of adiposity. To determine whether the age-associated increase in VAT $\gamma\delta$ T cells was specific to VAT, we examined $\gamma\delta$ T cell composition in blood, spleen, subcutaneous adipose tissue (SAT) and skin. The data show that the age-associated increase in $\gamma\delta$ T cells was unique to VAT, not being observed in blood, spleen, SAT, or skin (Fig. 3.2). Furthermore, to determine if these findings in mice translate to humans, we obtained VAT samples from discarded tissues specimens of patients undergoing operations at UK hospital. It is important to note here that the increase in $\gamma\delta$ T cells with aging was also observed in human VAT (Fig. 3.). Inversely, the percentage of conventional T cells (T_{conv} , i.e., $\alpha\beta$ T cells) decreased in the aged VAT, but total numbers were moderately increased by aging without a significant increase after adjusting for fat mass (Fig 3.4). All experiments for these studies were performed in three or more days to maximize biological repeats and to avoid technical error which may occur in a single day experiment. Full gating scheme to identify $\gamma\delta$ T and T_{conv} cells shown in Fig. 3.5.

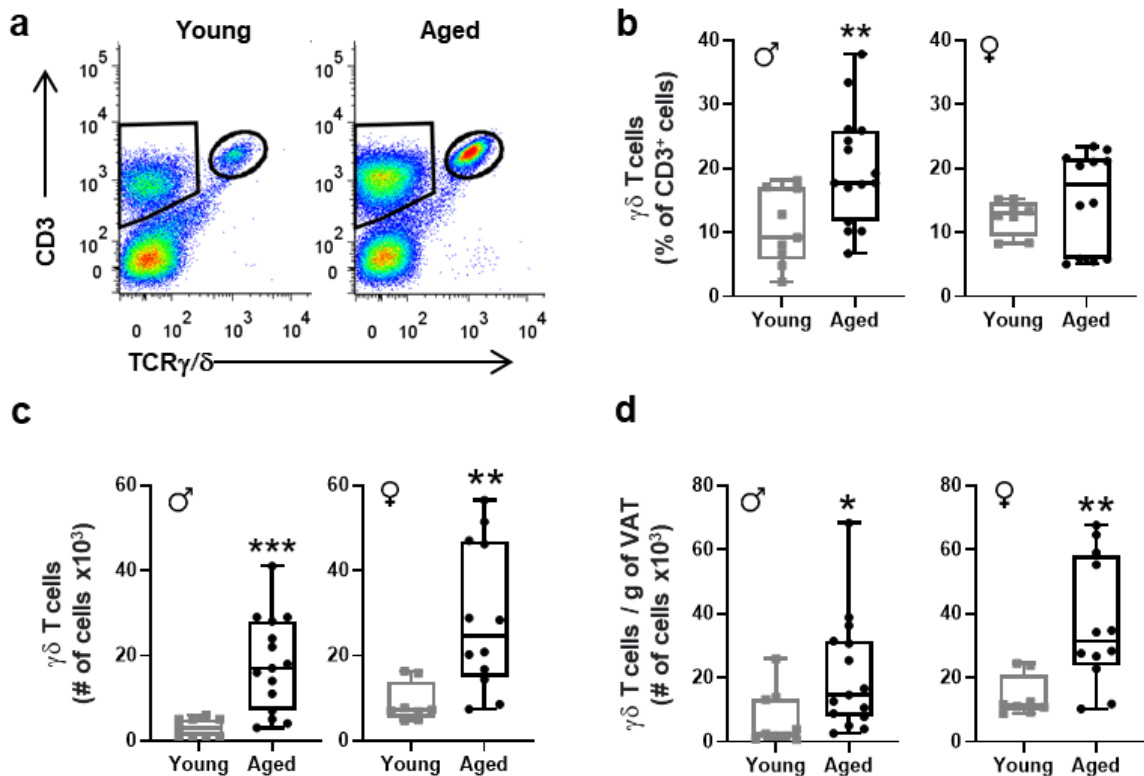


Fig. 3.1 $\gamma\delta$ T cells are increased by aging in visceral adipose tissue (VAT). a) Representative flow cytometry plots of $\gamma\delta$ T cells in VAT. b) Percentage, c) Total number, and d) Number per gram of adipose tissue of $\gamma\delta$ T cells was quantified in young (4–6 months) and aged (19–25 months) male (n = 9 young, n = 15 aged) and female (n = 8 young, n = 12 aged) C57BL/6 mice. Statistical differences were determined by two-way ANOVA with Fisher’s Least Significant Difference for multiple comparisons. Data are expressed in box plots from minimum to maximum values with a bar representing the mean; each symbol represents an individual mouse. *p < 0.05; **p < 0.01; ***p < 0.001. VAT, visceral adipose tissue. Reproduced with permission from Springer Nature.

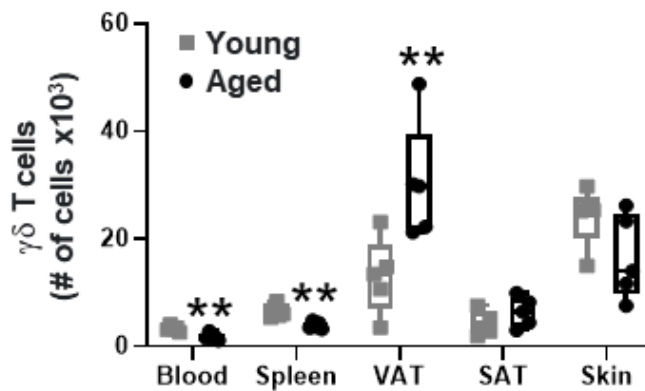


Fig. 3.2 $\gamma\delta$ T cells are increased by aging specifically in VAT. Number of $\gamma\delta$ T cells in blood and tissues of young and aged mice (n = 5, each; 6 and 19 months old, respectively). Statistical differences were determined by a two-sample Hotelling’s T2 test followed by Student’s t-test. Data are expressed in box plots from minimum to maximum values with a bar representing the mean; each symbol represents an individual mouse. *p < 0.05; **p < 0.01; ***p < 0.001. VAT, visceral adipose tissue; SAT, subcutaneous adipose tissue. Reproduced with permission from Springer Nature.

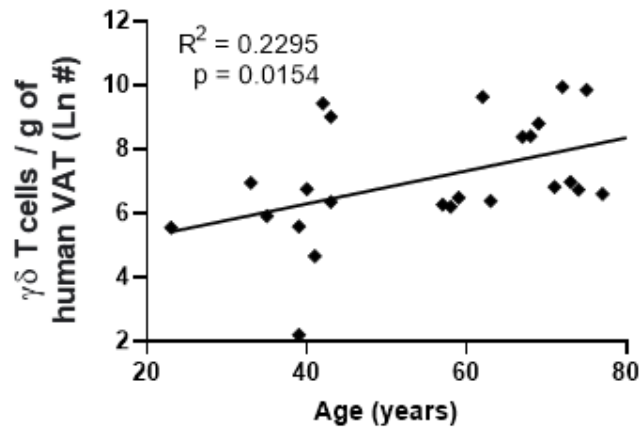


Fig. 3.3 $\gamma\delta$ T cells increase in human VAT by aging. Number of $\gamma\delta$ T cells per gram of human VAT according to age; each symbol represents a sample from an individual subject. Statistical significance of the correlation was assessed by Pearson correlation coefficient. VAT, visceral adipose tissue. Reproduced with permission from Springer Nature.

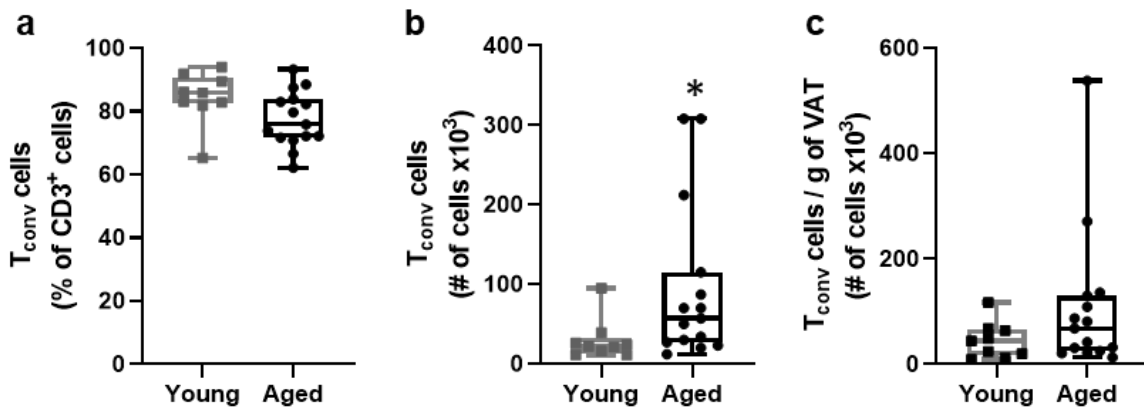


Fig. 3.4 Age-associated changes in the T_{conv} cells in VAT. a) Percentage, b) Total number, and c) Number per gram of adipose tissue of T_{conv} cells was quantified in young (4-6 months, $n=9$) and aged (19-25 months, $n=15$) male mice. Statistical differences were determined by Student's t-test. * $p < 0.05$. Reproduced with permission from Springer Nature.

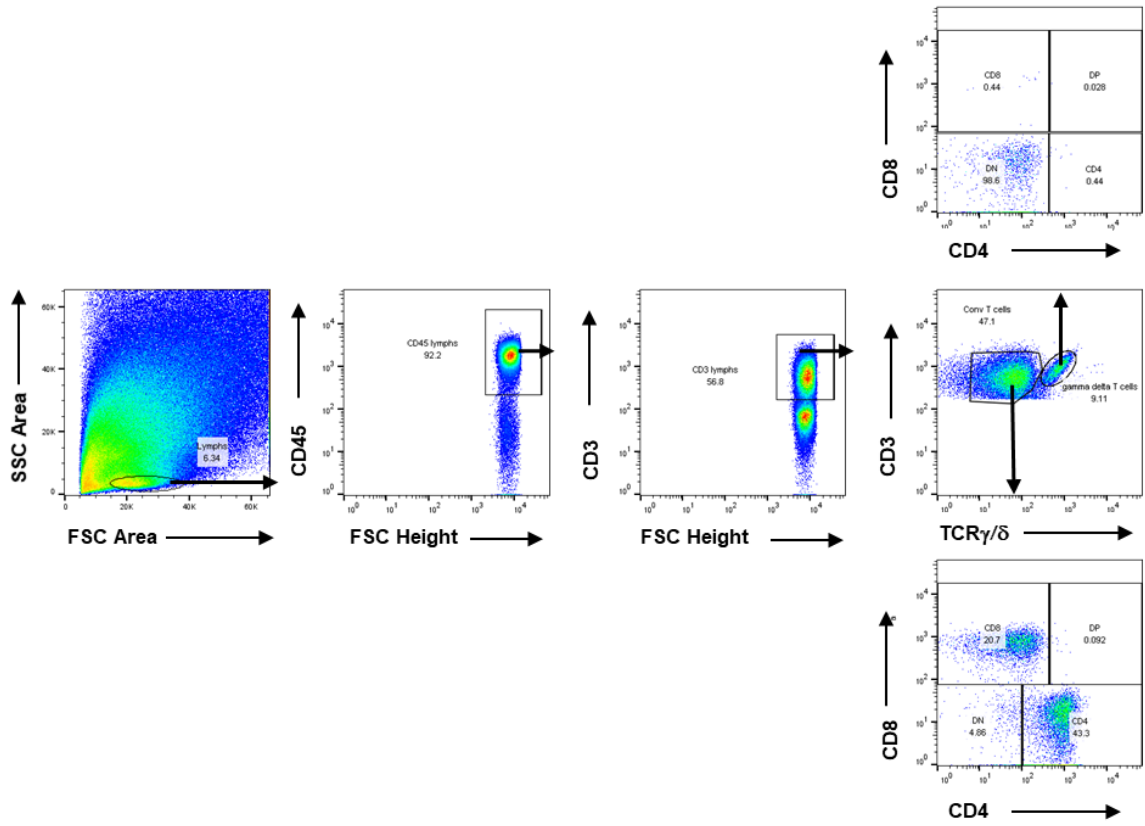


Fig. 3.5 Representative flow cytometry plots to identify $\gamma\delta$ T and T_{conv} cells. Reproduced with permission from Springer Nature.

3.2.2 Trend of $\gamma\delta$ T cells accumulation in VAT over the lifespan in mice

The data in Figure 3.1 showed an age-associated increase in $\gamma\delta$ T cells between young (4-5mo) and aged (19-24mo) mice; however, at what age this accumulation starts was not known. To identify the trend of $\gamma\delta$ T cells accumulation in VAT over the lifespan, $\gamma\delta$ T and T_{conv} cells were evaluated in parallel in seven age groups of mice (2mo, 4mo, 8mo, 12mo, 16mo, 20mo, 24mo). The percentage of $\gamma\delta$ T cells progressively increases in VAT with aging (Fig. 3.6a, $R^2= 0.4684$, $p<0.0001$) while the percentage of T_{conv} cells proportionately declines with age (Fig. 3.6b, $R^2=0.4335$, $p<0.0001$). The total number of $\gamma\delta$ T cells showed a significant increase in the middle-aged (12-16mo) compared to young (2-4mo); the number further increased significantly in the aged groups (20-24mo) compared to late middle-aged (16mo) (Fig. 3.6c). Contrarily, the number of T_{conv} cells significantly increases in the middle aged (12-16mo) compared to young (2-4mo), without further significant increase in old age groups (Fig. 3.6d). This suggests that the late age-associated increase is unique to $\gamma\delta$ T cells and absent in T_{conv} cells. To understand if adiposity plays a role in the accumulation, the number of cells was adjusted for fat mass. After adjusting for fat mass, $\gamma\delta$ T cells still showed a significant difference starting from late middle-age (16mo, Fig. 3.6e), suggesting that the increase in advanced age is primarily age-dependent while at middle-age (12mo), the increase is adiposity dependent. In contrast, significance for the age-associated increase was lost for T_{conv} cells after adjusting for fat mass (Fig. 3.6f), which suggests adiposity as a major determinant for T_{conv} accumulation in VAT. Natural adiposity pertaining to the body weight and epididymal fat mass of different age-groups of mice were measured (Fig. 3.7a-b). The total body weight (BW) increased from 2 months to 4 months and then reached a plateau. A significant difference in epididymal fat mass was observed only between 2 months to 12 months of age groups of mice in the cohorts of mice used for these studies.

As a comparison we evaluated $\gamma\delta$ T and T_{conv} cell profiles in peripheral lymph nodes. The percentage of $\gamma\delta$ T cells showed a significant increase in young adult (8mo) compared to young (2mo) which again decline in the middle age without further changes in the aged (Fig 3.8a). The percentage of T_{conv} cells remained statistically similar until late

middle age (16mo) and showed a decline in the aged (24mo) (Fig 3.8b). The total number of $\gamma\delta$ T cells in LN showed no influence of aging (Fig 3.8c) while the total number of T_{conv} cells were highest in the young (2mo) that declined and remained unchanged over the lifespan (Fig 3.8d). All experiments for these studies were performed in three or more days to maximize biological repeats and to avoid technical error which may occur in a single day experiment.

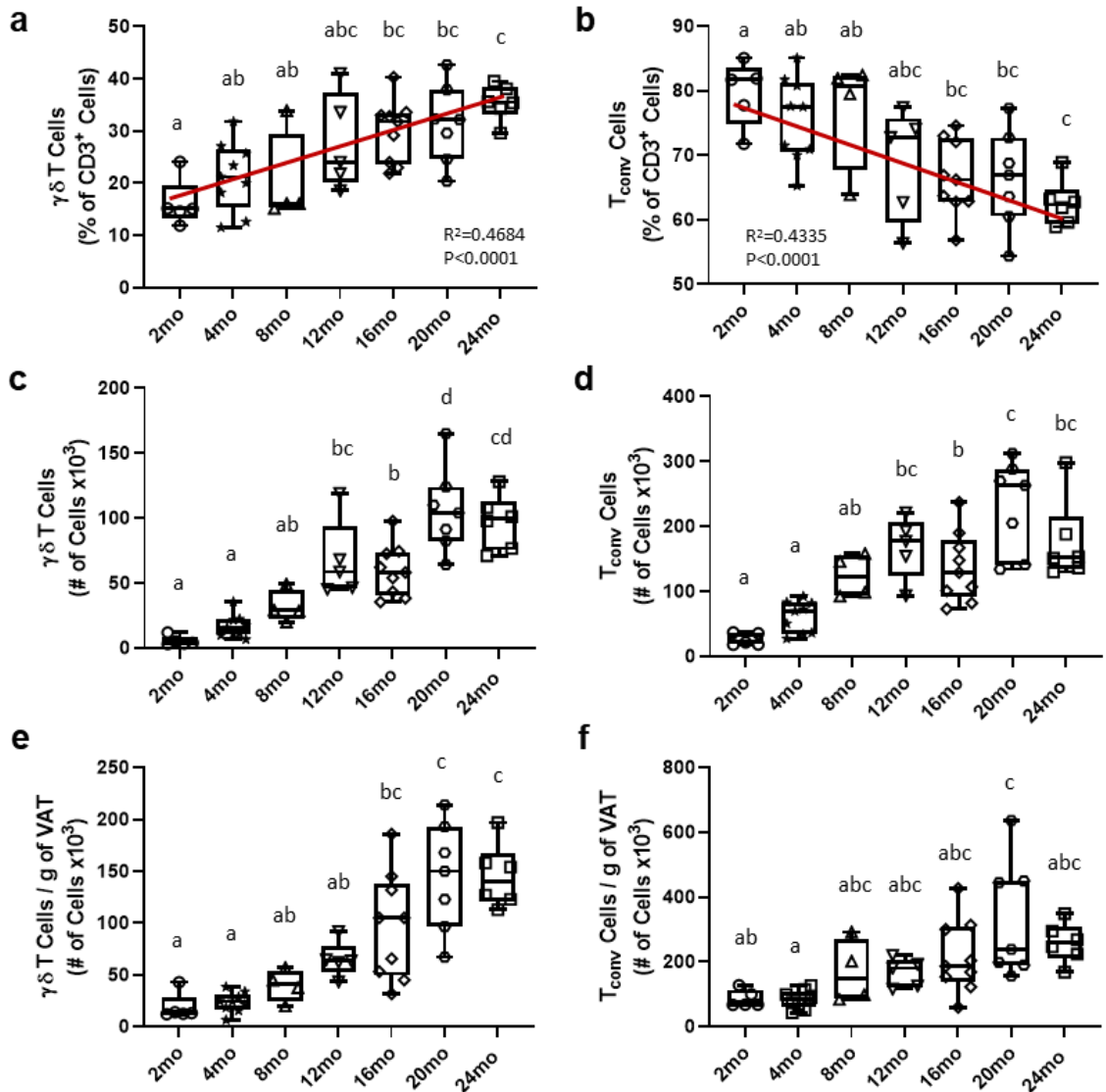


Fig. 3.6 Accumulation of $\gamma\delta$ T and T_{conv} cells in VAT over the lifespan in mice. a-b) Percentage, c-d) Total number, and e-f) Number per gram of VAT of $\gamma\delta$ T and T_{conv} cells were quantified among the total $CD3^+$ lymphocytes population in 2mo (n=5), 4mo (n=9), 8mo (n=4), 12mo (n=5), 16mo (n=9), 20mo (n=7), and 24mo (n=6) old male C57BL/6 mice. Data are expressed in box plots from minimum to maximum values with bars representing the mean; each symbol represents an individual mouse. Statistical differences were determined by one way ANOVA with Tukey Honest Significant difference for multiple comparisons. Age groups not connected by same letters (a,b,c,d) are significantly different; g: gram; mo: month; VAT: visceral adipose tissue.

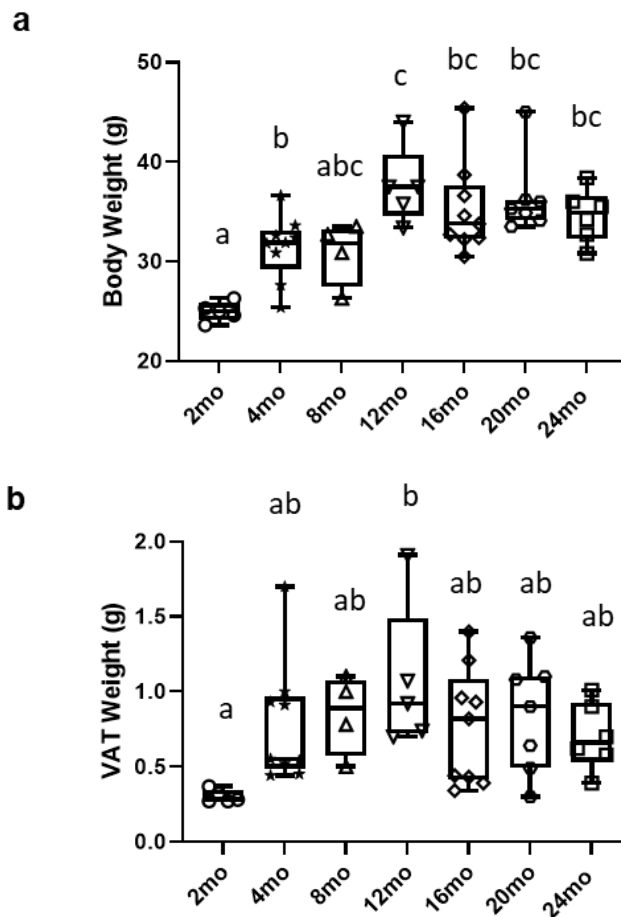


Fig. 3.7 Age and corresponding adiposity in mice. a) Body weight and b) VAT weight corresponding in 2mo (n=5), 4mo (n=9), 8mo (n=4), 12mo (n=5), 16mo (n=9), 20mo (n=7), and 24mo (n=6) old male C57BL/6 mice. Data are expressed in box plots from minimum to maximum values with bars representing the mean; each symbol represents an individual mouse. Statistical differences were determined by one way ANOVA with Tukey Honest Significant difference for multiple comparisons. Age groups not connected by same letters (a,b,c) are significantly different. g: gram; mo: month; VAT: visceral adipose tissue.

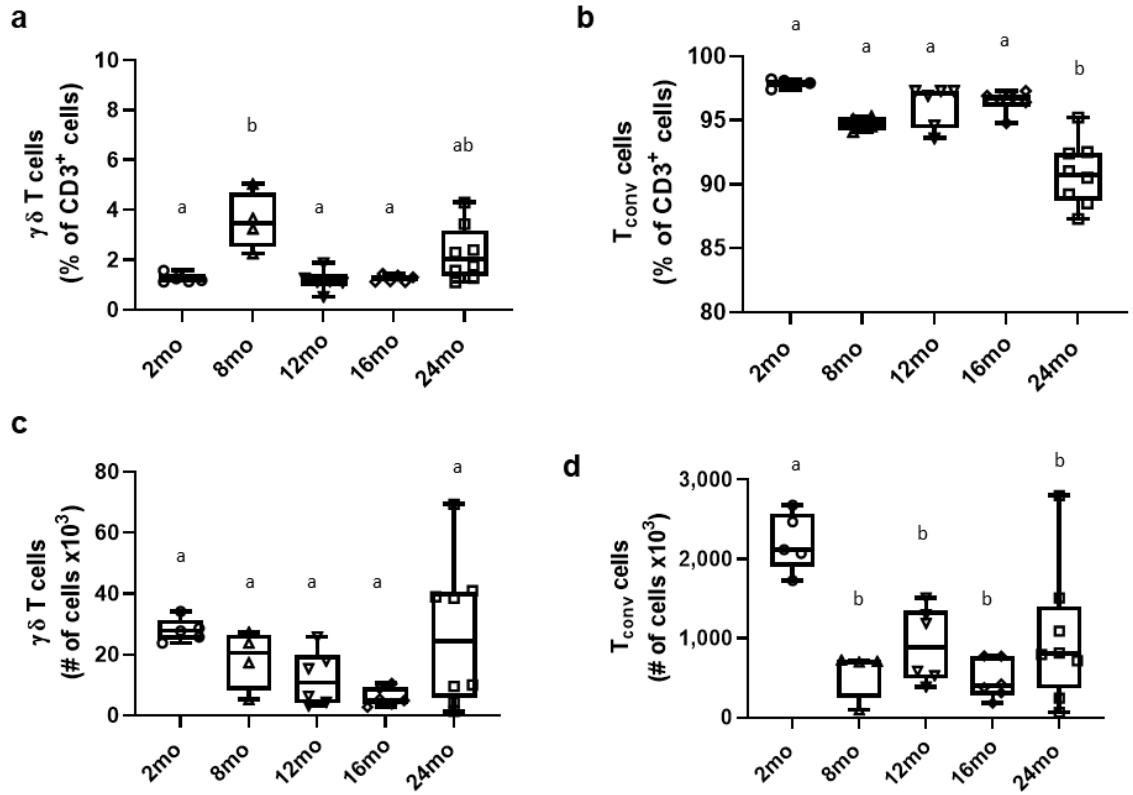


Fig. 3.8 $\gamma\delta$ T and T_{conv} cell profiling in lymph nodes (LN) over the lifespan. a-b) Percentage and c-d) Total number of $\gamma\delta$ T and T_{conv} cells were quantified among the total $CD3^+$ lymphocytes population in 2mo (n=5), 8mo (n=4), 12mo (n=6), 16mo (n=6) and 24mo (n=8) old male C57BL/6 mice. Data are expressed in box plots from minimum to maximum values with bars representing the mean; each symbol represents an individual mouse. Statistical differences were determined by one way ANOVA with Tukey Honest Significant difference for multiple comparisons. Age groups not connected by same letters (a,b) are significantly different. mo: month; LN: Lymph node.

3.2.3 $\gamma\delta$ T cells in VAT predominantly express IL-17A

$\gamma\delta$ T cells were categorized into subtypes based on IL-17A or IFN γ production, which distinguishes their functional programming. Intracellular staining for these two cytokines showed that IL-17A⁺ $\gamma\delta$ T cells made up the largest subset (3.9 Flow cytometry gating strategy). Approximately 50% of total $\gamma\delta$ T cells in young VAT and 65% of total $\gamma\delta$ T cells in aged VAT were single positive for IL-17A (Fig. 3.10a). Less than 10% of $\gamma\delta$ T cells in both age groups were single-positive for IFN γ . In addition to these mutually exclusive populations, a subset of $\gamma\delta$ T cells was positive or negative for both markers (double positive (DP) and double negative (DN), respectively). Total cell numbers per gram of VAT showed an age-associated increase for all $\gamma\delta$ T cell subsets, although the IL-17A⁺ subset was clearly the most prevalent and showed a profound age-associated increase (Fig. 3.10b). In contrast, T_{conv} cells in VAT showed a preference for IFN γ or lacked both markers, with little age-related variance (Fig. 3.11). In the spleen, $\gamma\delta$ T cells were equally distributed between IL-17A⁺, IFN γ ⁺, and DN subsets, while splenic T_{conv} cells were largely IFN γ ⁺ or DN, with little variance by age (Fig. 3.12).

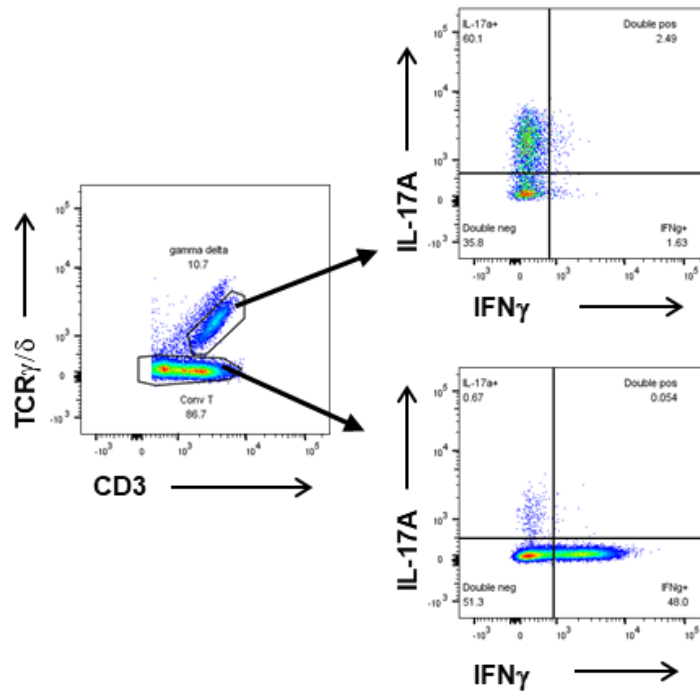


Fig. 3.9 Representative flow cytometry plots to identify $\gamma\delta$ T and T_{conv} cells based on IL-17A or IFN γ production. Reproduced with permission from Springer Nature.

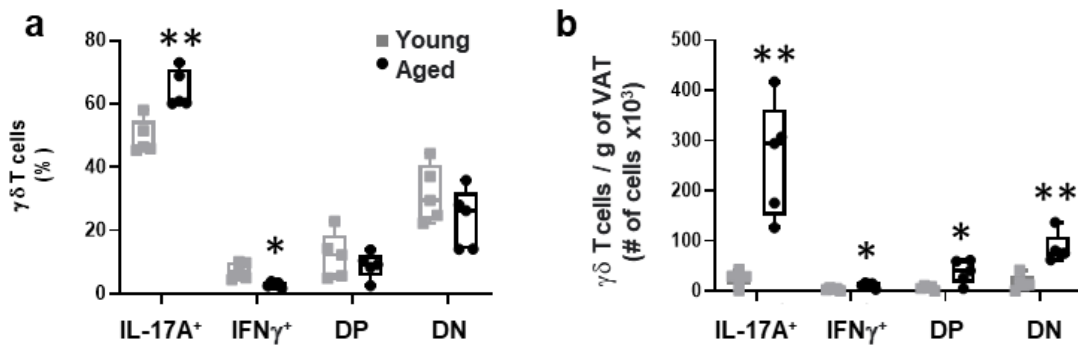


Fig. 3.10 $\gamma\delta$ T cells in VAT predominantly express IL-17A. a) Percentage of total $\gamma\delta$ T cells, and b) Number of $\gamma\delta$ T cell per gram of adipose tissue for each intracellular stain. Data are expressed in box plots from minimum to maximum values with a bar representing the mean; each symbol represents an individual mouse. Statistical differences were determined by Student's t-test. *p < 0.05; **p < 0.01. DP, double positive; DN, double negative. Reproduced with permission from Springer Nature.

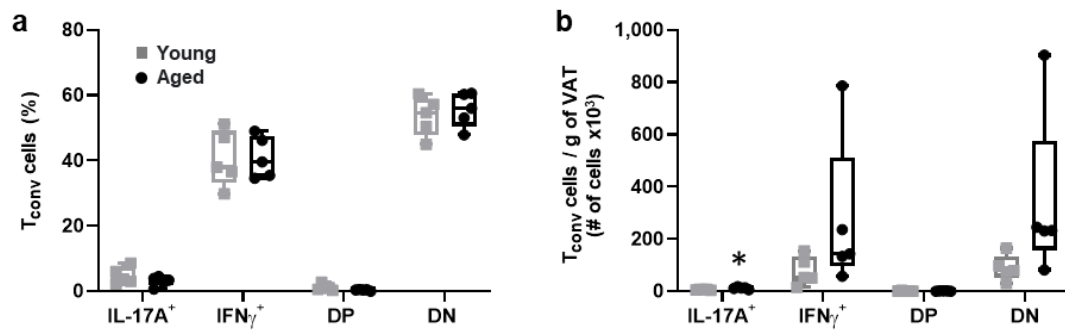


Fig. 3.11 IL-17A and IFN γ producing T_{conv} cells in VAT. T_{conv} cells from visceral adipose tissue of young (7 months, n=5) and aged (23-24 months, n=5) mice were assessed for intracellular IL-17A and IFN γ expression. a) Percentage of total T cells and b) Number of T_{conv} cells per gram of adipose tissue for each intracellular stain. Data are expressed in box plots from minimum to maximum values with a bar representing the mean; each symbol represents an individual mouse. Statistical differences were determined by Student's t-test. * p < 0.05. Reproduced with permission from Springer Nature.

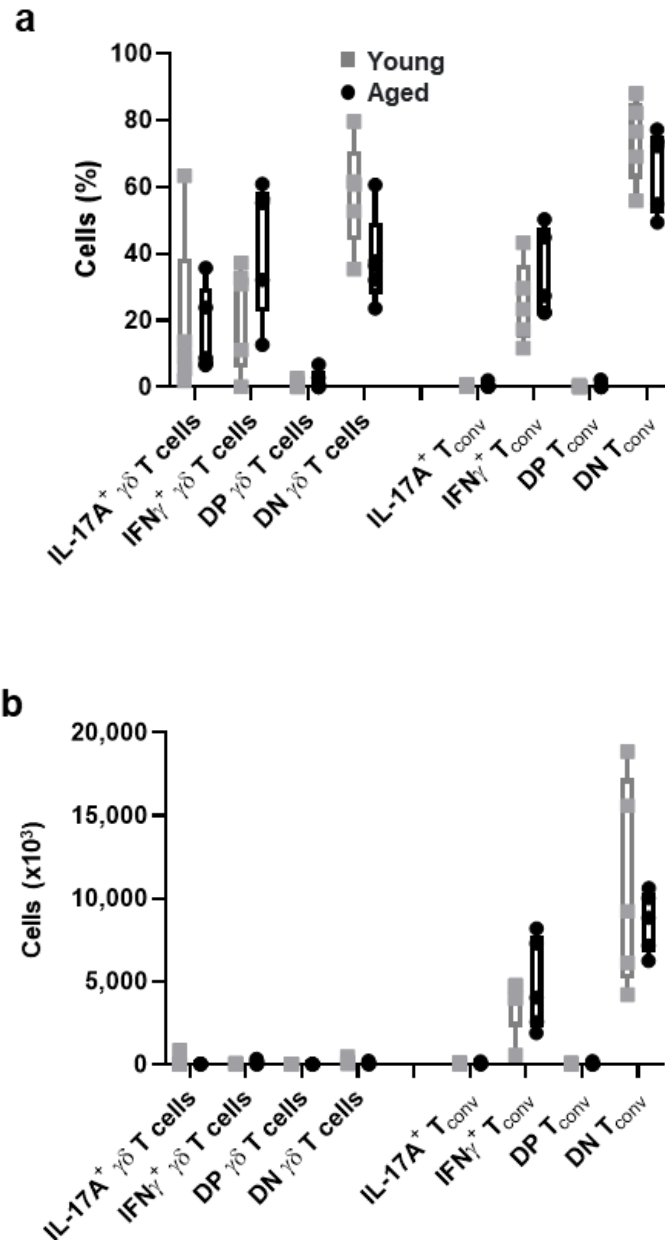


Fig. 3.12 IL-17A and IFN γ in splenic T cells. $\gamma\delta$ T cells and T_{conv} cells from spleen of young (7 months) and aged (23-24 months) mice were assessed for intracellular IL-17A and IFN γ expression. a) Percentage and b) Total number of T cells for each intracellular stain. Data are expressed in box plots from minimum to maximum values with a bar representing the mean; each symbol represents an individual mouse. Statistical differences were determined by Student's t-test (no significant differences were observed). Reproduced with permission from Springer Nature.

3.2.4 Reduced inflammation in aged mice lacking $\gamma\delta$ T cells (TCR δ KO)

To gain insight into the function of $\gamma\delta$ T cells, we utilized TCR δ KO mice, which lack functional $\gamma\delta$ T cells due to disruption of the δ chain of the TCR which is required for their development[89]. Aged WT and TCR δ KO mice were compared to evaluate systemic and VAT specific inflammation. IL-6, a well-known inflammaging marker was used as a surrogate for inflammation[90, 91]. A reduction in plasma IL-6 level was observed in the KO mice which indicates reduced age-associated inflammation systemically (Fig. 3.13a), IL-6 gene expression was also dramatically decreased in VAT of the KO mice, suggesting reduced local inflammation in the VAT (Fig. 3.13b) in the absence of $\gamma\delta$ T cells. To determine which cells in the VAT are responsible for IL-6 production and whether loss of $\gamma\delta$ T cells affects the cellular distribution of IL-6, I performed intracellular staining for IL-6 without stimulation. We identified that nonimmune cells (CD45^{neg}), as opposed to CD45⁺ immune cells, are the primary producers of IL-6 in the VAT (Fig. 3.14a). Total number of IL-6⁺ CD45^{neg} cells per gram of fat was significantly lower in TCR δ KO mice, suggesting that loss of $\gamma\delta$ T cells reduces IL-6 production from non-immune stromal cells (Fig. 3.14b). This cellular compartment is primarily composed of committed preadipocytes, adipose-derived stem cells (ADSC), and endothelial cells. Next, we compared IL-6 positivity among major immune (lymphocytes, macrophages, neutrophils) and nonimmune (preadipocytes/ADSCs, endothelial cells) subsets by gating with commonly used cell surface markers (see gating strategy in Table 2.2). The CD45^{neg}CD31^{neg} population, which excludes endothelial cells and consists of approximately 60% preadipocytes[92], was identified as the major subset of IL-6- producing cells. Additionally, the number of IL-6⁺ CD45^{neg}CD31^{neg} (preadipocytes/ADSCs) was significantly reduced in TCR δ KO mice (Fig. 3.14c), suggesting that $\gamma\delta$ T cells contribute to the inflammatory status of this cell subset. Unfortunately, we were unable to differentiate committed preadipocytes from ADSCs. Although immune cells are not responsible for the majority of IL-6 production in aged VAT, there is potential for their involvement in the signaling leading to IL-6 production. Thus, we performed a quantitative comparison of lymphocyte and macrophage subsets between WT and TCR δ KO mice (see gating strategy in Table 2.2). CD4⁺ and CD8⁺ T_{conv} cells showed a significant reduction whereas cells negative for CD4 and CD8 (double

negative (DN) T cells) showed a significant increase in TCR δ KO mice (Fig. 3.14d). Among the macrophage populations, M2-like (CD11c^{neg} CD206⁺) macrophages showed a significant reduction in TCR δ KO mice. On the other hand, M1-like macrophages gated as M1.1 (CD11c⁺CD206⁻) and M1.2 (CD11c⁺ CD206^{low}) were not significantly changed. DN macrophages (CD11c^{neg} CD206^{neg}) showed a significant increase in TCR δ KO mice (Fig. 3.14e). Comparative study in other tissues including kidney, lung, heart, and SAT did not show significant differences in IL-6, suggesting that reduced IL-6 in the KO mice is largely due to reduced IL-6 secretion by VAT (Fig. 3.15). Collectively, these data suggest that depletion of $\gamma\delta$ T cells in aged mice attenuates age-related inflammation, which results from an interplay between $\gamma\delta$ T cells and non-immune adipose stromal cells. All representative gating plots are shown in Fig. 3.16-3.18).

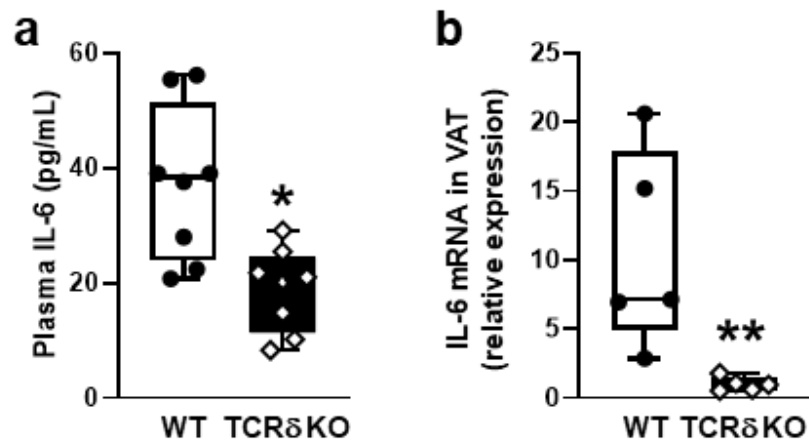


Fig. 3.13 Reduced inflammation in aged mice lacking $\gamma\delta$ T cells (TCR δ KO). Aged WT and aged TCR δ KO mice (24-27 months, n = 5-8) were euthanized for assessment of inflammatory cytokine IL-6. a) IL-6 level in plasma was measured by ELISA and b) IL-6 gene expression in VAT was measured by qRT-PCR. Statistical differences were assessed by Student's t-test. *p < 0.05; **p < 0.01. Reproduced with permission from Springer Nature.

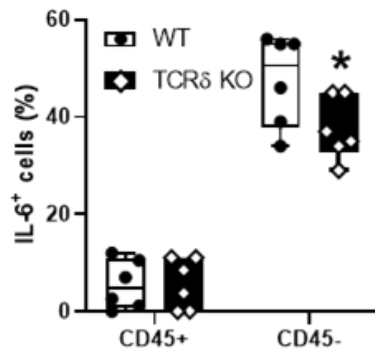
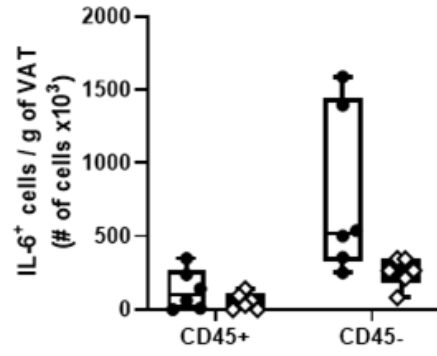
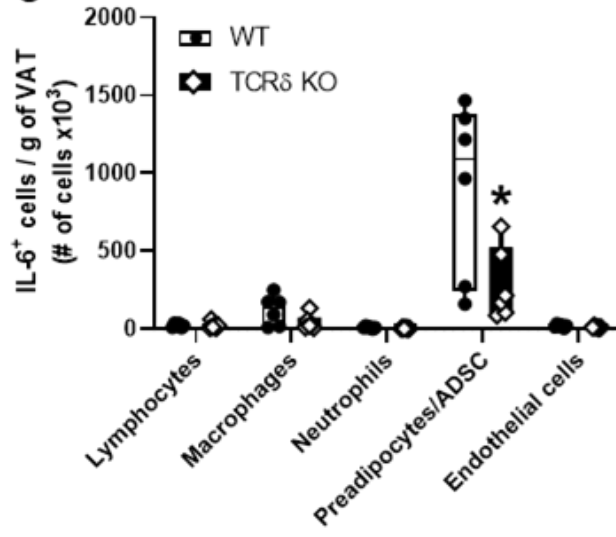
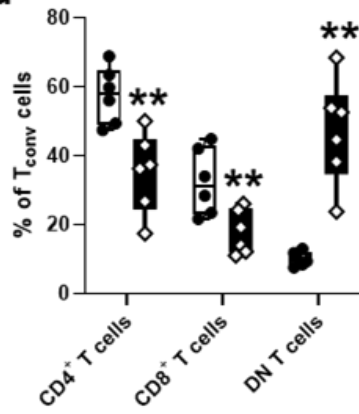
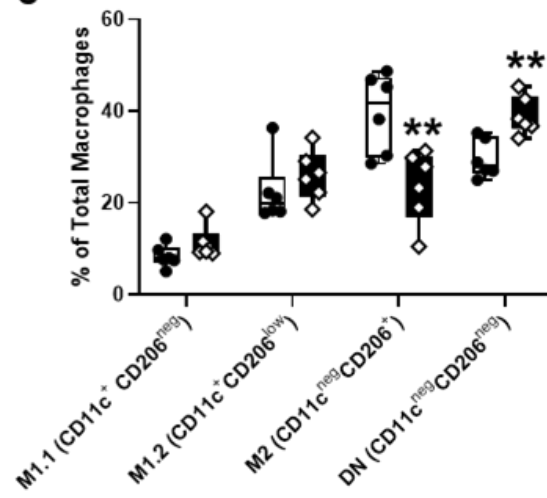
a**b****c****d****e**

Fig. 3.14 Non-immune cells are the primary IL-6 producers which decrease in aged mice lacking $\gamma\delta$ T cells (TCR δ KO). Intracellular staining of IL-6 in unstimulated cells was assessed by flow cytometry: a) Percentage of IL-6⁺ cells and b) Number of IL-6⁺ cells per gram of VAT compared between CD45⁺ immune cells and CD45 negative non-immune cells; c) Number of IL-6⁺ cells per gram of VAT among major immune and non-immune cell subsets. d) Percentage of T_{conv} cell subtypes and e) Percentage of macrophage subtypes compared between WT and TCR δ KO mice. Statistical differences were assessed by Student's t-test. *p < 0.05; **p < 0.01. Reproduced with permission from Springer Nature

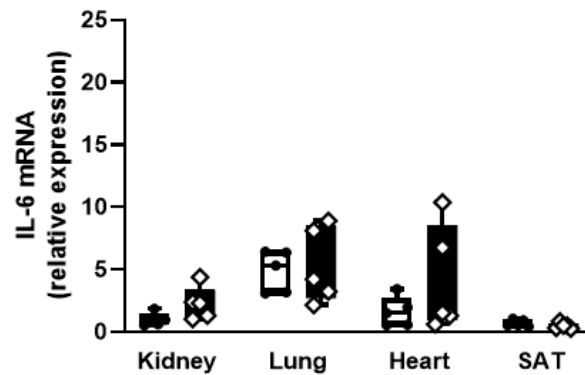


Fig. 3.15 IL-6 expression in tissues of WT vs. TCR δ KO mice. IL-6 gene expression in kidney, lung, heart, and subcutaneous adipose tissue (SAT) of aged WT and aged TCR δ KO mice (24-27 months, n=5) was measured by qRT-PCR. Reproduced with permission from Springer Nature.

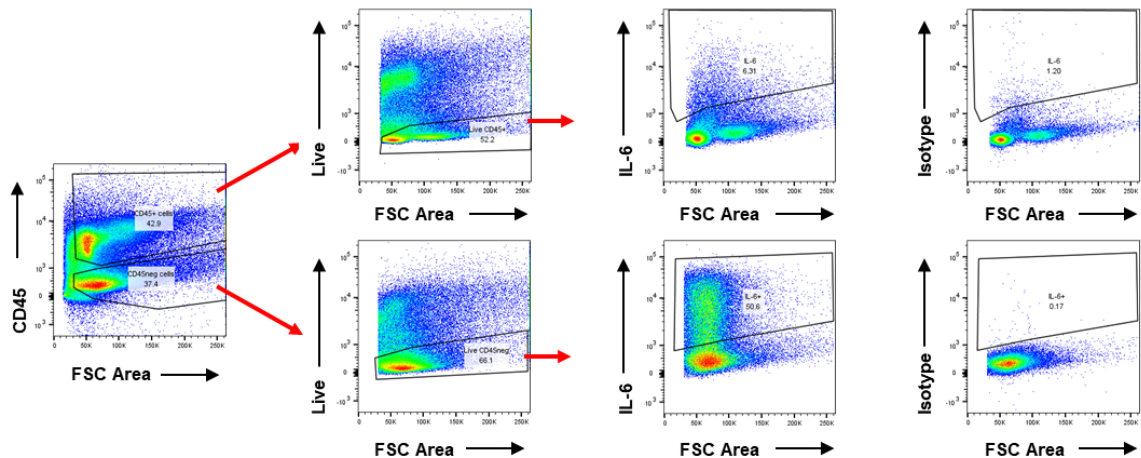


Fig. 3.16 Representative flow cytometry plots to identify IL-6 positive cells in the CD45 positive immune cells versus CD45 negative non-immune cells. Reproduced with permission from Springer Nature.

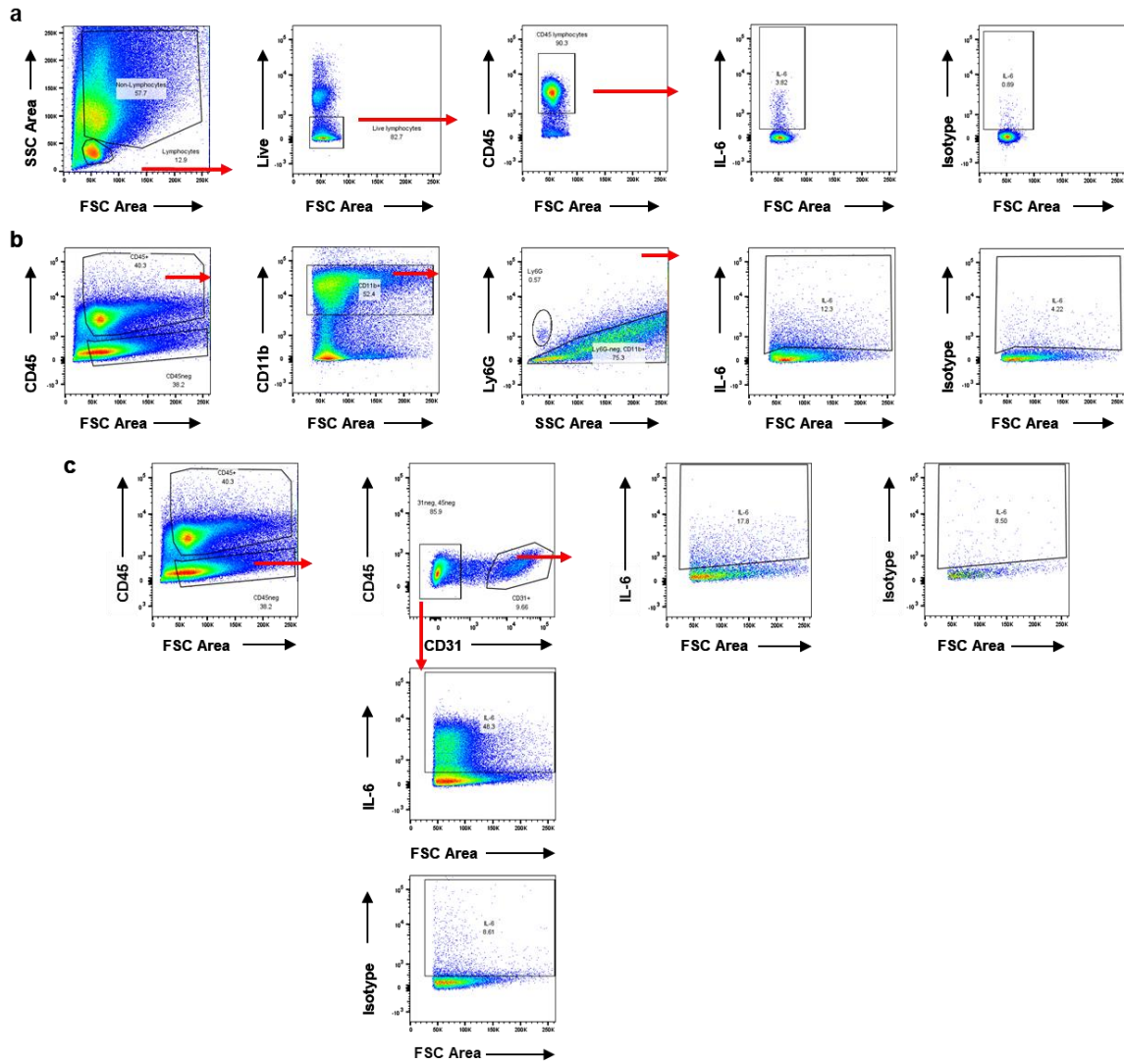


Fig. 3.17 Representative flow cytometry plots to identify IL-6 positive cells in stromal vascular cellular (SVFC) compartments. a) Lymphocytes, b) Myeloid cells, and c) Non-immune cells. Reproduced with permission from Springer Nature.

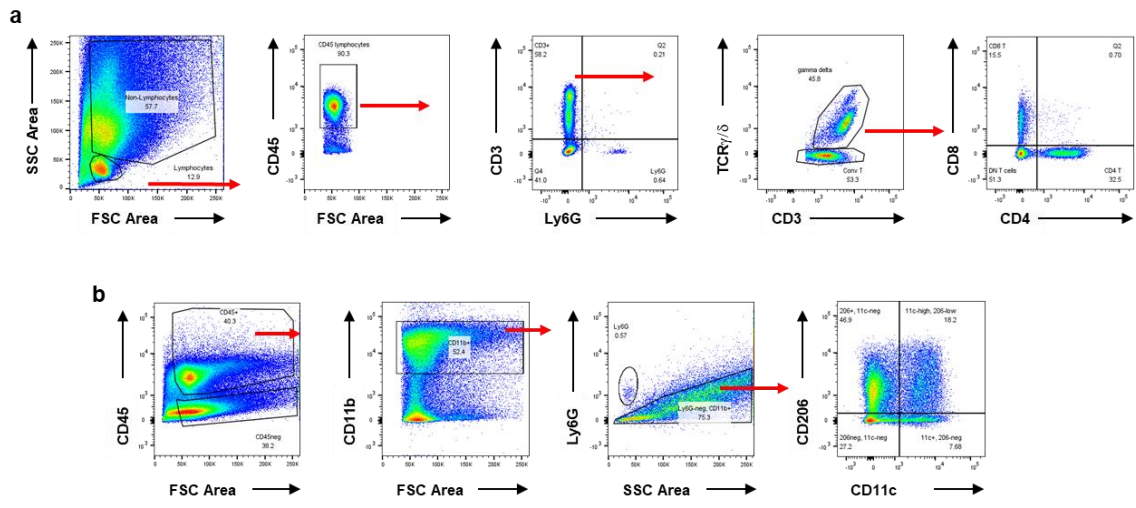


Fig. 3.18 Representative flow cytometry plots to identify immune cells among SVFC. a) lymphocyte and b) myeloid cell subsets. Reproduced with permission from Springer Nature.

3.3 Conclusions

$\gamma\delta$ T cells progressively accumulate over the lifespan in the VAT of mice and humans. The age-associated increase of $\gamma\delta$ T cells is consistent in both male and female mice. Furthermore, this accumulation is unique for VAT $\gamma\delta$ T cells as not observed in other tissues. Our data show that $\gamma\delta$ T cells accumulation is age-dependent and independent of adiposity at old age. However, this $\gamma\delta$ T cells accumulation is likely dependent on adiposity at middle age. The majority of $\gamma\delta$ T cells in VAT are IL-17A producing cells although both IL17A⁺ and IFN γ ⁺ $\gamma\delta$ T cells increase with aging. Studies with the genetic deletion mouse model (TCR δ KO) showed reduced systemic and local IL-6 levels in VAT and circulation compared to wild-type, which confirms that lack of $\gamma\delta$ T cells results in reduced inflammation. Preadipocytes/ADSC are the major IL-6 producing cells in VAT and mice lacking $\gamma\delta$ T cells have reduced number of IL-6⁺ preadipocytes/ADSC suggesting that $\gamma\delta$ T cells partly mediate IL-6 production from this cell type. Further mice lacking $\gamma\delta$ T cells have an altered immunophenotype with respect to other populations of lymphocytes and macrophages suggesting that $\gamma\delta$ T cells play a role in cellular homeostasis.

Chapter 4 THE CONTRIBUTIONS OF MIGRATION, PROLIFERATION AND APOPTOSIS IN AGE-ASSOCIATED $\gamma\delta$ T CELLS ACCUMULATION IN VAT

4.1 Objective

In the previous chapter my data demonstrated that $\gamma\delta$ T cells are resident in VAT where they show an age-associated increase in numbers and contribute to local and systemic chronic inflammation. However, maintenance of this population and mechanisms for the age-dependent accumulation are not known. The objective of this chapter was to understand the contributions of different physiological mechanisms to age-associated $\gamma\delta$ T cell accumulation in VAT. We first explored whether recruitment of peripheral $\gamma\delta$ T cells contributes to age-associated accumulation in VAT. In the absence of this finding, we shifted our focus to the tissue-resident population. Since tissue-resident immune cell numbers are tightly regulated by a balance between proliferation and programmed cell death, we further explored these processes to understand their impact on the increased VAT-resident $\gamma\delta$ T cell population in aging.

4.2 Results

4.2.1 Minimal peripheral migration of $\gamma\delta$ T cells was found in young and aged mice

Previous studies have reported VAT $\gamma\delta$ T cells in young mice to be a self-sustaining, tissue-resident population[45, 66]. Bruno et al 2022 previously showed that VAT $\gamma\delta$ T cells express tissue-resident memory phenotype in young and aged mice using surface markers[51]. However, as VAT of aged mice is known to produce increased levels of inflammatory cytokines and chemokines, we tested the hypothesis that the inflammatory microenvironment of aged VAT provides recruitment signals for peripheral $\gamma\delta$ T cells, which would contribute to accumulation. To address this hypothesis, we have used a parabiosis mouse model in which two animals are surgically conjoined for an extended period sharing the circulation. Recirculating cells will migrate into tissues between conjoined animals and establish equilibrium between the two, while tissue resident cells will not, demonstrating a lack of recirculation and peripheral migration.

For my study, isochronic parabiotic pairs of WT and TCR δ KO mice at both young and old age were used to evaluate peripheral $\gamma\delta$ T cell migration into VAT (Fig.4.1a). $\gamma\delta$ T cells in blood showed comparable chimerism between WT and TCR δ KO mice at both ages (Fig. 4.1b, young: 55.4 \pm 3.8% in WT vs 44.6 \pm 3.8% in KO; aged: 64.1 \pm 8.6% in WT vs 36 \pm 8.6% in KO) confirming the distribution of circulating cells and validating our model system. Interestingly, minimal recirculation of $\gamma\delta$ T cells was observed into the VAT of the TCR δ KO mouse from its WT pair for either age group (6.6 \pm 6.02% in young and 2.75 \pm 2.25% in the aged TCR δ KO) and there was no significant difference by aging (p=0.1239) (Fig. 4.1c) suggesting that $\gamma\delta$ T cells remain a self-sustaining tissue-resident population in VAT in both age groups. This is likely to be unique to VAT as we observed recirculation in liver (Fig. 4.1d young: 62.2 \pm 11.5% in WT vs 37.8 \pm 11.5% in KO; aged: 67.1 \pm 11.6% in WT vs 32.8 \pm 11.8% in KO) and spleen (Fig. 4.1e young: 60.2 \pm 3.5% in WT vs 39.8 \pm 3.5% in KO; aged: 54.5 \pm 12.2% in WT vs 45.5 \pm 12.2% in KO). From this study we concluded that peripheral migration plays a minimal role in the age-associated $\gamma\delta$ T cell accumulation, which requires exploring potential tissue specific mechanisms that would account for the age-associated $\gamma\delta$ T cells accumulation in VAT.

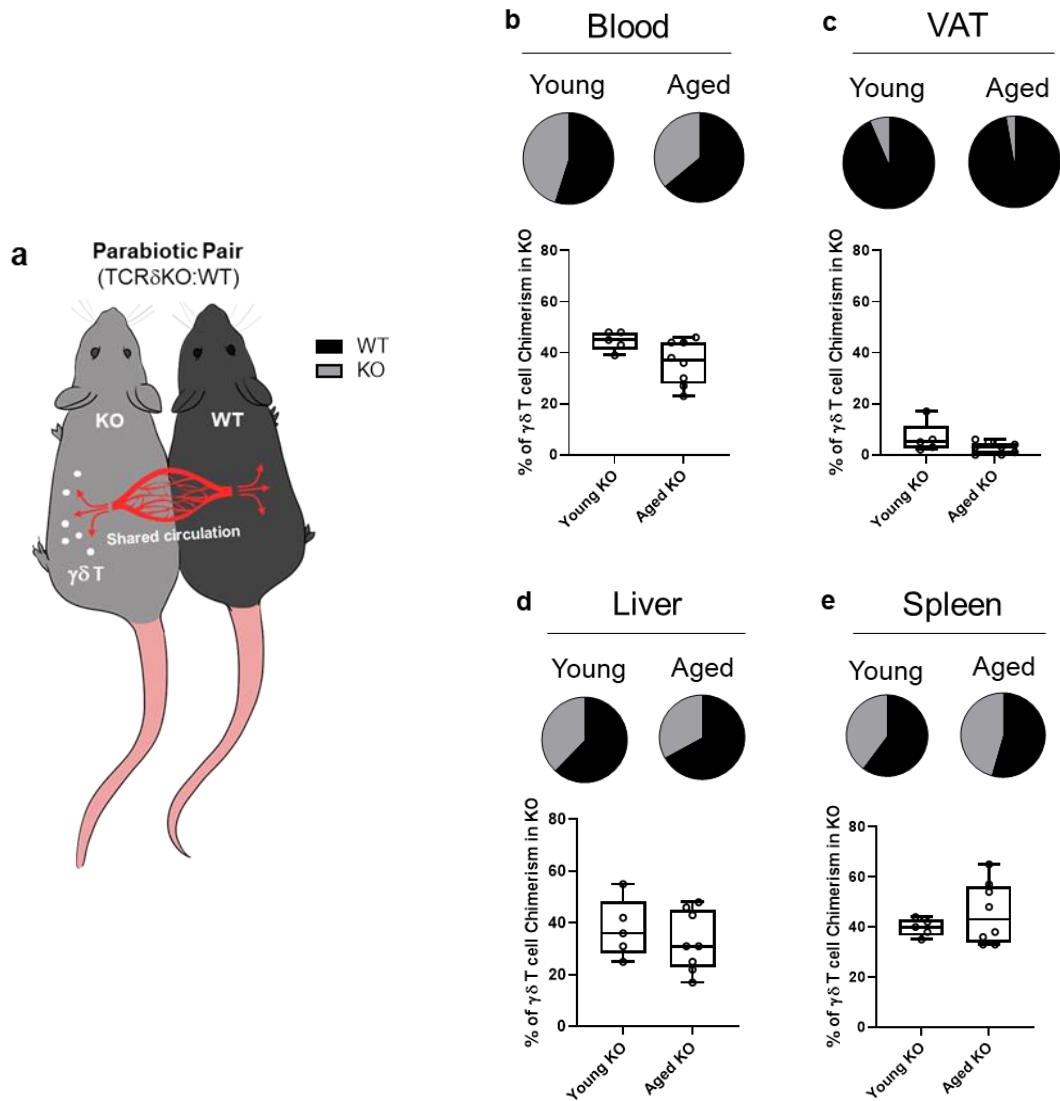


Fig. 4.1 Peripheral migration has a minimal role in age-associated $\gamma\delta$ T cell accumulation in VAT. $\gamma\delta$ T cell chimerism was evaluated 4 weeks after parabiosis surgery in young (n=5 WT:TCR δ KO pairs, 5-9mo old males) and aged (n=4 male pairs and n=4 female pairs, 21-24mo old; data from males and females were combined because no statistical differences were found between the sex groups) parabiotic pairs. (a) Representative diagram of isochronic parabiotic pairs. Average $\gamma\delta$ T cell chimerism in (b) Blood, (c) VAT, (d) Liver, and (e) Spleen for each genotype (WT and TCR δ KO) of the parabiotic pairs. Pie charts indicate the average proportion of $\gamma\delta$ T cells in each mouse of the parabiotic pair for both age groups. Proportions were calculated as the percentage of $\gamma\delta$ T cells in the KO (or WT) mouse over the sum of $\gamma\delta$ T cells in each WT and KO mouse of the parabiotic pair. Box plots show percent of $\gamma\delta$ T cells present in the TCR δ KO mouse pair at both age groups; each symbol represents an individual mouse, minimum to maximum values with bars representing the mean; Statistical differences were determined by two sample t-tests, no significant differences were observed. VAT: visceral adipose tissue.

4.2.2 Proliferating VAT-resident $\gamma\delta$ T cells increase in the aged

As *de novo* generation of $\gamma\delta$ T cells exists only in the thymus and peripheral recruitment to the VAT was minimal, we evaluated whether enhanced proliferation of tissue-resident $\gamma\delta$ T cells contributes to age-associated accumulation utilizing two different approaches: *in vivo* EdU incorporation and intracellular staining with the proliferation marker Ki67 (flow cytometry gating scheme shown in Fig. 4.2). Contrary to our hypothesis, the percentage of EdU⁺ $\gamma\delta$ T cells declined from young to aged (Fig. 4.3a, $p=0.0367$) suggesting that the proportion of proliferating to non-proliferating $\gamma\delta$ T cells decrease in the aged. The total number of EdU⁺ $\gamma\delta$ T cells per grams of VAT, however, showed a significant 6.3-fold increase in the aged (Fig. 4.3b, $p=0.0008$).

I subsequently utilized Ki67 as a proliferation marker and added middle-aged mice to further understand proliferation across the lifespan. The percentage of Ki67⁺ $\gamma\delta$ T cells (Fig. 4.3c) progressively declined from young to old age suggesting that the proportion of proliferating to non-proliferating $\gamma\delta$ T cells decrease by aging. The total number of Ki67⁺ $\gamma\delta$ T cells per gram of VAT, however, showed a significant 2-4-fold increase in the aged (Fig. 4.3d, young vs aged: 4.4-fold $p<0.0001$, middle-aged vs aged: 2.2-fold $p=0.0025$). No significant difference was found between young and middle aged ($p=0.2684$).

T_{conv} cells showed similar results. The percentage of EdU⁺ T_{conv} cells declined from young to aged (Fig. 4.4a), whereas the total number per grams of VAT increased in the aged (Fig 4.4b). Analyzing proliferation in three age groups revealed that the percentage of Ki67⁺ T_{conv} cells also declined from youth to middle age without any further change at old age (Fig. 4.4c). The total number of Ki67⁺ T_{conv} cells per gram of VAT, showed a significant 5-6-fold increase in the aged (Fig. 4.4d) without any significant difference between young and middle aged.

A comparison study in the lymph nodes revealed that the percentage of Ki67⁺ $\gamma\delta$ T cells in LN remain unchanged over the lifespan (Fig 4.5a) while the percentage of Ki67⁺ T_{conv} cells showed an increase in the aged (Fig. 4.5b). The total number of Ki67⁺ $\gamma\delta$ T cells significantly increased in the aged (Fig 4.5c) which was not found for T_{conv} cells (Fig. 4.5d).

Collectively, these results suggest that although, the proportion of proliferating to non-proliferating cells is reduced in the aged, the total number of proliferating cells within the population is increased in the aged and are likely contributing to the age-associated $\gamma\delta$ T cell accumulation.

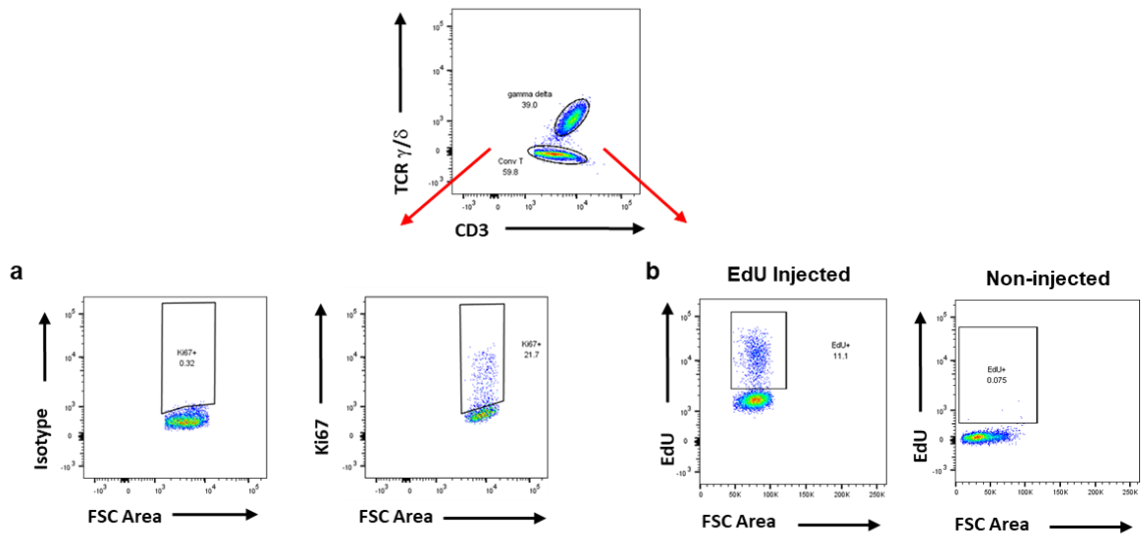


Fig. 4.2 Representative flow cytometry plots for proliferating T cells. a) Gating scheme for Ki67+ $\gamma\delta$ T and T_{conv} cells. b) Gating Scheme for EdU+ $\gamma\delta$ T and T_{conv} cells in EdU injected and non-injected mice.

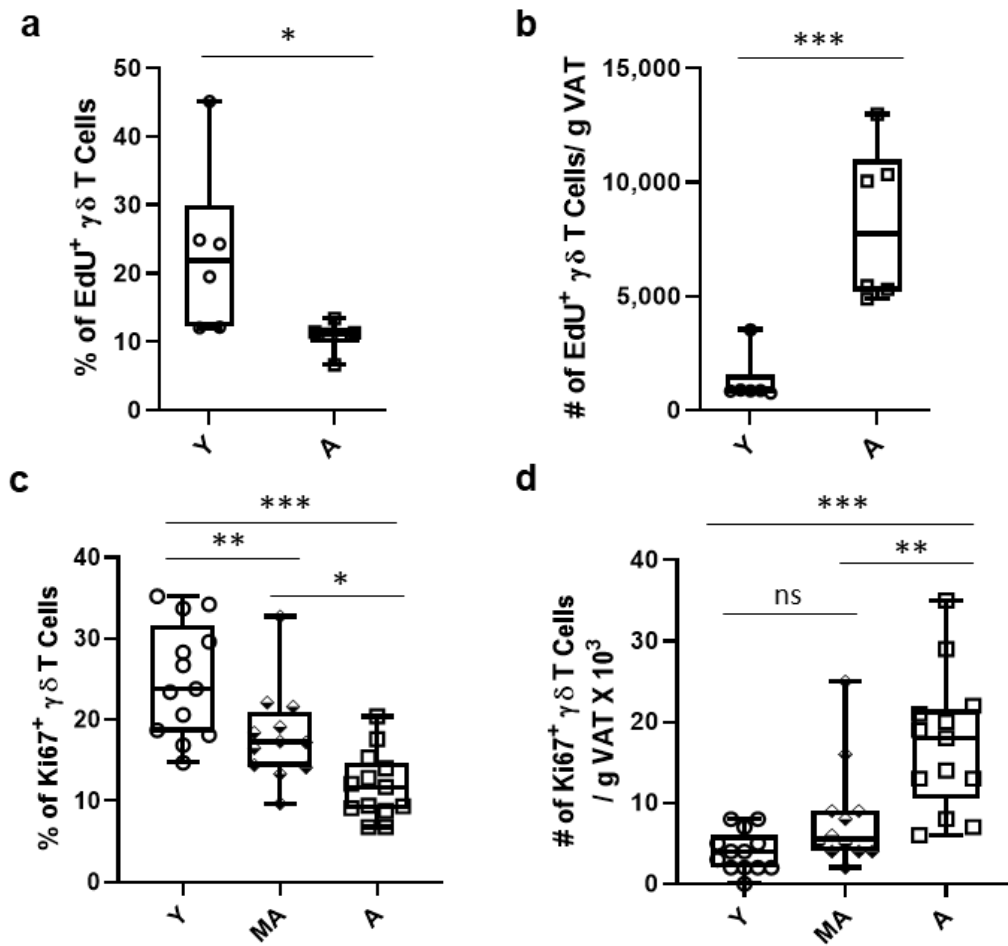


Fig. 4.3 Proliferating $\gamma\delta$ T cell profiling in VAT with aging. a) Percentage and b) number per gram of VAT of EdU⁺ $\gamma\delta$ T cells in young (n=6, 4mo), and aged (n=6, 23mo) male mice. c) Percentage and d) number per gram of VAT of Ki67⁺ $\gamma\delta$ T cells in young (Y, n=13, 4-6mo), middle aged (MA, n=12, 12-16mo) and aged (A, n=13, 21-25mo) male mice. Data are expressed in box plots from minimum to maximum values with bars representing the mean; each symbol represents an individual mouse. Statistical differences were determined by one way ANOVA with Tukey Honest Significant difference for multiple comparisons. *p<0.05, **p<0.01, ***p<0.001. VAT: visceral adipose tissue; EdU: 5-ethynyl-2'-deoxyuridine.

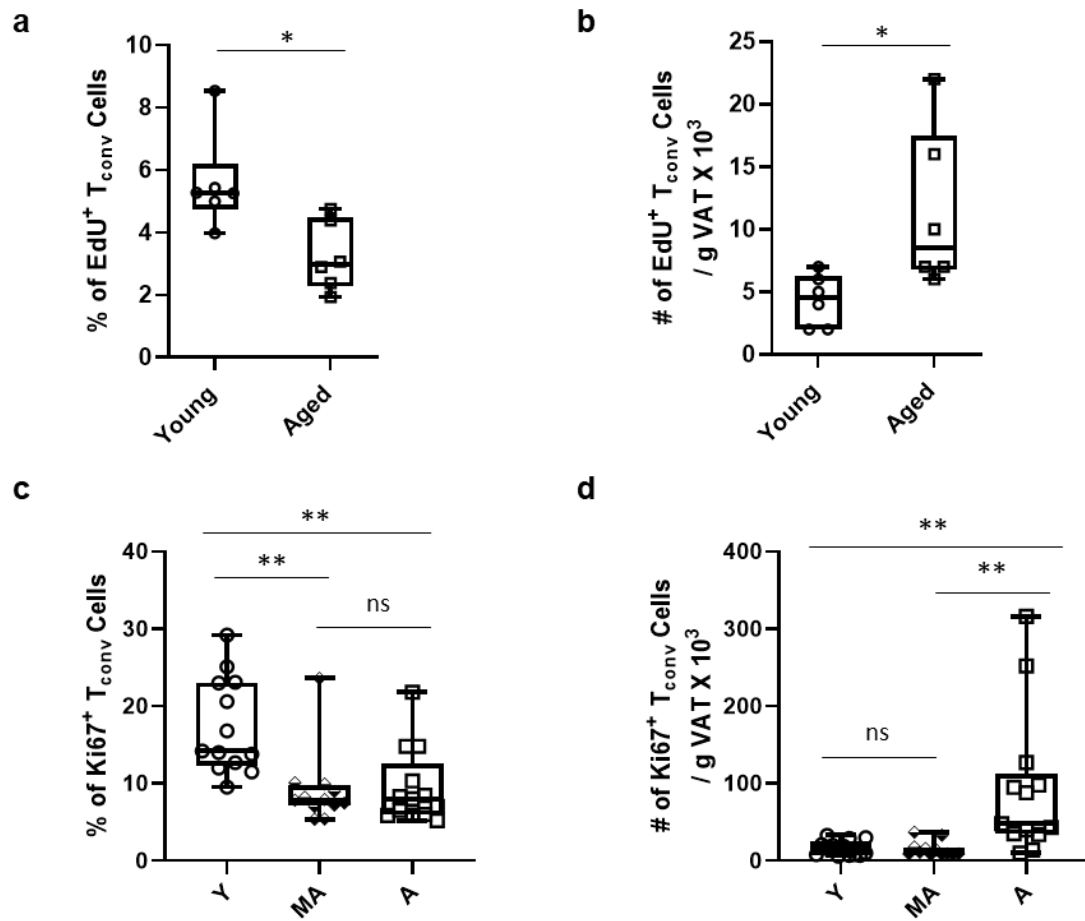


Fig. 4.4. Proliferating T_{conv} cell profiling in VAT with aging. (a) Percentage and (c) number of EdU⁺ T_{conv} cells per gram of VAT in young (n=6, 4mo), and aged (n=6, 23mo) male mice. (d) Percentage and (e) number of Ki67⁺ T_{conv} cells per gram of VAT in young (Y, n=13, 4-6mo), middle aged (MA, n=12, 12-16mo) and aged (A, n=13, 21-25mo) male mice. Data are expressed in box plots from minimum to maximum values with bars representing the mean; each symbol represents an individual mouse. Statistical differences were determined by one way ANOVA with Tukey Honest Significant difference for multiple comparisons. *p<0.05, **p<0.01, ***p<0.001. EdU: 5-ethynyl-2'-deoxyuridine; VAT: visceral adipose tissue.

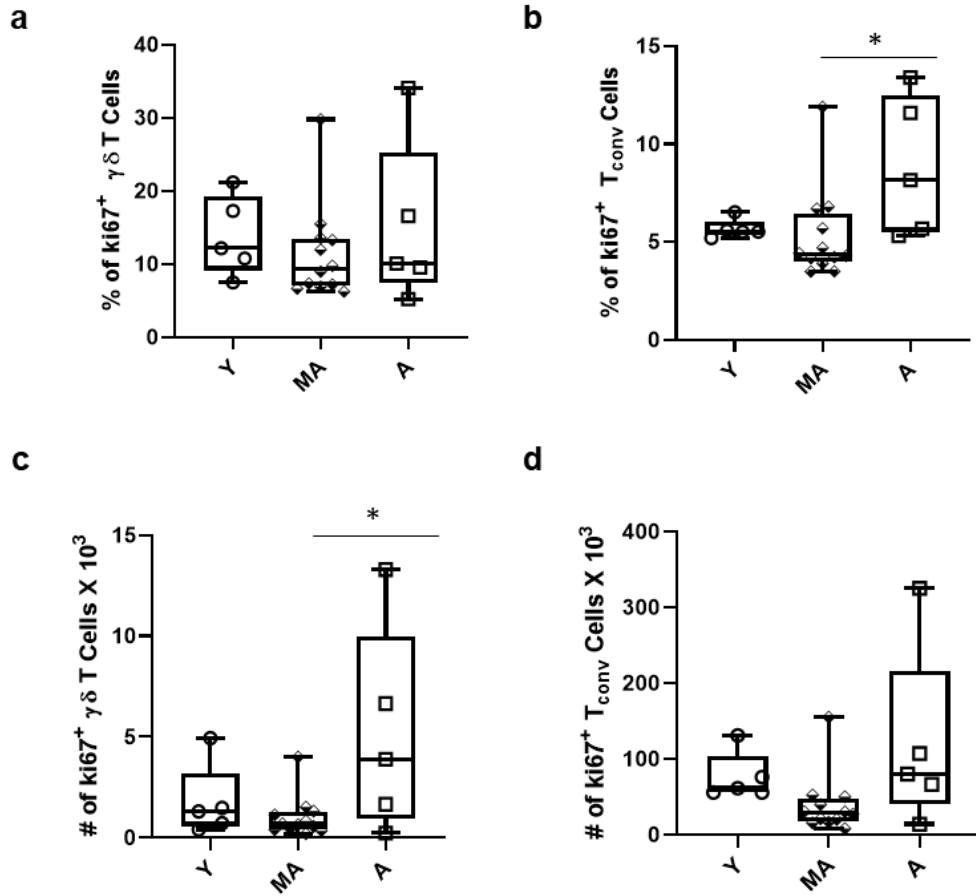


Fig. 4.5 Proliferating $\gamma\delta$ T and T_{conv} cell profiling in LN with aging. (a-b) Percentage and (c-d) number of $Ki67^+$ $\gamma\delta$ T and T_{conv} cells in LN T in young (Y, n=5, 4-6mo), middle aged (MA, n=12, 12-16mo) and aged (A, n=5, 21-25mo) male mice. Data are expressed in box plots from minimum to maximum values with bars representing the mean; each symbol represents an individual mouse. Statistical differences were determined by one way ANOVA with Tukey Honest Significant difference for multiple comparisons. * $p < 0.05$, ** $p < 0.01$, *** $p < 0.001$. LN: Lymph node.

4.2.3 Apoptosis of VAT-resident $\gamma\delta$ T cells declines at middle age

To understand whether aging influences VAT-resident $\gamma\delta$ T cell turnover, we analyzed apoptosis via caspase 3/7 activity. Caspase 3/7-positive cells are considered apoptotic cells. The proportion of apoptotic $\gamma\delta$ T cells significantly declined at middle-aged compared to young without any further change in the aged (Fig 4.6a). A concomitant increase in the proportion of live cells was also observed starting at middle aged (Fig 4.6b) suggesting that $\gamma\delta$ T cells are protected from apoptosis from middle-age onwards thus contributing to age-associated accumulation. However, the absolute number of both apoptotic and live $\gamma\delta$ T cells, after adjusting for fat mass was significantly higher in the old-age compared to other age groups, likely due to higher number of cells in this age group (Fig 4.6c-d).

To address the roles of anti-apoptotic proteins in $\gamma\delta$ T cell survival, apoptosis was induced by treating VAT SVF cells with a combination of two Bcl-2 family inhibitors called ABT737 (inhibitor of Bcl-2, Bcl-x1, and Bcl-w) and S63845 (inhibitor of Mcl-1). Apoptosis via caspase 3/7 activity in $\gamma\delta$ T cells was compared between control (treated with DMSO) and inhibitor-treated cells (Fig 4.6e). A significant induction of apoptosis was observed in young $\gamma\delta$ T cells upon BCL2 family inhibition (Fig. 4.6f). In contrast, no induction of apoptosis was observed in middle age suggesting that $\gamma\delta$ T cells are protected from apoptosis in the middle-aged via another anti-apoptotic mechanism. Interestingly, $\gamma\delta$ T cells from old mice showed blunted apoptotic induction compared to young which did not achieve the complete blocking of apoptosis observed at middle-age.

As a comparison, T_{conv} cells showed a significant decline in the proportion of apoptotic cells from young to middle age and an increase from middle age to old age (Fig 4.7a). Concomitantly, the proportion of live T_{conv} cells increased from young to middle age and then decreased from middle to old age (Fig 4.7b). The absolute number of apoptotic and live T_{conv} cells after adjusting for fat mass showed similar results to $\gamma\delta$ T cells (Fig 4.7c-d). Regarding the role of specific anti-apoptotic proteins inhibited by ABT737 and S63845 on the turnover of T_{conv} cells, a significant induction of apoptosis was observed in

all age groups in the presence of the inhibitors, suggesting that T_{conv} cells in VAT are not protected from apoptosis by these specific proteins (Fig 4.7e).

A comparative, study in the lymph nodes showed an increase in the proportion of apoptotic $\gamma\delta$ T cells at old age (Fig 4.8a), with a concomitant decline in the percentage of live cells (Fig 4.8b). However, the total number of both apoptotic (Fig 4.8c) and surviving cells (Fig 4.8d) did not significantly change over the lifespan. An induction of apoptosis was observed only in the young $\gamma\delta$ T cells and were absent in the other age groups (Fig 4.8e). T_{conv} cells in lymph nodes also showed an increase of apoptosis at old age compared to middle age (Fig 4.9a) with a concomitant decline in the percentage of live cells (Fig 4.9b). The total number of apoptotic cells declined in middle age compared to young without further changes into old age (Fig 4.9c). Total number of surviving cells showed a decline from young to old age, however, no change was observed in the middle age group (Fig 4.9d). Induction of apoptosis by selectively inhibiting several anti-apoptotic proteins was observed in young and old age but was not present in middle age (Fig 4.9e).

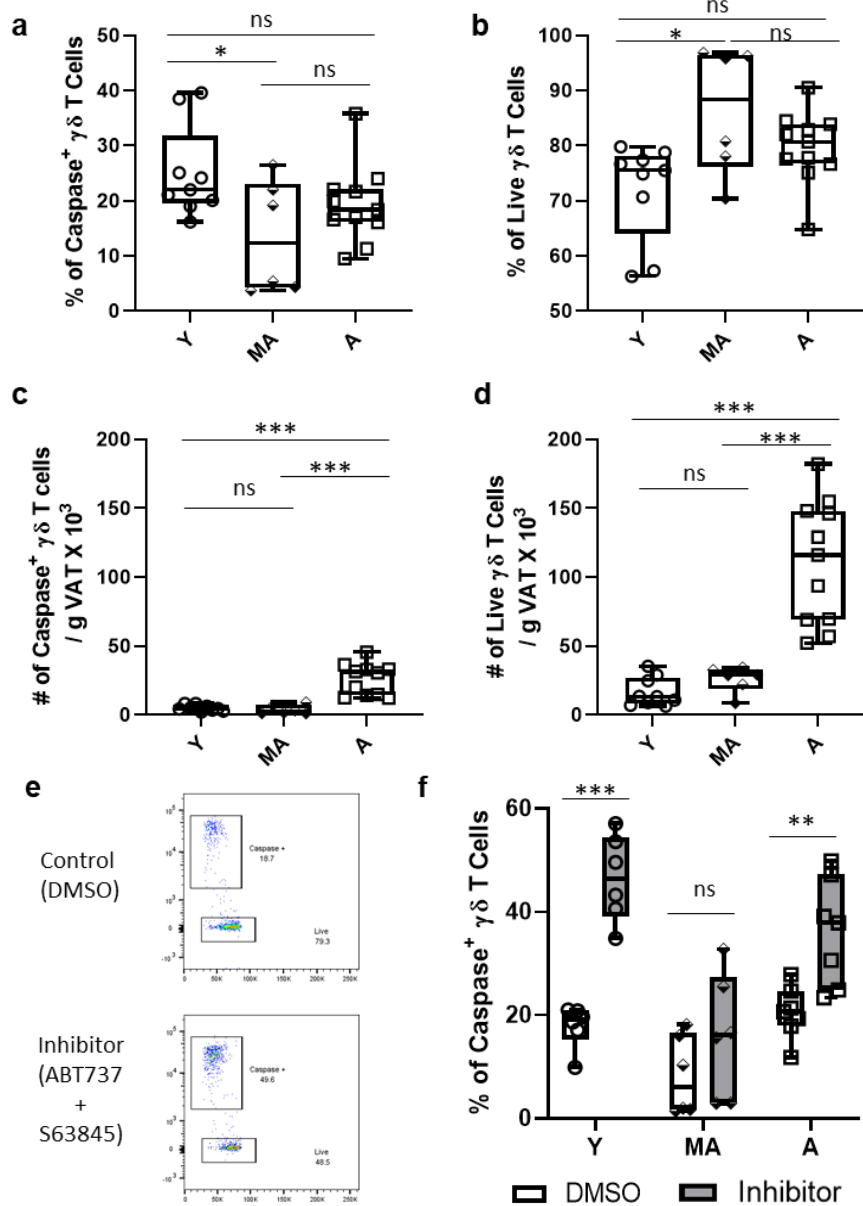


Fig. 4.6 $\gamma\delta$ T cells in VAT are protected from apoptosis at the middle age. (a-b) Percentage and (c-d) number per gram of VAT of apoptotic (Caspase 3/7⁺) and live (Caspase 3/7^{neg}) $\gamma\delta$ T cells in young (Y, n=9, 4mo), middle age (MA, n=6, 12mo) and aged (A, n=11, 22mo) male mice. (e) Flow cytometry plots of $\gamma\delta$ T cells treated with DMSO (control) and Bcl2 inhibitors following analysis of (f) activated caspase 3/7 expression in $\gamma\delta$ T cells in young (Y, n=6, 4mo), middle age (MA, n=6, 12mo) and aged (A, n=7, 22mo) male mice. Data are expressed in box plots from minimum to maximum values with bars representing the mean; each symbol represents an individual mouse. Statistical differences were determined by one way ANOVA with Tukey Honest Significant difference for multiple comparisons and Paired T test. *p<0.05, **p<0.01, ***p<0.001. VAT: visceral adipose tissue; g: gram.

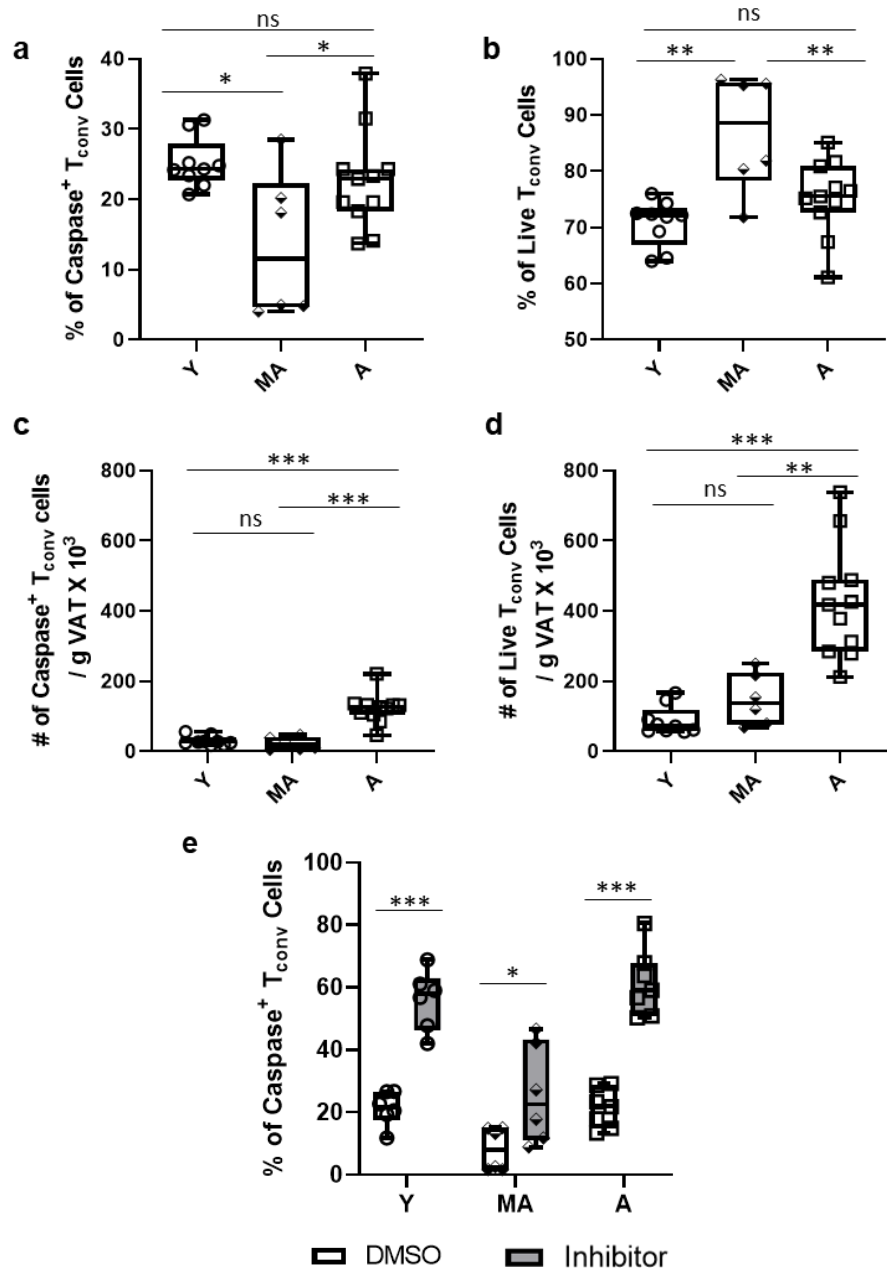


Fig. 4.7 Analysis of apoptosis in T_{conv} cells in VAT with aging. (a-b) Percentage and (c-d) number per gram of VAT of apoptotic (Caspase 3/7⁺) and live (Caspase 3/7^{neg}) T_{conv} cells in young (Y, n=9, 4mo), middle age (MA, n=6, 12mo) and aged (A, n=11, 22mo) male mice. (e) T_{conv} cells treated with DMSO (control) and Bcl-2 inhibitors following analysis of activated caspase 3/7 expression in T_{conv} cells in young (Y, n=6, 4mo), middle age (MA, n=6, 12mo) and aged (A, n=7, 22mo) male mice. Data are expressed in box plots from minimum to maximum values with bars representing the mean; each symbol represents an individual mouse. Statistical differences were determined by one way ANOVA with Tukey Honest Significant difference for multiple comparisons. *p<0.05, **p<0.01, ***p<0.001. VAT: visceral adipose tissue; g: gram.

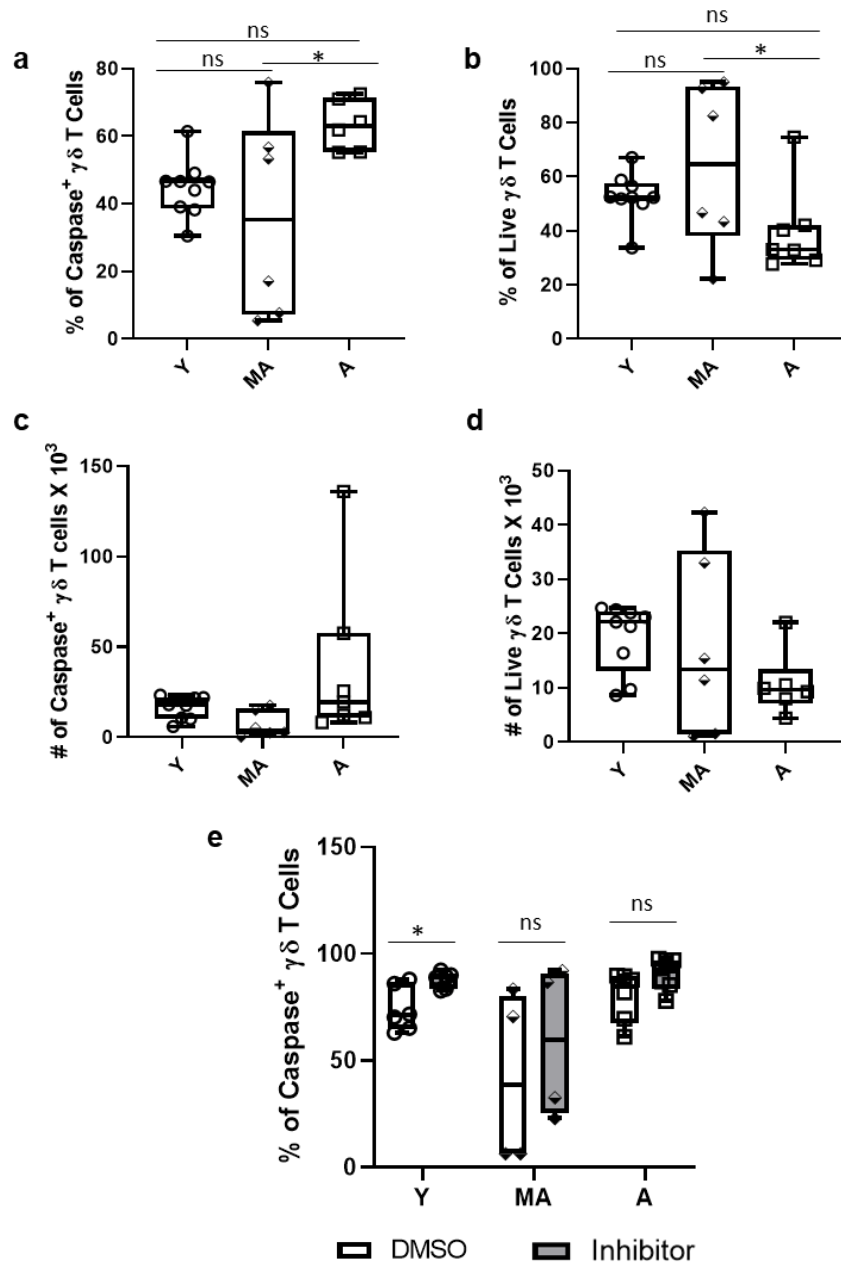


Fig. 4.8 Analysis of apoptosis in $\gamma\delta$ T cells in LN with aging. (a-b) Percentage and (c-d) number of apoptotic (Caspase 3/7⁺) and Live (Caspase 3/7^{neg}) $\gamma\delta$ T cells in LN in young (Y, n=9, 4mo), middle age (MA, n=6, 12mo) and aged (A, n=11, 22mo) male mice. (e) $\gamma\delta$ T cells treated with DMSO (control) and Bcl-2 inhibitors following analysis of activated caspase 3/7 expression in $\gamma\delta$ T cells in young (Y, n=6, 4mo), middle age (MA, n=6, 12mo) and aged (A, n=7, 22mo) male mice. Data are expressed in box plots from minimum to maximum values with bars representing the mean; each symbol represents an individual mouse. Statistical differences were determined by T-test and one way ANOVA with Tukey Honest Significant difference for multiple comparisons. *p<0.05, **p<0.01, ***p<0.001. LN: Lymph node.

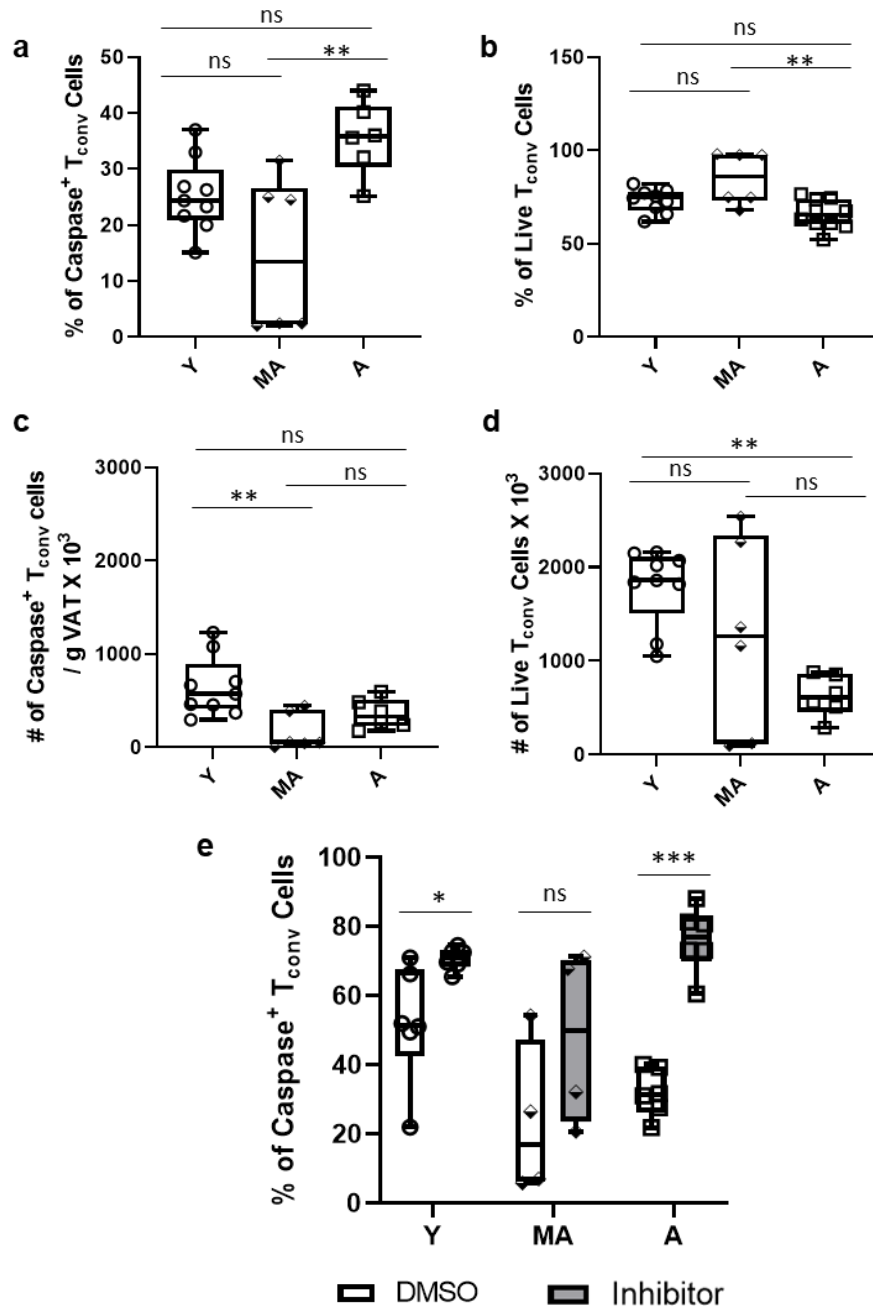


Fig. 4.9 Analysis of apoptosis in T_{conv} cells in LN with aging. (a-b) Percentage and (c-d) number per gram of VAT of apoptotic (Caspase 3/7⁺) and Live (Caspase 3/7^{neg}) T_{conv} cells in young (Y, n=9, 4mo), middle age (MA, n=6, 12mo) and aged (A, n=11, 22mo) male mice. (e) T_{conv} cells treated with DMSO (control) and Bcl-2 inhibitors following analysis of activated caspase 3/7 expression in T_{conv} cells in young (Y, n=6, 4mo), middle age (MA, n=6, 12mo) and aged (A, n=7, 22mo) male mice. Data are expressed in box plots from minimum to maximum values with bars representing the mean; each symbol represents an individual mouse. Statistical differences were determined by T-test and one way ANOVA with Tukey Honest Significant difference for multiple comparisons. * $p < 0.05$, ** $p < 0.01$, *** $p < 0.001$ LN: Lymph

4.3 Conclusions

In vivo parabiosis study between WT and TCR δ KO mice at both young and old age groups demonstrated a minimal recruitment of peripheral $\gamma\delta$ T cells into VAT without a significant change by aging, suggesting a minor contribution of migration to $\gamma\delta$ T cell accumulation with aging. However, it is impossible to eliminate the contribution of migrating $\gamma\delta$ T cells into VAT, as the small number of cells that do migrate into VAT may account for some accumulation over the lifespan.

Analyses of proliferation showed that the absolute number of proliferating $\gamma\delta$ T cells significantly increase in the aged VAT compared to young and middle age, indicating that an increase in the local proliferating $\gamma\delta$ T cell population contributes to age-associated accumulation. A protection from age-associated apoptosis was observed not only in $\gamma\delta$ T cells as well as T_{conv} cells in VAT, which resulted in a concomitant increase of the surviving population. This data indicates that lymphocytes in the aged VAT are likely to escape apoptosis. Furthermore, selective inhibition of several anti-apoptotic proteins revealed that the apoptosis in VAT $\gamma\delta$ T cells is regulated by differential mechanisms, which correspond to particular age groups over the lifespan. Collectively, these data suggest that increased number of proliferating $\gamma\delta$ T cells and increased survival due to a protection from apoptosis starting at middle age that continued into old age are the primary contributors to $\gamma\delta$ T cell accumulation in VAT with aging. However, a minor contribution of peripheral migration cannot be excluded.

Chapter 5 THE SUBPOPULATIONS OF $\gamma\delta$ T CELLS IN VAT

5.1 Objective

Unlike conventional T cells which display the $\alpha\beta$ TCR, $\gamma\delta$ TCR consists of one γ and one δ chain. There are different subtypes of $\gamma\delta$ T cells due to V(D)J recombination. My γ/δ -TCR profiling study is based on Heilig & Tonegawa nomenclature[73]. Previous studies in adipose tissue of young mice detected the expressions of $V\gamma 1$, $V\gamma 2$, $V\gamma 4$, $V\gamma 6$ and $V\delta 1$, $V\delta 3$, $V\delta 4$ genes by PCR indicating the presence of these subtypes[50]. Flow cytometric analyses confirmed that VAT of young mice is primarily composed of $V\gamma 6^+$ cells, while $V\gamma 1^+$ and $V\gamma 4^+$ cells appear in low abundance[45]. The objective of this chapter is to further characterize $\gamma\delta$ T cells in the aged VAT by determining which subpopulations of $\gamma\delta$ T cells are altered by aging.

5.2 Results

5.2.1 TCR- $V\gamma/V\delta$ profiling by PCR

The $\gamma\delta$ T cells in VAT were characterized by evaluating the gene expressions of different gamma (γ) and delta (δ) chains which constitute different subpopulations of $\gamma\delta$ T cells based on the rearrangements of the TCR with γ and δ chains. Pooled (n=4) PCR products for young (5mo) and aged (25mo) mice were used to identify the presence of the following subsets of $\gamma\delta$ T cells in the VAT: $V\gamma 1$, $V\gamma 2$, $V\gamma 4$, $V\gamma 5$, $V\gamma 6$, $V\gamma 7$ and $V\delta 1$, $V\delta 2$, $V\delta 3$, $V\delta 4$, $V\delta 6$. Blood and spleen were used for comparison (Fig 5.1). Based on this gene expression analysis, $\gamma 6$ and $\gamma 7$ appear to be the most abundant gamma chains in VAT while $\delta 1$ is the most abundant delta chain. An age-associated increase in expression was observed for $\gamma 1$, $\gamma 2$, $\gamma 4$, and $\gamma 6$ suggesting that these subpopulations may be increased by aging. In comparison, similar to VAT, $\gamma 6$ and $\gamma 7$ appear to be the most abundant gamma chains in blood as well, while $\delta 1$ and $\delta 4$ expressions were observed. An age-associated increase in expression was observed for $\gamma 2$ and $\gamma 6$ suggesting that these subpopulations may be increased by aging in blood. An age-associated decrease in expression was

observed for $\gamma 5$, $\delta 1$ and $\delta 4$ suggesting that these subpopulations may be decreased by aging in blood. $V\gamma 2$, $V\gamma 4$, $V\gamma 6$, appear to be the most abundant gamma chains in spleen and $\delta 1$, and $\delta 6$ is the most abundant delta chain. An age-associated increase in $\gamma 5$ was observed suggesting an increase of this populations, while age-associated decrease in expression was observed for $\delta 2$, $\delta 3$ and $\delta 6$ suggesting that these subpopulations may be decreased by aging in spleen. Individual samples were also analyzed to understand the variability among the mice and the gene expressions showed similar results to the pooled samples (Fig. 5.2).

The T_m was adjusted for individual primers. Of note, a smear was observed in several lanes i.e., $V\gamma 1$, $V\delta 4$ along with a band at the predicted size[87], suggesting the presence of multiple subpopulations within the $V\gamma 1$ and $V\delta 4$ populations as per Mehta et al[50]. A limitation of my study is that all the PCR reactions had equal number (38 cycles) of cycles which may have caused oversaturation for several bands. Further optimization of PCR cycles for individual genes may resolve this issue.

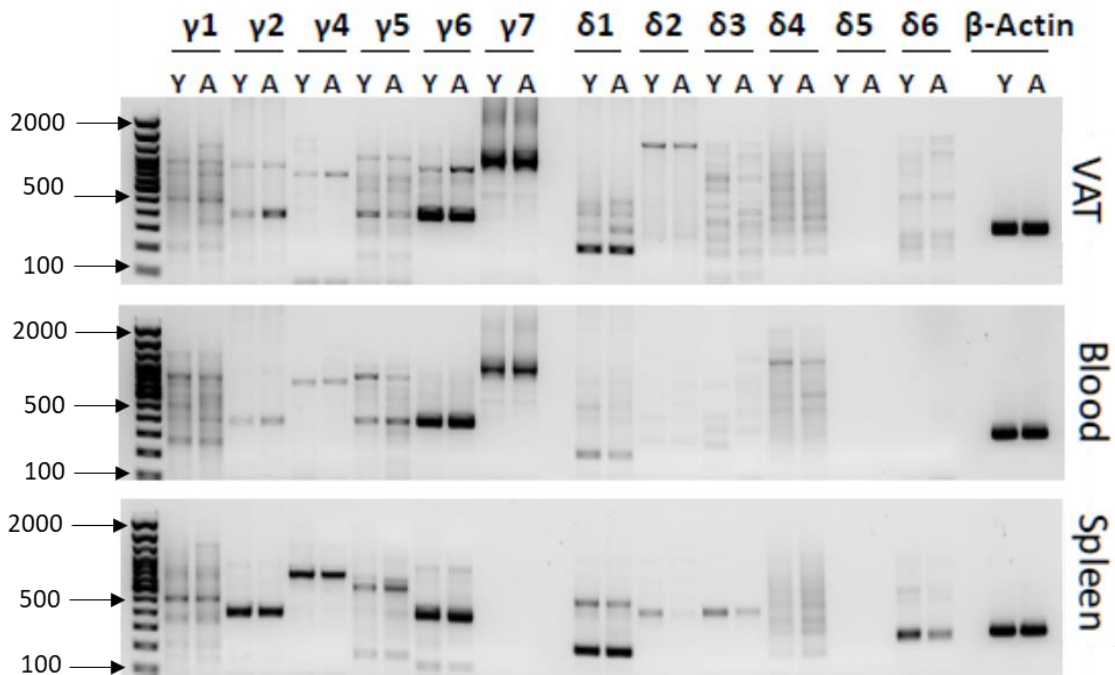
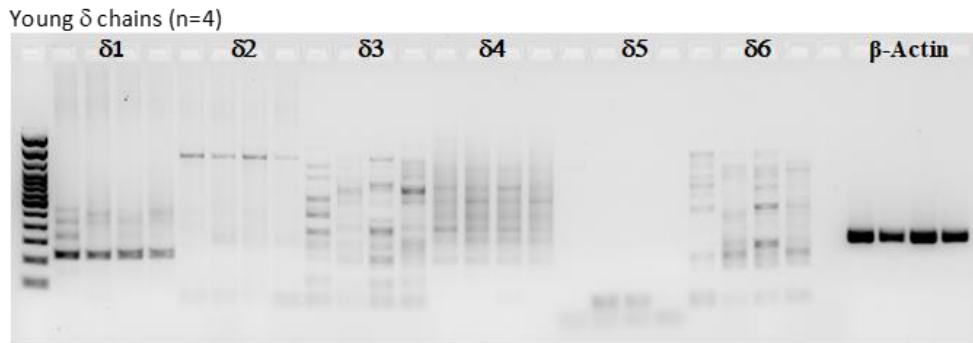
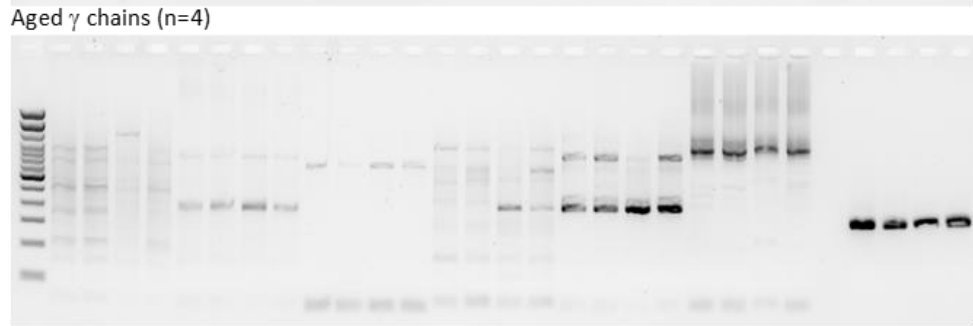
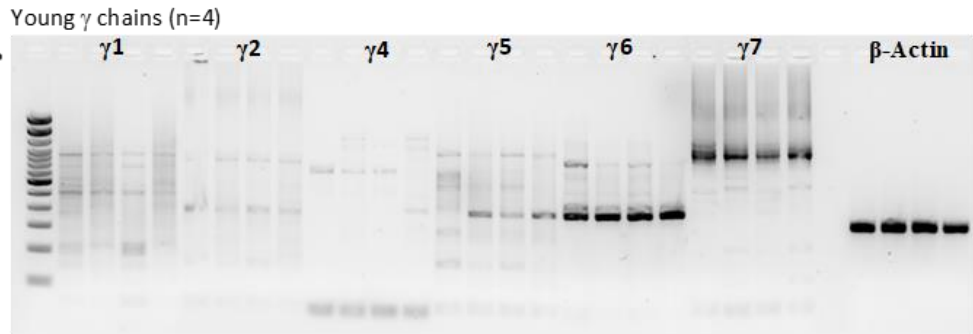


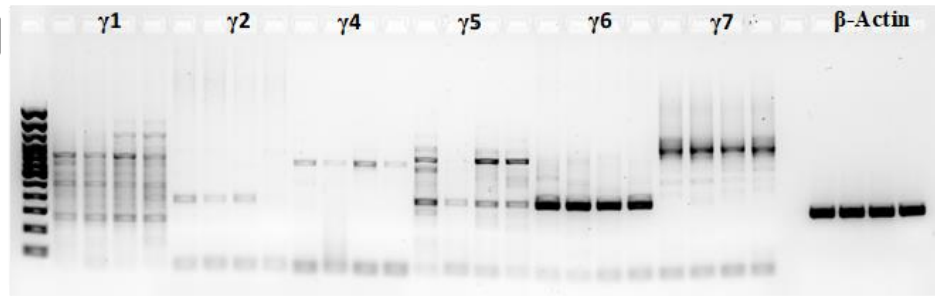
Fig. 5.1 Age-associated comparison of relative gene expressions of γ - δ chains by PCR. Data shown in VAT, blood, and spleen with pooled (n=4) samples of young (5mo) and aged (25mo) mice. Y: Young, A: Aged

a) VAT

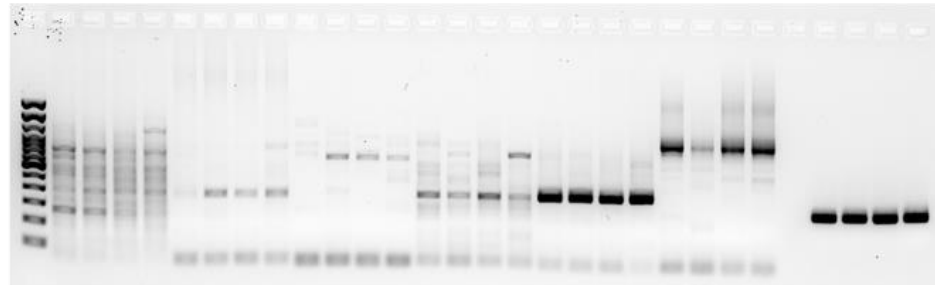


b) Blood

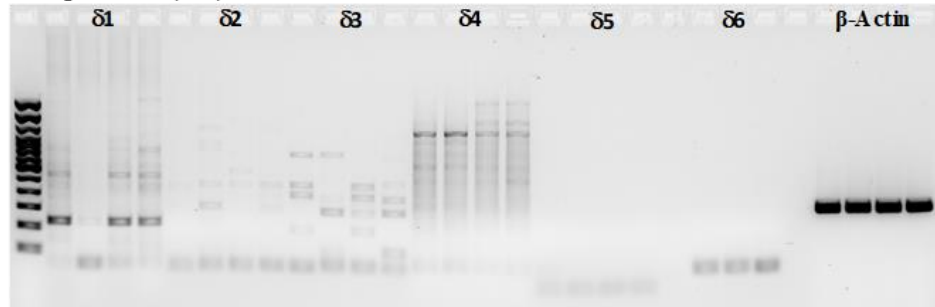
Young- γ Chains (n=4)



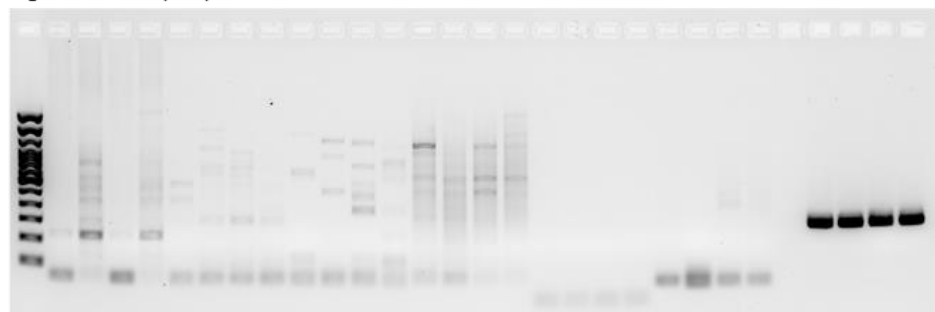
Aged- γ Chains (n=4)



Young- δ Chains (n=4)



Aged- δ Chains (n=4)



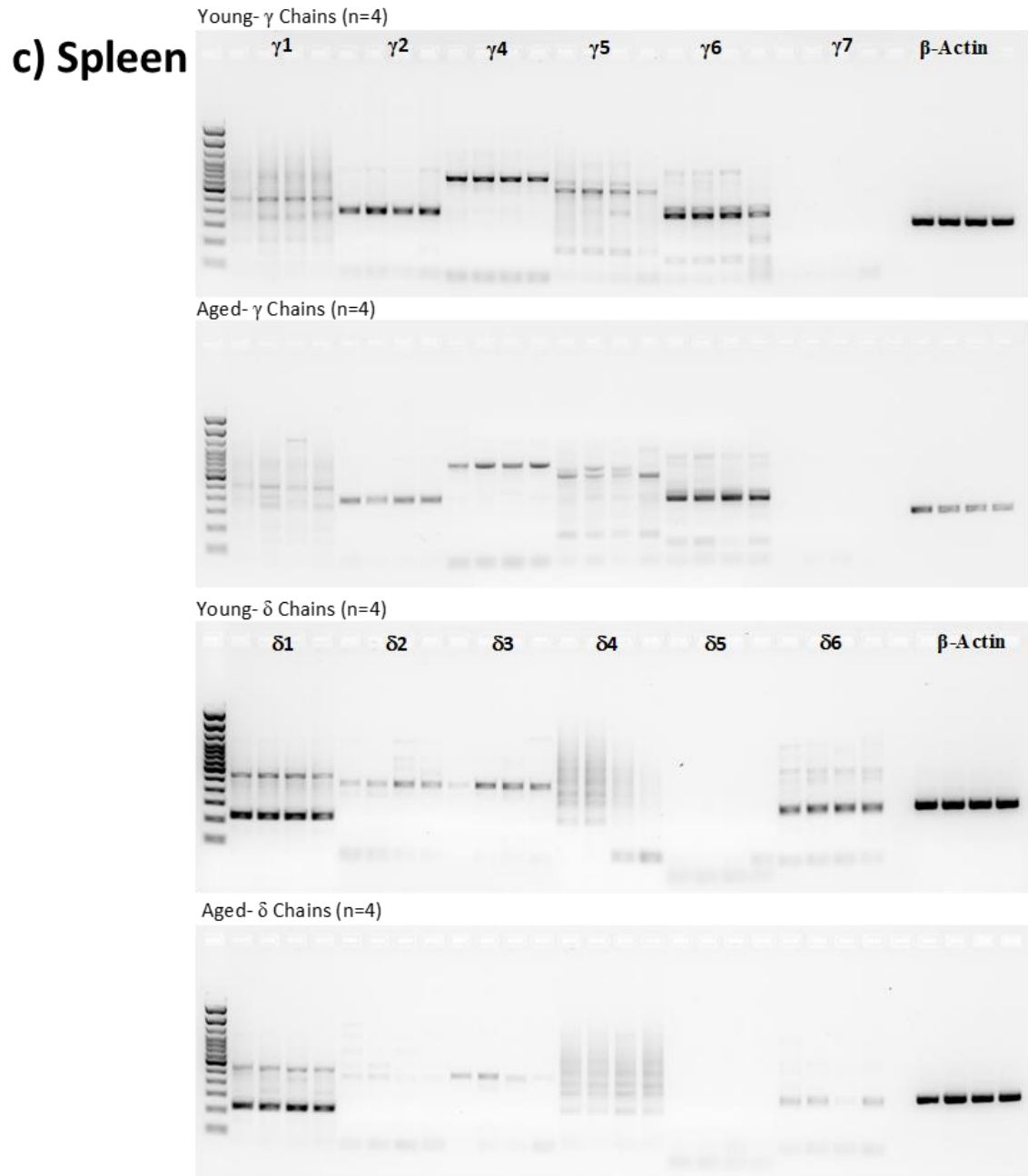


Fig. 5.2 Gene expression analysis on individual samples by PCR. Data shown in young (n=4, 5mo) and aged mice (n=4, 25mo). a) VAT b) Blood c) Spleen.

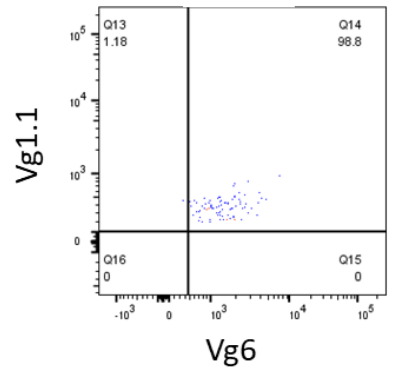
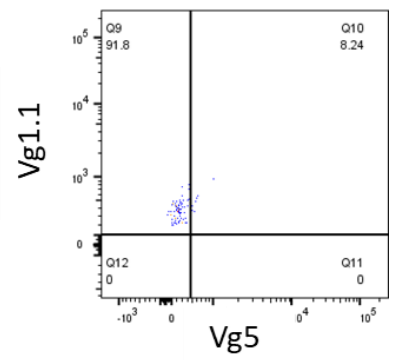
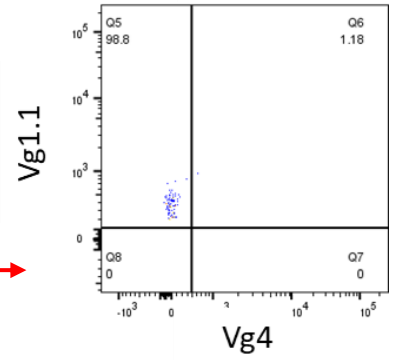
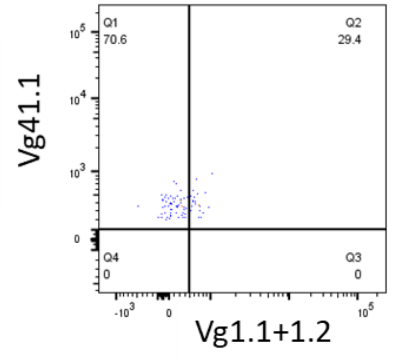
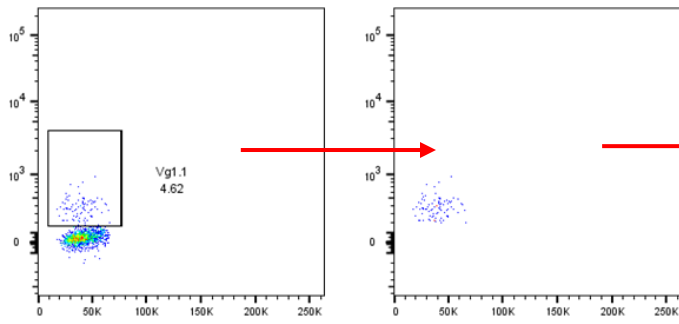
5.2.2 TCR-V γ /V δ profiling by flow cytometry

After identifying the gene expressions of different subpopulations in VAT, the next goal was to quantify $\gamma\delta$ T cells subpopulations in VAT in different age groups. I performed flow cytometry analysis in an attempt to determine the specific subpopulations that are increased in number in the aged. Surface staining was performed to the SVF cells with commercially available antibodies specific to V γ 1, V γ 2, V γ 4, V γ 5, V γ 6 (Table 5.1). However, several experiments in different tissues revealed that the commercially available antibodies lack specificity. Each of these antibodies must bind to a unique constant region of each gamma chain to provide a single-positive expression for individual subpopulations. In reality, all of the antibodies for each gamma chain showed co-expression with one or more antibodies for other chains (Fig 5.3a-e) demonstrating non-specific binding. With this technical limitation and lack of other commercially available antibodies, I was unable to reach reliable conclusions from this study.

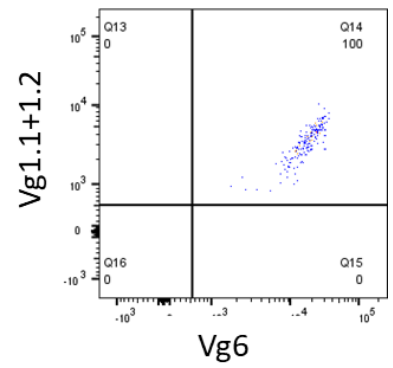
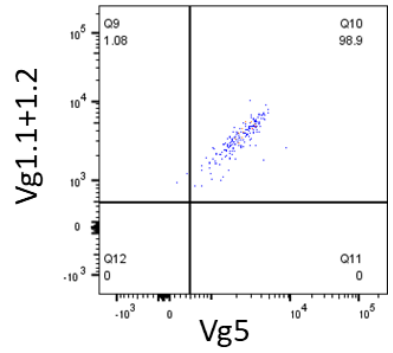
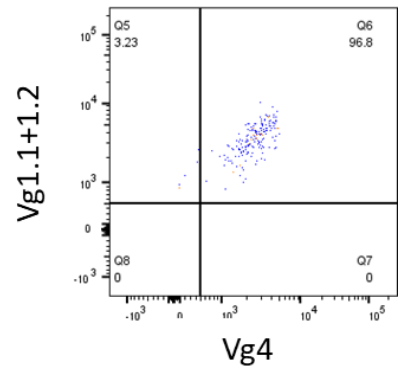
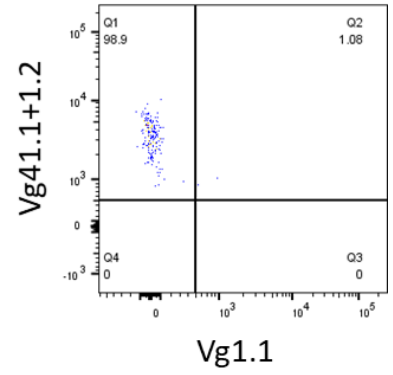
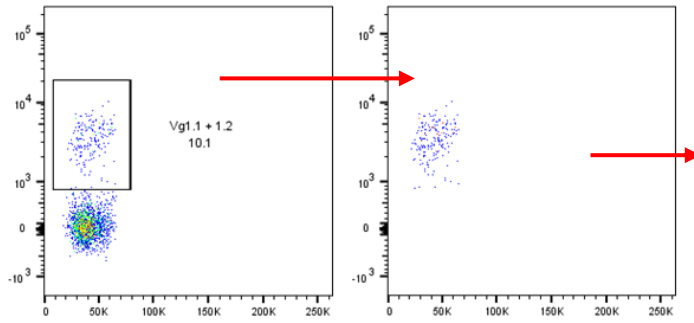
Table 5.1 Antibodies used for the Flow cytometry studies with γ chains.

Antigen	Conjugate	Manufacturer	Identifier
Mouse			
V γ 1(V γ 1.1)	FITC	BioLegend	141103
V γ 1 and 2(V γ 1.1+ V γ 1.2)	PE	BioLegend	142703
V γ 4	PerCP/Cyanine5.5	BioLegend	137711
V γ 5	APC	BioLegend	137505
V γ 6	Purified	BioLegend	160602
V γ 7	Purified	BioLegend	161702

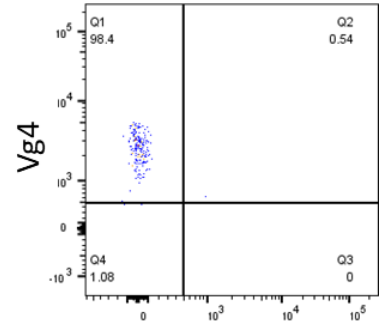
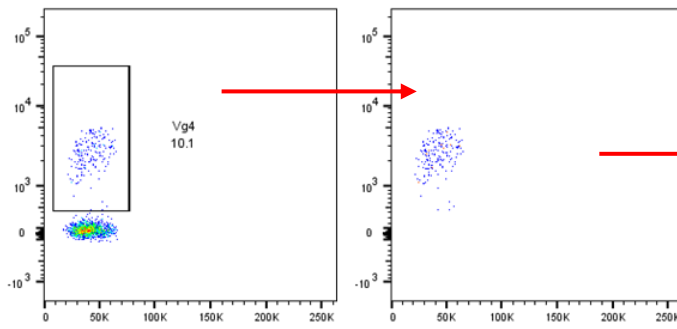
a V γ 1.1



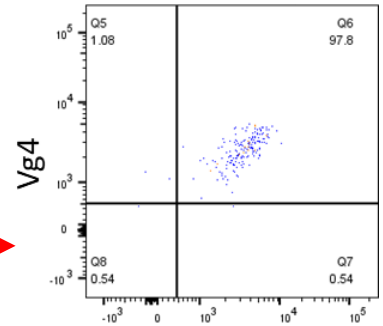
b V γ 1.1 + V γ 1.2



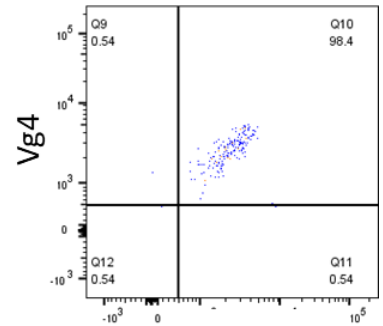
c V γ 4



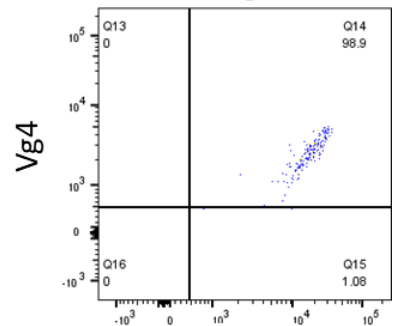
Vg1.1



Vg1.1 + 1.2

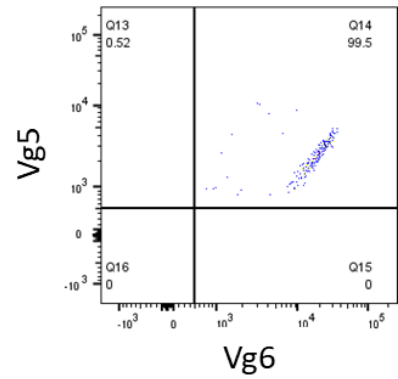
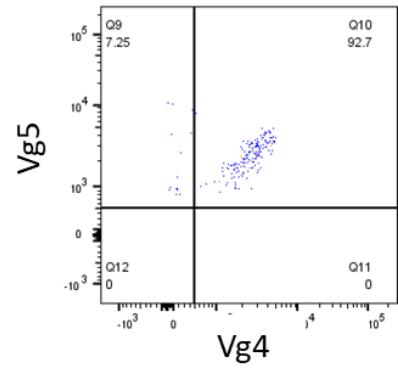
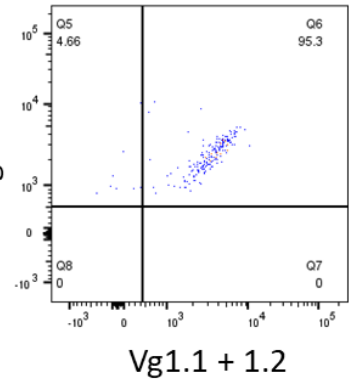
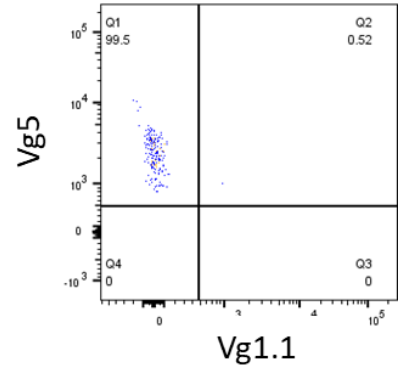
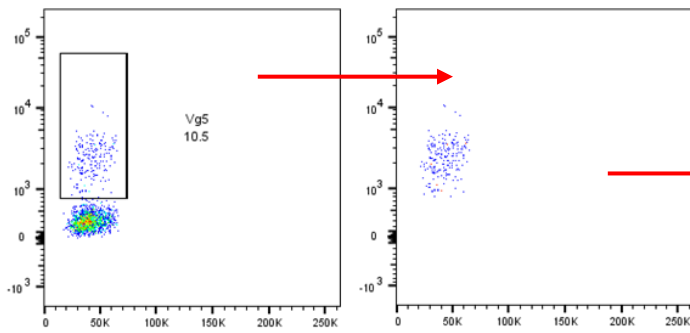


Vg5



Vg6

d $V_{\gamma 5}$



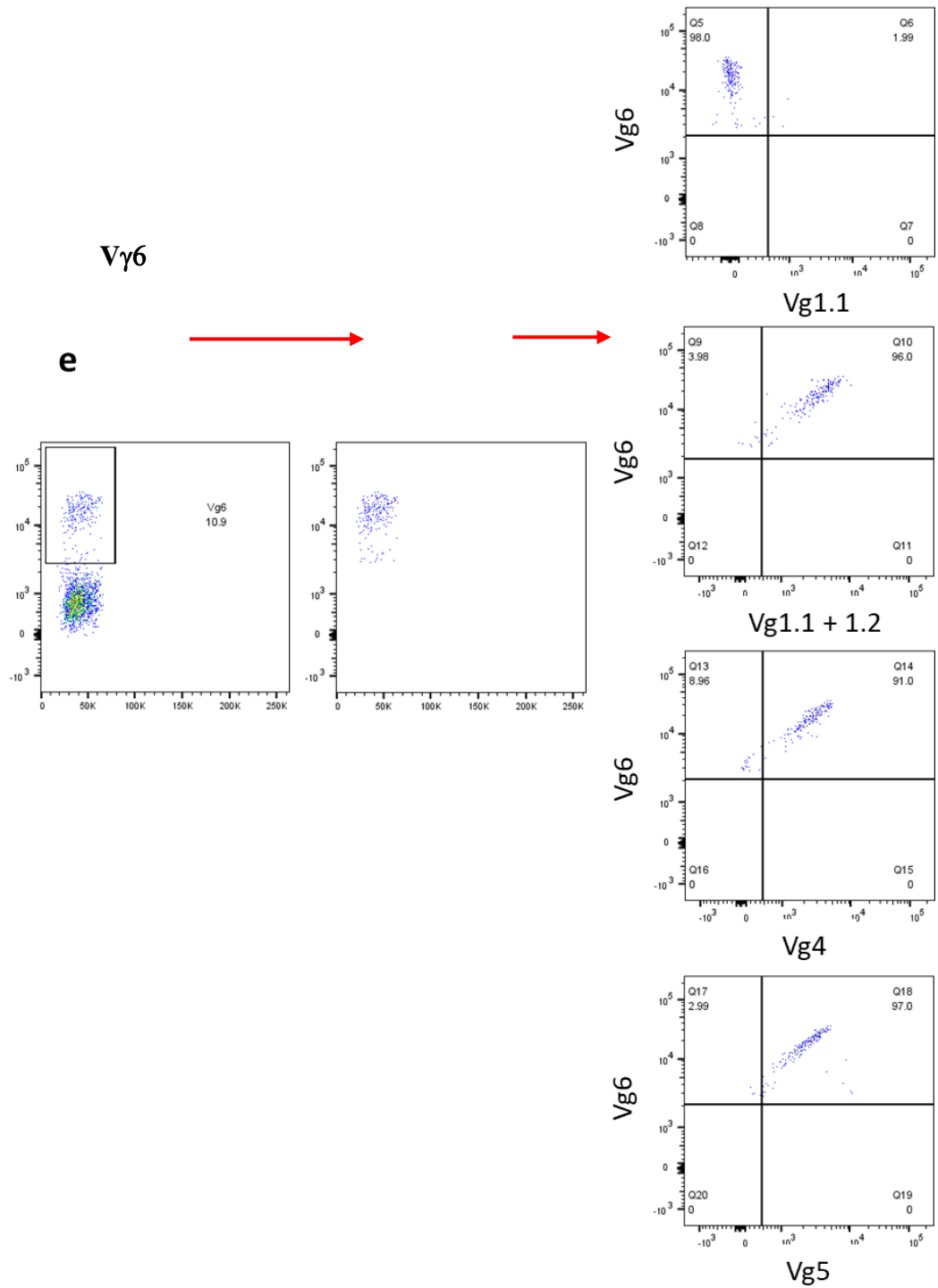


Fig. 5.3 Antibody co-expression for different γ chains. a) V γ 1.1 b) V γ 1.1+ V γ 1.2 c) V γ 4 d) V γ 5 e) V γ 6.

5.3 Conclusions

Studies from this chapter suggest that γ_6 and γ_7 appear to be the most abundant gamma chains in VAT while δ_1 is the most abundant delta chain. An age-associated increase in expression was observed for γ_1 , γ_2 , γ_4 , and γ_6 suggesting that these subpopulations may be increased by aging. However, as this data is based solely on gene expression by PCR, further studies are required to confirm this result.

Chapter 6 DISCUSSION, LIMITATIONS AND FUTURE DIRECTIONS

6.1 $\gamma\delta$ T cells progressively accumulate in VAT over the lifespan in mice

Changes in the immune profile are one of the major contributors of adipose tissue dysfunction[25, 27]. The majority of current knowledge regarding changes in the immune profile of visceral adipose tissue (VAT) with aging is focused on macrophages and regulatory T cells (Treg)[93-95]. Kohlgruber et al. recently showed that the number of $\gamma\delta$ T cells increase in VAT from juvenile (5weeks) to adult (28weeks) mice[45]. Previous studies from Dr. Starr's laboratory reported an age-associated (4mo vs. 24mo) increase in expression of T-cell receptor gamma, constant region (Tcr γ -C) in VAT, a gene expressed exclusively by $\gamma\delta$ T cells[88], which provided the platform to conduct my research on $\gamma\delta$ T cell accumulation in VAT with aging. Our initial experiments confirmed an age-associated increase in $\gamma\delta$ T cells in VAT that was independent of sex and adiposity by comparing two age groups. Importantly, we further showed that the age-associated increase in $\gamma\delta$ T cells in VAT was consistent in humans. Comparisons among different tissues demonstrated this increase to be specific to VAT. However, whether the age-associated increase in $\gamma\delta$ T cells is a late age-event or occurs linearly over the lifespan was not known. Seven age groups of mice were studied to identify the trend of $\gamma\delta$ T cell increase in VAT over the lifespan. The percentage of $\gamma\delta$ T cells among CD3⁺ lymphocytes increased in a progressive manner with a proportional decrease in T_{conv} cells. The actual number of $\gamma\delta$ T cells showed an initial increase in VAT at middle aged (12-16mo) compared to young (2-4mo), likely due to midlife weight gain as the trend follows the raise in body weight and epididymal fat weight. Supporting this, the number of $\gamma\delta$ T cells per gram of VAT is not significantly different in young and 12mo old mice suggesting dependence on adiposity at this age. Other studies have previously shown that high-fat diet feeding for short term increases the number of $\gamma\delta$ T cells, which was proportional to the increase of fat mass[45, 50, 72, 75]. $\gamma\delta$ T cell numbers further increase significantly at the old age groups (20-24mo) compared to the late middle age (16mo) without an increase in the body weight or fat mass. The number of T_{conv} cells showed similar results until middle age without further significant increase at the old age groups. To eliminate adiposity as a primary factor, cell

numbers were adjusted for fat mass. The absolute number of $\gamma\delta$ T cells after adjusting for fat mass showed a unique age-associated increase which reaches plateau after 16 months of age, whereas the increase in T_{conv} cells were primarily adiposity-dependent. The proportionate increase in the percentage of $\gamma\delta$ T cells compared to T_{conv} cells in VAT with aging indicates a functional replacement of the lymphocytes within the tissue which led to the studies to understand the role of $\gamma\delta$ T cells in inflammation and cellular homeostasis in the aged VAT.

6.2 Adipose tissue-resident $\gamma\delta$ T cells promote inflammation

IL-17A is a pro-inflammatory cytokine that is considered a kick starter of inflammation [96]. A prior report highlighted that the majority of adipose tissue $\gamma\delta$ T cells produce IL-17A, and that adipose tissue IL-17A is derived primarily from $\gamma\delta$ T cells [72]. One study with high fat diet fed mice showed a role for $\gamma\delta$ T cells in promoting obesity-driven inflammation by demonstrating reduced infiltration of pro-inflammatory macrophages into VAT, and reduced inflammation in VAT, skeletal muscle and liver in the mice lacking $\gamma\delta$ T cells [50]. Kohlgruber et al. identified the PLZF⁺ $\gamma\delta$ T cell subset as the largest subset in VAT which are IL-17A-producing cells in young adult mice. Age-associated changes in $\gamma\delta$ T cell phenotypes were not studied before. My study further confirmed that the majority of VAT $\gamma\delta$ T cells are IL-17A-producing and both percentage and total number of IL-17A⁺ $\gamma\delta$ T cells increased significantly by aging. This finding indicates that VAT $\gamma\delta$ T cells are not likely to lose functionality with age which raises the hypothesis that the increase in IL-17A⁺ $\gamma\delta$ T cells in VAT promotes chronic adipose tissue inflammation in the aged.

We studied the functional importance of $\gamma\delta$ T cells on inflammation using aged mice lacking $\gamma\delta$ T cells (TCR δ KO). We identified a significant reduction in gene expression of IL-6 in VAT and plasma of the aged TCR δ KO mice compared to WT mice. This is suggestive of a more youthful phenotype given that increased IL-6 in aging is a well-known inflammaging marker and has long been associated with a decline in physical function, heightened inflammation, senescence, and mortality [27, 32, 90, 91]. A recent study demonstrated that IL-6 itself can drive frailty in mice [97]. My study showed that a

population of cells including preadipocytes and ADSCs (CD45^{neg}CD31^{neg} cells) are the major IL-6-producing cells in VAT of aged mice, and that a significant reduction of IL-6⁺ cells in this subset is responsible for the overall reduction of IL-6 in aged mice lacking $\gamma\delta$ T cells. This suggests that $\gamma\delta$ T cells mediate IL-6 production by preadipocytes/ADSCs, either by direct communication or via signaling with other immune cells. IL-17A, which is almost exclusively produced by $\gamma\delta$ T cells in VAT, has been shown to induce the expression[72] and secretion[79] of IL-6 in cultured preadipocytes as well as fibroblasts[98], supporting the premise that $\gamma\delta$ T cells may directly induce preadipocyte IL-6 production via IL-17A signaling. Further studies are required to test this hypothesis. Additionally, changes in the abundance of other immune cell populations mediated by the loss of $\gamma\delta$ T cells may contribute to the overall decrease in inflammation. For example, CD4⁺ and CD8⁺ T_{conv} cells are increased in adipose tissue with age and promote inflammation[99-101]. My data showed a decrease in the number of these cells in the aged TCR δ KO mice which could potentially reduce age-related T_{conv} cell-mediated inflammation. Adipose tissue macrophages (ATM) play an important role in mediating inflammation during obesity and are well-known IL-6 producers. However, alterations in macrophages are distinct in aging when compared to obesity. While macrophage infiltration in obesity is well studied, their numbers do not significantly change during aging[93]. While the numbers do not change, one study identified macrophage as major IL-6 producers in adipose tissue and observed an age-associated increase in IL-6 production by ATM[99]. However, my data did not show macrophages as primary IL-6 producers in VAT.

Another mechanism in the adipose tissue known to promote inflammation is senescence[27, 102]. Senescent preadipocytes are known to accumulate in adipose tissue with age and secrete a wide array of inflammatory mediators in detriment of metabolic homeostasis[102, 103]. While we did not directly evaluate senescence in my studies, IL-6 is often utilized as a marker of senescence. Our data show that IL-6 is specifically decreased in the preadipocyte fraction of TCR δ KO mice. This may suggest a decrease in the proportion of senescent to non-senescent preadipocytes in VAT and raises the hypothesis that $\gamma\delta$ T cells contribute to preadipocyte senescence. Such hypothesis also requires further investigation.

6.3 Adipose tissue-resident $\gamma\delta$ T cells mediate cellular homeostasis

Very few studies have reported physiological roles of $\gamma\delta$ T cells in adipose tissue regarding cellular homeostasis[45, 50]. Obese mice lacking $\gamma\delta$ T (TCR δ KO) cells have reduced accumulation of pro-inflammatory macrophages in VAT compared to obese WT mice, specifically CD11c⁺CD206⁻ M1 and TNF α ⁺ macrophages. Additionally, no differences in the accumulation of anti-inflammatory M2 macrophages in the obese TCR δ KO vs. obese WT mice suggest a role of $\gamma\delta$ T cells in the infiltration of pro-inflammatory macrophages during obesity. Moreover, increased number of anti-inflammatory M2 macrophages were observed in obese V γ 4 and V γ 6 double knock-out mouse model demonstrating a role of V γ 4 and V γ 6 subsets to preventing the accumulation of M2 macrophages[50]. *In vivo* studies with TCR δ KO mice showed that $\gamma\delta$ T cells act on the adipose stromal cells via IL-17A to produce IL-33 which is required for Treg accumulation and homeostasis in VAT of young adult mice. The lack of inflammation in young VAT raises the possibility of the existence of a feedback loop which prevents local inflammation as the accumulation of pro-inflammatory $\gamma\delta$ T cells is concomitant with increase in anti-inflammatory Treg cells accumulation. My study with aged TCR δ KO mice demonstrated a significant reduction of CD4⁺ and CD8⁺ T cells and M2 macrophages compared to aged WT mice, suggesting a role of $\gamma\delta$ T cells in the maintenance of these cell types in the aged VAT. Reduced inflammation in the aged VAT of TCR δ KO mice may also compensate the necessity of anti-inflammatory M2 accumulation to maintain tissue homeostasis. On the other hand, an increase in CD4⁻CD8⁻ T cells and CD11c⁻CD206⁻ macrophages in the TCR δ KO mice indicates that $\gamma\delta$ T cells may prevent enrichment of these cells in aged VAT. No changes in the M1 macrophage population suggests that, in contrast to obesity, aging has distinct mechanisms to influence macrophage accumulation.

6.4 Peripheral migration plays a minor role in age-associated $\gamma\delta$ T cell accumulation in VAT

As *de novo* generation of $\gamma\delta$ T cells exists only in the thymus[104, 105], we investigated different physiological mechanisms to elucidate the age-associated $\gamma\delta$ T cell accumulation in VAT. The initial migration of $\gamma\delta$ T cells into peripheral tissues to take residency during the gestation period are well known[106]. Previous studies have found VAT $\gamma\delta$ T cells to be a tissue-resident population in young mice, using a parabiosis model with congenic CD45.1 and CD45.2 pairs[45, 66]. However, aged VAT serves as a primary source of inflammatory mediators in the body and pro-inflammatory cytokines and chemokines have been shown to recruit $\gamma\delta$ T cells into several tissues[107-109]. Moreover, the number of circulating $\gamma\delta$ T cells declines in aged mice[51] and humans[52-58], suggesting potential redistribution to VAT. Whether peripheral $\gamma\delta$ T cell recruitment to the VAT is enhanced by the inflammatory microenvironment in the aged was determined by comparing migration of $\gamma\delta$ T cells in young and aged WT:TCR δ KO isochronic parabiotic pairs. While blood and other peripheral tissues showed chimerism between WT and TCR δ KO mice, minimal migration of $\gamma\delta$ T cells into TCR δ KO VAT of both age groups was observed, suggesting that the majority of $\gamma\delta$ T cells remain as a self-sufficient tissue resident population over the lifespan. However, it is impossible to eliminate the contribution of a small amount of migrating $\gamma\delta$ T cells into VAT. In the young adult parabiotic pair, the VAT of the TCR δ KO animal achieved 7% chimerism on average indicating that circulating $\gamma\delta$ T cells are indeed able to migrate into the VAT. While on the low end compared to other tissues which ranged from 35-65% chimerism, this level of infiltration could lead to accumulation of cells over the lifespan. In the aged parabiotic pair, chimerism in the VAT of the parabiotic pair was lower, 2% on average, although not significantly different from the young. This low level chimerism was similar to those observed by others using young CD45.1:CD45.2 parabiotic pairs[45, 66]. A decline in migration in the aged could be explained as the number of the $\gamma\delta$ T cells within VAT may already have reached capacity to provide exclusion signals preventing the further recruitment of additional cells.

6.5 Increased number of proliferating $\gamma\delta$ T cells contribute to age-associated accumulation in VAT.

Minimal migration of $\gamma\delta$ T cells into VAT indicated a self-sustaining tissue resident population. My findings identified a progressive trend of $\gamma\delta$ T cells accumulation over the lifespan which may occur due to a clonal expansion of the $\gamma\delta$ T cell population via proliferation. Contrary to our hypothesis, the proportion of proliferating to non-proliferating $\gamma\delta$ T cells progressively declines from young to old age suggesting a decrease in the proliferative capacity by aging. However, the absolute number of proliferating $\gamma\delta$ T cells in VAT showed a significant age-associated increase which was sustained after adjusting for fat mass. Collectively, these results suggest that while the proportion of proliferating to non-proliferating $\gamma\delta$ T cells declines with age, the actual number of proliferating cells increases in accord with the total increase in the population of cells due to the exponential nature of clonal expansion. The presence of higher numbers of cells within the tissue and clonal expansion of these cells in VAT not only maintains, but rather expands the population contributing to age-associated $\gamma\delta$ T cell accumulation. Interestingly, there was no difference in the number of proliferating $\gamma\delta$ T cells from young to middle-age suggesting that the initial increase of $\gamma\delta$ T cells at middle age is not due to proliferation. It is possible that middle-age weight gain results in $\gamma\delta$ T cell recruitment which expands the population during aging. This could be tested with parabiosis in middle-aged mice. In fact, our data show that the middle-age increase in $\gamma\delta$ T cells corresponds with weight gain uniquely at that age. VAT $\gamma\delta$ T cells also express CD69, a signature phenotype of tissue-resident memory (TRM) cells[50, 51] which further corroborates that once $\gamma\delta$ T cells move into VAT, they lose exit signals. This population expands into older age with clonal expansion and contributes to maintaining the increased population. Another possibility is that a particular subpopulation of $\gamma\delta$ T cells may proliferate to increase the population in the aged. At this time, we are unable to determine subpopulation specifics due to lack of commercially available antibodies for the different γ and δ chains.

6.6 Decreased apoptosis beginning at middle-age contributes to increased survival and age-associated accumulation of $\gamma\delta$ T cells in VAT

DNA damage and oxidative stress during aging has a profound impact on cellular turnover, which generally results in increased cellular apoptosis with aging. However, the continuous accumulation of $\gamma\delta$ T cells in VAT over the lifespan without an increase in the proportion of proliferating cells indicate a potential increase in cell survival. To address this possibility, I evaluated the effect of aging on apoptosis of $\gamma\delta$ T cells in VAT. My data showed a decrease in the proportion of apoptotic $\gamma\delta$ T cells with a concomitant increase in the live (non-apoptotic) population in the middle-aged which continued into old age indicating that $\gamma\delta$ T cells in VAT are protected from apoptosis from the middle age onwards. Recent studies have shown that V γ 6⁺ $\gamma\delta$ T cells in the skin are protected from apoptosis via Bcl1a1 family proteins[110]. Using a similar experimental design, I explored this possible mechanism for VAT $\gamma\delta$ T cell protection from apoptosis. An induction of apoptosis was observed with the inhibition of Bcl-2, Bcl-xl, Bcl-w or Mcl1 proteins in young and aged VAT $\gamma\delta$ T cells suggesting a role of these anti-apoptotic proteins, either individually or in combination, to provide protection from apoptosis in these age groups. Whereas middle-aged VAT $\gamma\delta$ T cells are protected from apoptosis via other anti-apoptotic Bcl-2 family proteins that was not inhibited in my study, which is likely to be Bcl-2a1 proteins, as Bcl-2a1 has been shown to protect skin $\gamma\delta$ T cells from apoptosis [110]. Overall, my data showed that the anti-apoptotic Bcl-2 family proteins act differentially on VAT $\gamma\delta$ T cells in different age groups.

T_{conv} cells showed similar results with a significant increase in live cells and a decrease in the apoptotic population in middle-age. Contrary to the effect of aging on different cells of other tissues, the data collectively suggest that VAT lymphocytes are likely to escape apoptosis through aging. My data indicates that apoptosis in the T_{conv} cells are primarily regulated by Bcl-2, Bcl-xl, Bcl-w or Mcl1 or a combination of them in all three age groups: young, middle-age and aged. On the other hand, both $\gamma\delta$ T cells and T_{conv} cells in the lymph nodes have an increased age-associated apoptosis with a reduced live

cell population indicating that the protection from age-associated apoptosis is unique to VAT lymphocytes.

In conclusion, $\gamma\delta$ T cells showed a progressive trend of accumulation in VAT over the lifespan in mice and humans. Reduced inflammation, both locally and systemically, was observed in the absence of $\gamma\delta$ T cells, demonstrating their role in promoting inflammation. Consequently, mechanisms of age-associated accumulation of $\gamma\delta$ T cells were explored. In the absence of evidence suggesting that $\gamma\delta$ T cells traffic to VAT with aging, we focused on mechanisms supporting tissue-resident cell homeostasis. My findings indicated that $\gamma\delta$ T cells in VAT are protected from apoptosis from middle age onwards contributing to enhanced cell survival. This, in combination with an increased number of proliferating cells in the aged due to clonal expansion, not only maintains the growing population, but leads to the observed age-associated accumulation of $\gamma\delta$ T cells. These mechanisms are illustrated in a model (Fig 6.1). These findings are important to better understand how immune cells mediate adipose tissue dysfunction with aging and will aid in finding novel therapeutic interventions to reduce the burden of inflammaging associated diseases among the elderly.

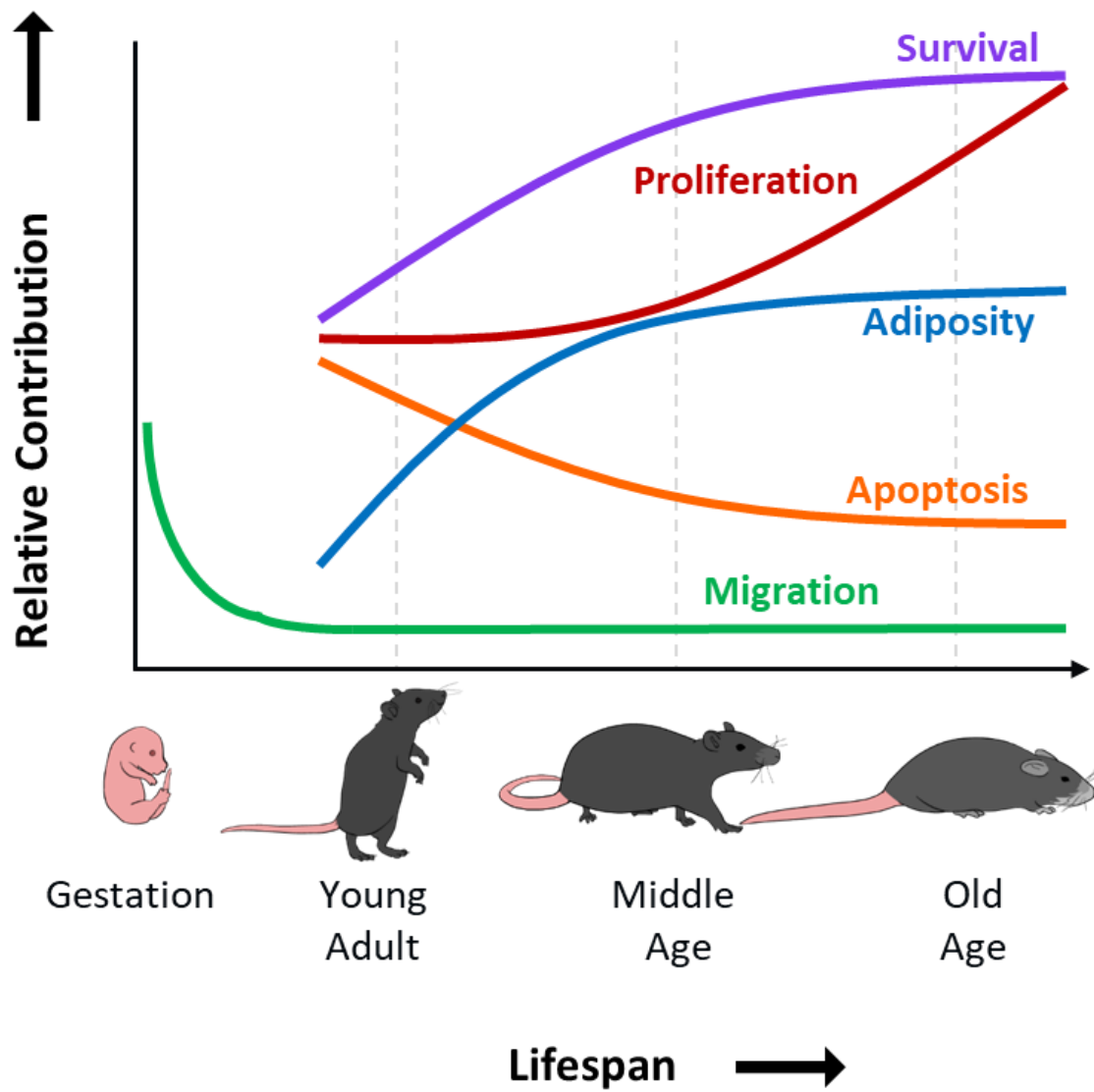


Fig. 6.1 A putative model demonstrating the interplay of global mechanisms to $\gamma\delta$ T cells accumulation in VAT with aging.

6.7 Limitations and future directions

The mice obtained for all of my studies were from either The Jackson Laboratory or National Institute on Aging. I acknowledge that various housing strategies in different institutes have an impact on mouse health, body weight, food habit and intake, microbiome, and overall adiposity, and thus influence the result. I also recognize that it would have been ideal to perform the studies with littermates and to age all the mice in the same environment. However, the use of at least three or more biological replicates for each experiment performed over several months along with high statistical power for each experiment have substantially minimized technical errors.

Another limitation of this study specific to the parabiosis model, is that TCR δ KO mice might lack the necessary recruitment signals for $\gamma\delta$ T cells due to lacking these cells in the system. This could be resolved by using congenic CD45.1 and CD45.2 parabiosis pairs; however, these mice would have to be aged for 2 years. Thus, we opted to use our available aging TCR δ KO colony to pursue the migration study. Although my studies were focused on young and aged groups, it would be of interest to identify whether migration is enhanced during middle-age by constructing parabiotic pairs at 12 months of age; however, we were not able to complete those studies at this time. It would be of interest to identify whether migration was enhanced during the middle age. Use of middle-aged mice would help us to understand whether $\gamma\delta$ T cell recruitment to VAT occurs during middle-age when weight gain and adiposity are also increased.

Another limitation is that $\gamma\delta$ T cell accumulation in the aged VAT can be subpopulation specific as it has been found in lymph nodes[63]. We were not capable of identifying different subpopulations in VAT as the commercially available antibodies showed co-expression with one or more antibodies for different proteins demonstrating non-specific binding. A single-cell RNA-Seq study in the future will help better understand the $\gamma\delta$ T cells subpopulations in VAT. Previous studies found that the majority of VAT $\gamma\delta$ T cells are V γ 6⁺[45]. Lymph node and thymic V γ 6⁺ cells are believed to have higher motility and traffic between tissues under homeostasis and in response to inflammation[110], which leads us to speculate that a certain population of V γ 6⁺ $\gamma\delta$ T cell

could migrate into VAT over the lifespan and maintain this population. Proliferation and apoptosis may also affect subpopulations differently and unique differences may be masked by our data on the total $\gamma\delta$ T cell population. We are currently conducting scRNAseq to address subpopulations specific differences which will allow us to generate additional hypotheses regarding the importance of different subpopulations to age-associated $\gamma\delta$ T cell accumulation and role in inflammaging.

It is established that the number of $\gamma\delta$ T cells increase with adiposity[50, 51], however, the source of these cells is yet to be explained. Previous studies have shown that circulating $\gamma\delta$ T cells are TNF α -producing and exhibit an activated CD69⁺ phenotype in the elderly due to presence of an inflamed environment known as inflammaging [54, 55]. VAT $\gamma\delta$ T cells demonstrate an activated phenotype in both young and aged mice[51] and maintain functionality with an increased number of IL-17A-producing cells in the aged. Whether the aged VAT microenvironment with elevated inflammatory mediators play any role in this activation and drive the proliferation is yet to be studied. Also, the functional importance of selective expansion of IL-17A⁺ $\gamma\delta$ T cells among lymphocytes requires further exploration.

My data demonstrated that the population of cells which includes preadipocytes and ADSC are the primary IL-6 producers in aged VAT and the number of IL-6-producing preadipocytes and ADSC cell subsets decreases in absence of $\gamma\delta$ T cells. Whether $\gamma\delta$ T cells directly act on preadipocytes via cytokine such as IL-17A or acts via other cellular crosstalk are yet to be studied. It is also possible that $\gamma\delta$ T cells may promote senescence of preadipocytes, which would become the primary IL-6 producers. The hypothesis that $\gamma\delta$ T cells contribute to preadipocyte senescence also requires further investigation.

In summary, my dissertation work has helped to elucidate how $\gamma\delta$ T cells come to be expanded in the VAT with aging. Future research to further elucidate their role in inflammaging both locally in VAT and systemically are warranted and will provide important information for aging biology.

Table 6.1 Nonstandard abbreviations and Acronyms.

Abbreviations	
AT	Adipose tissue
BAT	Brown adipose tissue
VAT	Visceral adipose tissue or visceral gonadal fat pads
SAT	Subcutaneous adipose tissue or inguinal fat pads
LN/pLN	Peripheral lymph node
TCR	T cell receptor
$\gamma\delta$ T	Gamma delta T cells
T _{conv}	Conventional T cells
T _{reg}	Regulatory T cells
Th17	T-helper 17 cells
MSC	Mesenchymal stem cells
WT	Wild type
KO	Knock out
TCR δ KO	T cell receptor delta knock out (lacks functional $\gamma\delta$ T cells)
Tcrg-C	T-cell receptor gamma, constant region
RPE	Retinal pigment epithelium
IVC	Inferior vena cava
RBC	Red blood cell
WBC	White blood cell
SVF	Stromal vascular fraction
DNA	Deoxyribonucleic acid
RNA	Ribonucleic acid
mi-RNA	MicroRNA
PCR	Polymerase Chain Reaction
RT-PCR	Reverse transcription-polymerase chain reaction
qRT-PCR	Quantitative real-time RT-PCR
IL-17A and IL-17F	Interleukin 17A and F
IL-17RA and IL-17RC	IL-17 Receptor A and C
IFN γ	Interferon gamma
TNF α	Tumor necrosis factor alpha
IL-6	Interleukin 6
IL-33	Interleukin 33
TGF β	Transforming growth factor beta
DP	Double positive
DN	Double negative
CD	Cluster of differentiation protein
PLZF	promyelocytic leukemia zinc finger

Table 6.1 Nonstandard abbreviations and Acronyms (Continued)

Abbreviations	
BCL2	B-cell leukemia/lymphoma 2 protein
PPAR γ	Peroxisome proliferator-activated receptor gamma
UCP1	Uncoupling Protein 1
AdipoR1	Adiponectin receptor 1
T _{RM}	Tissue-resident memory phenotype
SASP	Senescence associated secretory phenotype
HFD	High fat diet
T2 diabetes	Type 2 diabetes
AMD	Age-related macular degeneration
EdU	5-ethynyl-2'-deoxyuridine
FACS	fluorescence activated cell sorting
MFI	Mean fluorescence intensity
ANOVA	Analysis of variance
g	Gram
mo	Month
Y	Young
MA	Middle-aged
A	Aged

REFERENCES

1. Rose, M.R., *Evolutionary biology of aging*. 1991, New York: Oxford University Press. ix, 221 p.
2. Dominguez, L.J., et al., *Healthy Aging and Dietary Patterns*. *Nutrients*, 2022. **14**(4).
3. Fredriksen Goldsen, K. and B. de Vries, *Global Aging With Pride: International Perspectives on LGBT Aging*. *Int J Aging Hum Dev*, 2019. **88**(4): p. 315-324.
4. Rudnicka, E., et al., *The World Health Organization (WHO) approach to healthy ageing*. *Maturitas*, 2020. **139**: p. 6-11.
5. Vespa, J., *The U.S. Joins Other Countries With Large Aging Populations*. 2018.
6. Hafez, G., *The "greying" of the nations*. 1994.
7. Vespa, J., *The U.S. Joins Other Countries With Large Aging Populations*. 2018.
8. Richard J. Hodes, M.D., *NIA Congressional Budget Justification Fiscal year 2024 Budget*. 2023, NIA.
9. Bautmans, I., et al., *WHO working definition of vitality capacity for healthy longevity monitoring*. *Lancet Healthy Longev*, 2022. **3**(11): p. e789-e796.
10. Carmona, J.J. and S. Michan, *Biology of Healthy Aging and Longevity*. *Rev Invest Clin*, 2016. **68**(1): p. 7-16.
11. Kanasi, E., S. Ayilavarapu, and J. Jones, *The aging population: demographics and the biology of aging*. *Periodontol 2000*, 2016. **72**(1): p. 13-8.
12. Lopez-Otin, C., et al., *Hallmarks of aging: An expanding universe*. *Cell*, 2023. **186**(2): p. 243-278.
13. Guo, J., et al., *Aging and aging-related diseases: from molecular mechanisms to interventions and treatments*. *Signal Transduct Target Ther*, 2022. **7**(1): p. 391.
14. Moskalev, A., et al., *Targeting aging mechanisms: pharmacological perspectives*. *Trends Endocrinol Metab*, 2022. **33**(4): p. 266-280.
15. Imbert, I., *Biomarkers and aging*. *Biomark Med*, 2014. **8**(5): p. 621-3.
16. De Winter, G., *Aging as disease*. *Med Health Care Philos*, 2015. **18**(2): p. 237-43.
17. Jaul, E. and J. Barron, *Age-Related Diseases and Clinical and Public Health Implications for the 85 Years Old and Over Population*. *Front Public Health*, 2017. **5**: p. 335.
18. Callahan, C.M., et al., *Translational research on aging: clinical epidemiology as a bridge between the sciences*. *Transl Res*, 2014. **163**(5): p. 439-45.
19. Dunn, K.M., *Extending conceptual frameworks: life course epidemiology for the study of back pain*. *BMC Musculoskelet Disord*, 2010. **11**: p. 23.
20. Brenner, H. and V. Arndt, *Epidemiology in aging research*. *Exp Gerontol*, 2004. **39**(5): p. 679-86.
21. Kevin Flurkey, J.M.C., D.E. Harrison, *Chapter 20 - Mouse Models in Aging Research*. *The Mouse in Biomedical Research (Second edition)*. Vol. 3. 2007.
22. Patel, P. and N. Abate, *Body fat distribution and insulin resistance*. *Nutrients*, 2013. **5**(6): p. 2019-27.
23. Batra, A. and B. Siegmund, *The role of visceral fat*. *Dig Dis*, 2012. **30**(1): p. 70-4.
24. Huffman, D.M. and N. Barzilai, *Role of visceral adipose tissue in aging*. *Biochim Biophys Acta*, 2009. **1790**(10): p. 1117-23.

25. Palmer, A.K. and J.L. Kirkland, *Aging and adipose tissue: potential interventions for diabetes and regenerative medicine*. *Exp Gerontol*, 2016. **86**: p. 97-105.
26. Zhang, Y.X., et al., *Adipose tissue aging is regulated by an altered immune system*. *Front Immunol*, 2023. **14**: p. 1125395.
27. Stout, M.B., et al., *Physiological Aging: Links Among Adipose Tissue Dysfunction, Diabetes, and Frailty*. *Physiology (Bethesda)*, 2017. **32**(1): p. 9-19.
28. Longo, M., et al., *Adipose Tissue Dysfunction as Determinant of Obesity-Associated Metabolic Complications*. *Int J Mol Sci*, 2019. **20**(9).
29. Reyes-Farias, M., et al., *White adipose tissue dysfunction in obesity and aging*. *Biochem Pharmacol*, 2021. **192**: p. 114723.
30. Von Bank, H., C. Kirsh, and J. Simcox, *Aging adipose: Depot location dictates age-associated expansion and dysfunction*. *Ageing Res Rev*, 2021. **67**: p. 101259.
31. Franceschi, C., et al., *Inflamm-aging. An evolutionary perspective on immunosenescence*. *Ann N Y Acad Sci*, 2000. **908**: p. 244-54.
32. Franceschi, C. and J. Campisi, *Chronic inflammation (inflammaging) and its potential contribution to age-associated diseases*. *J Gerontol A Biol Sci Med Sci*, 2014. **69 Suppl 1**: p. S4-9.
33. Zamboni, M., et al., *How does adipose tissue contribute to inflammaging? Exp Gerontol*, 2021. **143**: p. 111162.
34. Palmer, A.K., et al., *Cellular Senescence in Type 2 Diabetes: A Therapeutic Opportunity*. *Diabetes*, 2015. **64**(7): p. 2289-98.
35. Maticchione, G., et al., *Senescent macrophages in the human adipose tissue as a source of inflammaging*. *Geroscience*, 2022. **44**(4): p. 1941-1960.
36. Fulop, T., et al., *Immunology of Aging: the Birth of Inflammaging*. *Clin Rev Allergy Immunol*, 2023. **64**(2): p. 109-122.
37. Zheng, J., et al., *gammadelta-T cells: an unpolished sword in human anti-infection immunity*. *Cell Mol Immunol*, 2013. **10**(1): p. 50-7.
38. Legut, M., D.K. Cole, and A.K. Sewell, *The promise of gammadelta T cells and the gammadelta T cell receptor for cancer immunotherapy*. *Cell Mol Immunol*, 2015. **12**(6): p. 656-68.
39. Lockhart, E., A.M. Green, and J.L. Flynn, *IL-17 production is dominated by gammadelta T cells rather than CD4 T cells during Mycobacterium tuberculosis infection*. *J Immunol*, 2006. **177**(7): p. 4662-9.
40. Shibata, K., et al., *Resident Vdelta1+ gammadelta T cells control early infiltration of neutrophils after Escherichia coli infection via IL-17 production*. *J Immunol*, 2007. **178**(7): p. 4466-72.
41. Hamada, S., et al., *IL-17A produced by gammadelta T cells plays a critical role in innate immunity against listeria monocytogenes infection in the liver*. *J Immunol*, 2008. **181**(5): p. 3456-63.
42. Vantourout, P. and A. Hayday, *Six-of-the-best: unique contributions of gammadelta T cells to immunology*. *Nat Rev Immunol*, 2013. **13**(2): p. 88-100.
43. Bank, I., *The Role of Gamma Delta T Cells in Autoimmune Rheumatic Diseases*. *Cells*, 2020. **9**(2).
44. Kabelitz, D., *Gamma Delta T Cells (gammadelta T Cells) in Health and Disease: In Memory of Professor Wendy Havran*. *Cells*, 2020. **9**(12).

45. Kohlgruber, A.C., et al., *gammadelta T cells producing interleukin-17A regulate adipose regulatory T cell homeostasis and thermogenesis*. Nat Immunol, 2018. **19**(5): p. 464-474.
46. Ribot, J.C., N. Lopes, and B. Silva-Santos, *gammadelta T cells in tissue physiology and surveillance*. Nat Rev Immunol, 2021. **21**(4): p. 221-232.
47. Cai, Y., et al., *Pivotal role of dermal IL-17-producing gammadelta T cells in skin inflammation*. Immunity, 2011. **35**(4): p. 596-610.
48. Pantelyushin, S., et al., *Rorgammata⁺ innate lymphocytes and gammadelta T cells initiate psoriasiform plaque formation in mice*. J Clin Invest, 2012. **122**(6): p. 2252-6.
49. Sebestyen, Z., et al., *Translating gammadelta (gammadelta) T cells and their receptors into cancer cell therapies*. Nat Rev Drug Discov, 2020. **19**(3): p. 169-184.
50. Mehta, P., A.M. Nuotio-Antar, and C.W. Smith, *gammadelta T cells promote inflammation and insulin resistance during high fat diet-induced obesity in mice*. J Leukoc Biol, 2015. **97**(1): p. 121-34.
51. Bruno, M.E.C., et al., *Accumulation of gammadelta T cells in visceral fat with aging promotes chronic inflammation*. Geroscience, 2022. **44**(3): p. 1761-1778.
52. Singh, P., et al., *Age-dependent frequency of unconventional T cells in a healthy adult Caucasian population: a combinational study of invariant natural killer T cells, gammadelta T cells, and mucosa-associated invariant T cells*. Geroscience, 2022. **44**(4): p. 2047-2060.
53. Clark, B.L. and P.G. Thomas, *A Cell for the Ages: Human gammadelta T Cells across the Lifespan*. Int J Mol Sci, 2020. **21**(23).
54. Colonna-Romano, G., et al., *Gamma/delta T lymphocytes are affected in the elderly*. Exp Gerontol, 2002. **37**(2-3): p. 205-11.
55. Romano, G.C., et al., *Early activation of gammadelta T lymphocytes in the elderly*. Mech Ageing Dev, 2000. **121**(1-3): p. 231-8.
56. Argentati, K., et al., *Numerical and functional alterations of circulating gammadelta T lymphocytes in aged people and centenarians*. J Leukoc Biol, 2002. **72**(1): p. 65-71.
57. Michishita, Y., et al., *Age-associated alteration of gammadelta T-cell repertoire and different profiles of activation-induced death of Vdelta1 and Vdelta2 T cells*. Int J Hematol, 2011. **94**(3): p. 230-240.
58. Vasudev, A., et al., *gamma/delta T cell subsets in human aging using the classical alpha/beta T cell model*. J Leukoc Biol, 2014. **96**(4): p. 647-55.
59. Tan, C.T., et al., *Vdelta2⁺ and alpha/ss T cells show divergent trajectories during human aging*. Oncotarget, 2016. **7**(29): p. 44906-44918.
60. Colonna-Romano, G., et al., *Impairment of gamma/delta T lymphocytes in elderly: implications for immunosenescence*. Exp Gerontol, 2004. **39**(10): p. 1439-46.
61. Kallemeijn, M.J., et al., *Next-Generation Sequencing Analysis of the Human TCRgammadelta⁺ T-Cell Repertoire Reveals Shifts in Vgamma- and Vdelta-Usage in Memory Populations upon Aging*. Front Immunol, 2018. **9**: p. 448.
62. Mazzocchi, G., et al., *A timetable of 24-hour patterns for human lymphocyte subpopulations*. J Biol Regul Homeost Agents, 2011. **25**(3): p. 387-95.

63. Chen, H.C., et al., *IL-7-dependent compositional changes within the gammadelta T cell pool in lymph nodes during ageing lead to an unbalanced anti-tumour response*. EMBO Rep, 2019. **20**(8): p. e47379.
64. Prinz, I. and I. Sandrock, *Dangerous gammadelta T cells in aged mice*. EMBO Rep, 2019. **20**(8): p. e48678.
65. Cheng, M., et al., *Intrinsically altered lung-resident gammadeltaT cells control lung melanoma by producing interleukin-17A in the elderly*. Aging Cell, 2020. **19**(2): p. e13099.
66. Goldberg, E.L., et al., *Ketogenesis activates metabolically protective gammadelta T cells in visceral adipose tissue*. Nat Metab, 2020. **2**(1): p. 50-61.
67. Shibata, K., et al., *Notch-Hes1 pathway is required for the development of IL-17-producing gammadelta T cells*. Blood, 2011. **118**(3): p. 586-93.
68. Turchinovich, G. and D.J. Pennington, *T cell receptor signalling in gammadelta cell development: strength isn't everything*. Trends Immunol, 2011. **32**(12): p. 567-73.
69. Zarin, P., et al., *Gamma delta T-cell differentiation and effector function programming, TCR signal strength, when and how much?* Cell Immunol, 2015. **296**(1): p. 70-5.
70. Ribot, J.C., et al., *CD27 is a thymic determinant of the balance between interferon-gamma- and interleukin 17-producing gammadelta T cell subsets*. Nat Immunol, 2009. **10**(4): p. 427-36.
71. Sadler, A.J., et al., *BTB-ZF transcriptional regulator PLZF modifies chromatin to restrain inflammatory signaling programs*. Proc Natl Acad Sci U S A, 2015. **112**(5): p. 1535-40.
72. Zuniga, L.A., et al., *IL-17 regulates adipogenesis, glucose homeostasis, and obesity*. J Immunol, 2010. **185**(11): p. 6947-59.
73. Heilig, J.S. and S. Tonegawa, *Diversity of murine gamma genes and expression in fetal and adult T lymphocytes*. Nature, 1986. **322**(6082): p. 836-40.
74. Sun, H., et al., *Tissue-resident lymphocytes: from adaptive to innate immunity*. Cell Mol Immunol, 2019. **16**(3): p. 205-215.
75. Caspar-Bauguil, S., et al., *Adipose tissues as an ancestral immune organ: site-specific change in obesity*. FEBS Lett, 2005. **579**(17): p. 3487-92.
76. Bonneville, M., R.L. O'Brien, and W.K. Born, *Gammadelta T cell effector functions: a blend of innate programming and acquired plasticity*. Nat Rev Immunol, 2010. **10**(7): p. 467-78.
77. Papotto, P.H., et al., *IL-23 drives differentiation of peripheral gammadelta17 T cells from adult bone marrow-derived precursors*. EMBO Rep, 2017. **18**(11): p. 1957-1967.
78. Ahmed, M. and S.L. Gaffen, *IL-17 in obesity and adipogenesis*. Cytokine Growth Factor Rev, 2010. **21**(6): p. 449-53.
79. Shinjo, T., et al., *IL-17A synergistically enhances TNFalpha-induced IL-6 and CCL20 production in 3T3-L1 adipocytes*. Biochem Biophys Res Commun, 2016. **477**(2): p. 241-6.
80. Hu, B., et al., *gammadelta T cells and adipocyte IL-17RC control fat innervation and thermogenesis*. Nature, 2020. **578**(7796): p. 610-614.

81. Ahmed, M. and S.L. Gaffen, *IL-17 inhibits adipogenesis in part via C/EBPalpha, PPARgamma and Kruppel-like factors*. Cytokine, 2013. **61**(3): p. 898-905.
82. Teijeiro, A., et al., *Inhibition of the IL-17A axis in adipocytes suppresses diet-induced obesity and metabolic disorders in mice*. Nat Metab, 2021. **3**(4): p. 496-512.
83. LaMarche, N.M., A.C. Kohlgruber, and M.B. Brenner, *Innate T Cells Govern Adipose Tissue Biology*. J Immunol, 2018. **201**(7): p. 1827-1834.
84. Zhao, Z., et al., *gammadelta T cells as a major source of IL-17 production during age-dependent RPE degeneration*. Invest Ophthalmol Vis Sci, 2014. **55**(10): p. 6580-9.
85. Shibata, S., et al., *Adiponectin regulates psoriasiform skin inflammation by suppressing IL-17 production from gammadelta-T cells*. Nat Commun, 2015. **6**: p. 7687.
86. Kamran, P., et al., *Parabiosis in mice: a detailed protocol*. J Vis Exp, 2013(80).
87. Andrew, E.M., et al., *Delineation of the function of a major gamma delta T cell subset during infection*. J Immunol, 2005. **175**(3): p. 1741-50.
88. Starr, M.E., et al., *Gene expression profile of mouse white adipose tissue during inflammatory stress: age-dependent upregulation of major procoagulant factors*. Aging Cell, 2013. **12**(2): p. 194-206.
89. Itohara, S., et al., *T cell receptor delta gene mutant mice: independent generation of alpha beta T cells and programmed rearrangements of gamma delta TCR genes*. Cell, 1993. **72**(3): p. 337-48.
90. Ershler, W.B., *Interleukin-6: a cytokine for gerontologists*. J Am Geriatr Soc, 1993. **41**(2): p. 176-81.
91. Maggio, M., et al., *Interleukin-6 in aging and chronic disease: a magnificent pathway*. J Gerontol A Biol Sci Med Sci, 2006. **61**(6): p. 575-84.
92. Church, C.D., R. Berry, and M.S. Rodeheffer, *Isolation and study of adipocyte precursors*. Methods Enzymol, 2014. **537**: p. 31-46.
93. Garg, S.K., et al., *Changes in adipose tissue macrophages and T cells during aging*. Crit Rev Immunol, 2014. **34**(1): p. 1-14.
94. Kolodin, D., et al., *Antigen- and cytokine-driven accumulation of regulatory T cells in visceral adipose tissue of lean mice*. Cell Metab, 2015. **21**(4): p. 543-57.
95. Bapat, S.P., et al., *Depletion of fat-resident Treg cells prevents age-associated insulin resistance*. Nature, 2015. **528**(7580): p. 137-41.
96. Papotto, P.H., J.C. Ribot, and B. Silva-Santos, *IL-17(+) gammadelta T cells as kick-starters of inflammation*. Nat Immunol, 2017. **18**(6): p. 604-611.
97. Jergovic, M., et al., *IL-6 can singlehandedly drive many features of frailty in mice*. Geroscience, 2021. **43**(2): p. 539-549.
98. Hwang, S.Y., et al., *IL-17 induces production of IL-6 and IL-8 in rheumatoid arthritis synovial fibroblasts via NF-kappaB- and PI3-kinase/Akt-dependent pathways*. Arthritis Res Ther, 2004. **6**(2): p. R120-8.
99. Lumeng, C.N., et al., *Aging is associated with an increase in T cells and inflammatory macrophages in visceral adipose tissue*. J Immunol, 2011. **187**(12): p. 6208-16.
100. Kalathookunnel Antony, A., Z. Lian, and H. Wu, *T Cells in Adipose Tissue in Aging*. Front Immunol, 2018. **9**: p. 2945.

101. Trott, D.W., et al., *T lymphocyte depletion ameliorates age-related metabolic impairments in mice*. *Geroscience*, 2021. **43**(3): p. 1331-1347.
102. Tchkonina, T., et al., *Fat tissue, aging, and cellular senescence*. *Aging Cell*, 2010. **9**(5): p. 667-84.
103. Zhu, Y., et al., *Cellular senescence and the senescent secretory phenotype in age-related chronic diseases*. *Curr Opin Clin Nutr Metab Care*, 2014. **17**(4): p. 324-8.
104. Prinz, I., B. Silva-Santos, and D.J. Pennington, *Functional development of gammadelta T cells*. *Eur J Immunol*, 2013. **43**(8): p. 1988-94.
105. Parker, M.E. and M. Ciofani, *Regulation of gammadelta T Cell Effector Diversification in the Thymus*. *Front Immunol*, 2020. **11**: p. 42.
106. Haas, J.D., et al., *Development of interleukin-17-producing gammadelta T cells is restricted to a functional embryonic wave*. *Immunity*, 2012. **37**(1): p. 48-59.
107. Xu, P., et al., *Recruitment of gammadelta T cells to the lesion via the CCL2/CCR2 signaling after spinal cord injury*. *J Neuroinflammation*, 2021. **18**(1): p. 64.
108. Severa, M., et al., *IFN-beta and multiple sclerosis: cross-talking of immune cells and integration of immunoregulatory networks*. *Cytokine Growth Factor Rev*, 2015. **26**(2): p. 229-39.
109. Taub, D.D., et al., *Chemotaxis of T lymphocytes on extracellular matrix proteins. Analysis of the in vitro method to quantitate chemotaxis of human T cells*. *J Immunol Methods*, 1995. **184**(2): p. 187-98.
110. Tan, L., et al., *Single-Cell Transcriptomics Identifies the Adaptation of Scart1(+) Vgamma6(+) T Cells to Skin Residency as Activated Effector Cells*. *Cell Rep*, 2019. **27**(12): p. 3657-3671 e4.

VITA

EDUCATION

- Ph.D.** in Pharmacology (GPA: 3.7/4.0) August 2018 – Present
University of Kentucky Advisor: [Dr. Marlene Starr](#)
Dissertation: *Age-associated increase of $\gamma\delta$ T cells in visceral adipose tissue and mechanisms of their accumulation.*
- M.S.** (with [Thesis](#)) in Biology (GPA: 3.9/4.0) August 2016 – August 2018
Indiana University of Pennsylvania Advisor: [Dr. Robert Major](#)
- M.Sc.** in Zoology Aug. 2012 – Nov. 2014
University of Calcutta, India. GPA: First-class
- B.Sc.** in Zoology June 2009 – July 2012
University of Calcutta, India. GPA: First-class

PROFESSIONAL EXPERIENCE

- Graduate Research Assistant** August 2018 – Present
Department of Pharmacology and Nutritional Science. University of Kentucky
- Tutor: Biology, Biochemistry, Chemistry and English** April 2017 – July 2018
Skill Zone, ISSS Indiana University of Pennsylvania
- Volunteer Tutor** July 2017
American Culture and English (ACE) Tutoring. Indiana University of Pennsylvania
- High School Teacher (Biology, Chemistry)** December 2014 – August 2015
Dreamland School West Bengal, India

AWARDS and HONORS

- **Best Poster Pitch Award**, American Aging Association (2022)
- **Graduate Student Thesis Award Nominee**, Dept of Pharmacology and Nutritional Sciences, College of Medicine, UKY (2022)
- **Outstanding Graduate Student Award Nominee**, Dept of Pharmacology and Nutritional Sciences, College of Medicine, UKY (2022)
- **Graduate Student Travel Award**, American Aging Association (2021)

- **Graduate Student Research Grant**, Indiana University of Pennsylvania (2017-18)
- **Library Employees' Scholarship Award**, Indiana University of Pennsylvania (2017)
- **International Tuition Waiver Scholarship**, Indiana University of Pennsylvania (2016-18)
- **Certificate of Achievement for Outstanding Participation in Women in Mathematics, Science and Technology**, Indiana University of Pennsylvania (2018, 2017)
- **Certificate of Excellence for Outstanding Scholarship and Service Activities**, Department of Biology, Indiana University of Pennsylvania (2018)
- **Graduate Research Assistantship Award**, University of Kentucky (2018-present)

PUBLICATIONS

- [J04] Lyon A, Meeks C, Tripathi R, He D, Wu Y, Liu J, Wang C, Chen J, Zhu H, **Mukherjee S**, Ganguly S, and Plattner R. ReversABLE drug resistance in NRAS-mutant melanomas. *Cancers*. 2023; 2;15(3):954.
- [J03] Bruno MEC*, **Mukherjee S***, Powell WL, Mori SF, Wallace FK, Balasuriya BK, Su LC, Stromberg AJ, Cohen DA, Starr ME. Accumulation of $\gamma\delta$ T cells in visceral fat with aging promotes chronic inflammation. *Geroscience*. 2022;44(3):1761-1778. (*Both authors contributed equally)
- [J02] Bruno MEC, **Mukherjee S**, Stromberg AJ, Saito H, Starr ME. Visceral fat-specific regulation of plasminogen activator inhibitor-1 in aged septic mice. *J Cell Physiol*. 2022;237(1):706-719.
- [J01] Zwischenberger BA, Balasuriya BK, Harris DD, Nataraj N, Owen AM, Bruno MEC, **Mukherjee S**, Ortiz-Soriano V, O'Connor W, Ke C, Stromberg AJ, Chang PK, Neyra JA, Saito H, Starr ME. Adipose-derived inflammatory and coagulant mediators in patients with sepsis. *Shock*. 2021;55(5):596-606.

POSTERS

- Aged visceral adipose tissue microenvironment mediates enhanced proliferation and accumulation of resident $\gamma\delta$ -T cells in mice, *American Aging Association*, San Antonio, TX, May 2022. (**Best Poster Pitch Award**)

- Peripheral migration contributes to age-associated $\gamma\delta$ -T cell accumulation in visceral adipose tissue in mice, *American Aging Association*, Madison, WI, July 2021. (**Graduate Student Travel Award**)

CERTIFICATIONS

- Certification for **Kentucky Science Advocate** for participating in Student Advocacy Workshops, Kentucky Academy of Science (2022)
- Certificate of Training in **Responsible Conduct of Research (RCR)** (2022)
- Certificate of Training in **Methods to Promote Data Reproducibility in Laboratory Research**, The University of Kentucky Good Research Practice (GRP) Resource Center (2019)

MEMBERSHIP and PARTICIPATIONS

- 2021- Ongoing Member - American Aging Association
- 2019- Ongoing Member-Women in Medicine and Science, University of Kentucky
- 2020- Ongoing Member - Nutritional Sciences and Pharmacology Students member
- 2019- Kentucky Advocates for Science Policy and Research
- 2020- 2021- American Heart Association
- 2019- COMPASS Science Communication Training
- 2019- SciPhD Workshop
- 2019- Faculty-Trainee Book Club - *Next Gen Ph.D* by Melanie Sinche

SCIENTIFIC COMMUNITY and OUTREACH ACTIVITIES

- 2022- Served as a Judge for Postdoctoral Poster Presentation, 13th Annual COM trainee Poster Session, University of Kentucky.
- 2022- Volunteered as BGSO Buddies mentor – College of Medicine, University of Kentucky
- 2021, 2019- Served as a Judge for Poster Presentation- Undergraduate Research Experience in Environmental Health Sciences (SURES) Program, University of Kentucky
- 2019- Near peer mentor- SURES Program, University of Kentucky